AD-A062 340 DAVID W TAYLOR NAVAL SHIP RESEARCH AND DEVELOPMENT CE--ETC F/G 13/10
HYDRODYNAMIC LOADING COEFFICIENTS FOR THE AGEH-1 MAIN STRUT-POD--ETC(U)
MAY 78 D W CODER, D E LAYNE

UNCLASSIFIED DTNSRDC/SPD-0332-05 NL

1 OF
AD
A062340

END
DATE FILMED
3 -79
DDC

LEVEL II

DAVID W. TAYLOR NAVAL SHIP RESEARCH AND DEVELOPMENT CENTER

Bethesda, Md. 20084

AD A062340

DDC FILE COPY

HYDRODYNAMIC LOADING COEFFICIENTS FOR THE AGEH-1 MAIN STRUT-POD-FOIL SYSTEM AS DERIVED FROM THE 1975 FLAP INCIDENCE CONTROL EXPERIMENT by D.W. Coder & D.E. Layne DTNSRDC/SPD-0332-05

(6) HYDRODYNAMIC LOADING COEFFICIENTS FOR THE AGEH-1 MAIN STRUT-POD-FOIL SYSTEM AS DERIVED FROM THE 1975 FLAP INCIDENCE CONTROL EXPERIMENT

by

(10) David W. Coder
Douglas E. Layne

APPROVED FOR PUBLIC RELEASE: DISTRIBUTION UNLIMITED

SHIP PERFORMANCE DEPARTMENT

(9) DEPARTMENTAL REPORT

(11) May 1978 (12) 87 p. (14) DTNSRDC/SPD-0332-05

389 694

78 12 14 031

MAJOR DTNSRDC ORGANIZATIONAL COMPONENTS

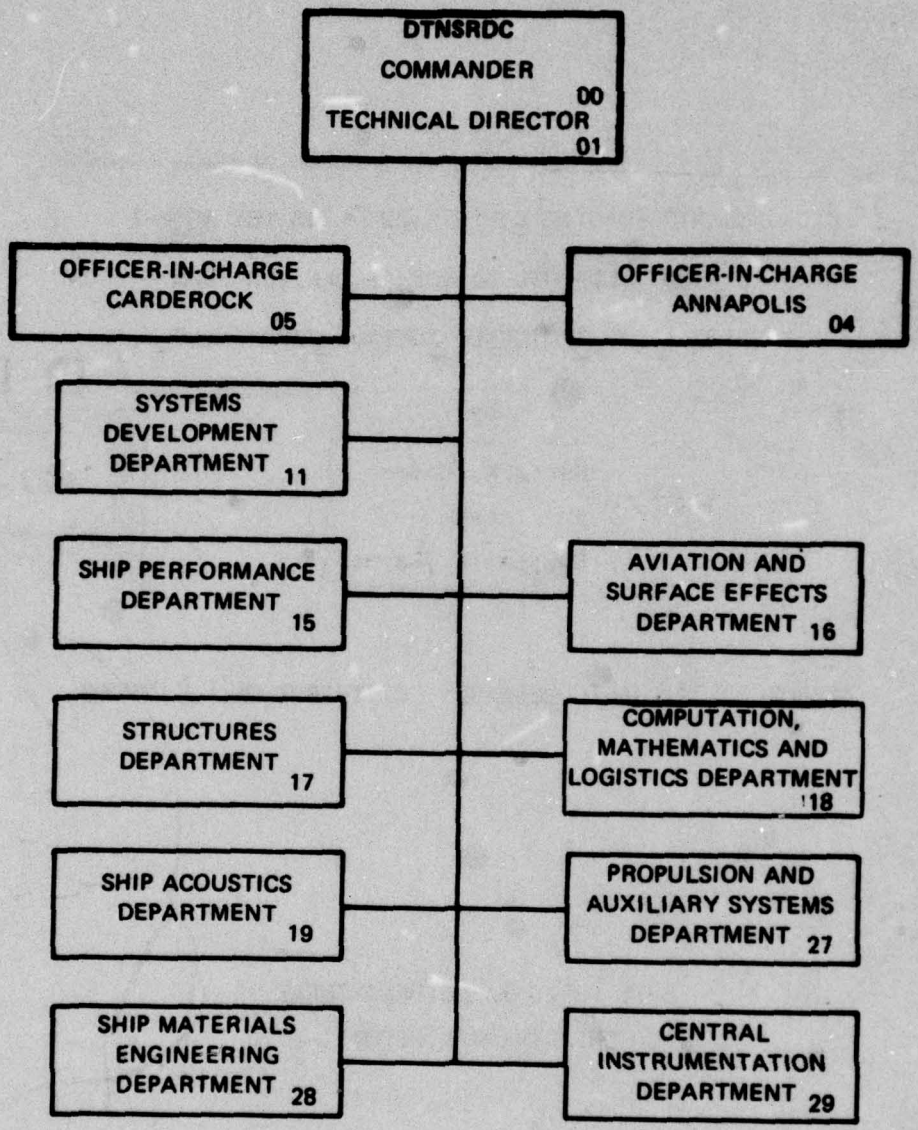

UNCLASSIFIED

SECURITY CLASSIFICATION OF THIS PAGE (When Data Entered)

REPORT DOCUMENTATION PAGE		READ INSTRUCTIONS BEFORE COMPLETING FORM
1. REPORT NUMBER 78-SPD-332-05	2. GOVT ACCESSION NO.	3. RECIPIENT'S CATALOG NUMBER
4. TITLE (and Subtitle) HYDRODYNAMIC LOADING COEFFICIENTS FOR THE AGEH-1 MAIN STRUT-POD-FOIL SYSTEM AS DERIVED FROM THE 1975 FLAP INCIDENCE CONTROL EXPERIMENT		5. TYPE OF REPORT & PERIOD COVERED Departmental 6. PERFORMING ORG. REPORT NUMBER
7. AUTHOR(s) D.W. Coder and D.E. Layne		8. CONTRACT OR GRANT NUMBER(s)
9. PERFORMING ORGANIZATION NAME AND ADDRESS David W. Taylor Naval Ship R&D Center Bethesda, Maryland 20084		10. PROGRAM ELEMENT, PROJECT, TASK AREA & WORK UNIT NUMBERS Project S4606, Task 01703 Work Unit 1153-503
11. CONTROLLING OFFICE NAME AND ADDRESS Naval Sea Systems Command Washington, DC 20362		12. REPORT DATE May 1978 13. NUMBER OF PAGES 79
14. MONITORING AGENCY NAME & ADDRESS(if different from Controlling Office)		15. SECURITY CLASS. (of this report) UNCLASSIFIED 15a. DECLASSIFICATION/DOWNGRADING SCHEDULE

16. DISTRIBUTION STATEMENT (of this Report)

APPROVED FOR PUBLIC RELEASE: DISTRIBUTION UNLIMITED

17. DISTRIBUTION STATEMENT (of the abstract entered in Block 20, if different from Report)

18. SUPPLEMENTARY NOTES

19. KEY WORDS (Continue on reverse side if necessary and identify by block number)

Flap Incidence Control
AGEH-1
Hydrofoils

20. ABSTRACT (Continue on reverse side if necessary and identify by block number)

As part of an investigation into minimizing control power requirements for hydrofoil craft, a technique has been developed for obtaining complete hydrodynamic lift and moment characteristics of a flapped hydrofoil from equilibrium data obtained in flap incidence control experiments with a freely pivoting foil. This method employs a simple mathematical model and various crossplots of the data to separate the effects of camber, foil incidence angle, and flap angle using a minimum amount of data. (cont'd)

DD FORM 1 JAN 73 1473 EDITION OF 1 NOV 65 IS OBSOLETE
S/N 0102-LF-014-6601

UNCLASSIFIED

SECURITY CLASSIFICATION OF THIS PAGE (When Data Entered)

Existing model data for the AGEH-1 main strut-pod-foil system under subcavitating conditions have been analyzed by this method, and effects of depth and velocity are described. Velocity effects were attributed to air and/or water flow out of the pod. Relatively high values of flap lift effectiveness (0.3 to 0.4) were obtained. Centers of pressure (lines of action) for lift due to camber, angle of attack, and flap angle are presented. Recommendations are given for improving the accuracy of the measurement and analysis techniques.

TABLE OF CONTENTS

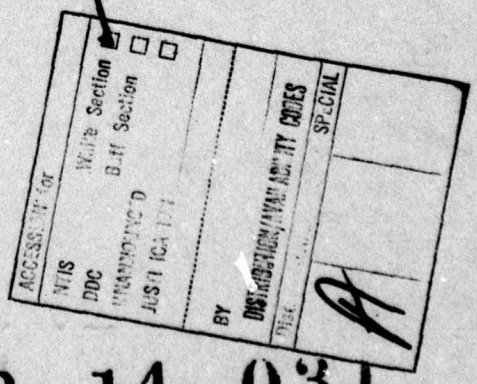

LIST OF FIGURES

LIST OF TABLES

NOTATION

b	Intercept of flap angle-foil angle curve ($= (\varphi)_{\alpha=0}$)
C_H	Moment coefficient ($= H/q\,S\bar{c}$)
C_{HC}	Camber moment coefficient
$C_{H\alpha}$	Foil-moment-curve slope ($=\partial C_H/\partial\alpha$)
$C_{H\varphi}$	Flap-moment-curve slope ($=\partial C_H/\partial\varphi$)
C_L	Lift coefficient ($= L/qS$)
C_{LC}	Camber lift coefficient
$C_{L\alpha}$	Foil-lift-curve slope ($=\partial C_L/\partial\alpha$)
$C_{L\varphi}$	Flat-lift-curve slope ($=\partial C_L/\partial\varphi$)
C_M	Bias moment coefficient ($=M/qS\bar{c}$)
$\bar{c}$	Mean geometric chord based on foil planform extended to pod centerline
E_H	Flap moment effectiveness ($= C_{H\varphi}/C_{H\alpha}$)
E_L	Flap lift effectiveness ($= C_{L\varphi}/C_{L\alpha}$)
H	Hydrodynamic moment
h	Depth from free surface to foil
L	Hydrodynamic lift
M	Bias moment
m	Slope of flap angle-foil angle curve ($=\partial\varphi/\partial\alpha$)
q	Dynamic pressure ($= (1/2)\rho U^2$)
S	Planform area of foil extended to pod centerline
U	Free stream velocity or carriage velocity
W	Flap lift center of pressure location from the leading edge in mean geometric chords

X or x	Foil pivot location from the leading edge in mean geometric chords
Y or y	Planform lift center of pressure location from the leading edge in mean geometric chords
Z or z	Camber lift center of pressure location from the leading edge in mean geometric chords
α	Foil angle relative to pod
β	Flap angle relative to foil
ρ	Density of fluid

ABSTRACT

As part of an investigation into minimizing control power requirements for hydrofoil craft, a technique has been developed for obtaining complete hydrodynamic lift and moment characteristics of a flapped hydrofoil from equilibrium data obtained in flap incidence control experiments with a freely pivoting foil. This method employs a simple mathematical model and various crossplots of the data to separate the effects of camber, foil incidence angle, and flap angle using a minimum amount of data.

Existing model data for the AGEH-1 main strut-pod-foil system under subcavitating conditions have been analyzed by this method, and effects of depth and velocity are described. Velocity effects were attributed to air and/or water flow out of the pod. Relatively high values of flap lift effectiveness (0.3 to 0.4) were obtained. Centers of pressure (lines of action) for lift due to camber, angle of attack, and flap angle are presented. Recommendations are given for improving the accuracy of the measurement and analysis techniques.

ADMINISTRATIVE INFORMATION

The work presented here was sponsored by the Naval Sea Systems Command (NAVSEA SYSCOM) under Project S4606, Task 01703, and performed under the David W. Taylor Naval Ship Research and Development Center (DTNSRDC) Work Unit 1153-503.

INTRODUCTION

Of recent interest to the U.S. Navy have been methods of reducing the control power requirements for hydrofoil craft. In a theoretical study of four different hydrofoil configurations in a seaway, Remington

and Bender[1] concluded that the configuration using a trailing edge flap for incidence control of a freely pivoting foil required the least amount of power. An existing model of the AGEH main strut-pod-foil with a trailing edge flap on the foil* has been modified for flap incidence control. The foil was made freely pivoting in pitch (incidence angle) about the existing transverse axis through the pod. The motion of the flap and foil angles were coupled together by a series of linkages to obtain a passive control system. An experiment performed at DTNSRDC using this modified model has been reported by Coder and Wisler.[2] The purpose of that experiment, labeled here as the "1975 Flap Incidence Control Experiment," was to determine whether equilibrium flap-foil angle conditions ("stable flying situations") could be obtained. The velocities were low (7.31 to 12.86 m/s) so that the foil was fully wetted (no cavitation) for most of the conditions tested. Equilibrium conditions were obtained and are reported in Reference 2. While those data were being reduced, it was discerned that the moment at zero flap and foil angles and the variance of moment with flap angle alone could be obtained from the data using what will be called here the "indirect method." After those results were published, this "indirect method" was expanded to include consideration of the lift data (not published in Reference 2 but included here in Appendix A) to determine other hydrodynamic loading characteristics.

---

[1]References are listed on page 79.

* This model was previously used for work reported informally by A.C. Conolly in DTNSRDC Report SPD-332-H-02 in February 1973.

This "indirect method" is based on that two-dimensional representation of the foil developed in Coder, et al.[3] - the lift and moment were assumed to be the sum total of the parts due to foil camber, foil angle of attack, and tab/flap. Here the equations for lift and moment are written in coefficient form as given in Equations [1] and [2] of the ANALYSIS section. Using the straight-line fits to the flap angle-foil angle equilibrium data from Coder and Wisler,[2] and appropriate crossplots of those data and the lift data from Appendix A, the six coefficients on the right-hand side of Equations [1] and [2] are determined. Also, it will be seen that the lift and moment effectiveness and the lines of action of the various lift components may be determined from the resulting coefficients.

The objective of the present work is to determine with actual data whether this "indirect method" produces reasonable results. Since it is planned to conduct further flap incidence control experiments with an improved model and under cavitating conditions, this "indirect method" may prove to be a viable method to determine these lift and moment coefficients as a byproduct of studying the equilibrium conditions and the control system. Further, it may prove to be more advantageous from a testing point of view to determine the loading characteristics using this "indirect method" since much data is obtained rather quickly and efficiently.

The remainder of the report describes this "indirect method," presents and discusses the results for the data from the 1975 Flap Incidence Control Experiments, and makes recommendations as to the future employment of this method.

ANALYSIS

The lift and moment in coefficient form for a fully wetted flapped foil at small angles may be represented by

$$C_L = C_{L\alpha}\alpha + C_{LC} + C_{L\beta}\beta \qquad [1]$$

$$C_H = C_{H\alpha}\alpha + C_{HC} + C_{H\beta}\beta \qquad [2]$$

where

C_L is lift coefficient (= lift/qS)

$C_{L\alpha}$ is foil lift-curve slope (= $\partial C_L/\partial\alpha$)

C_{LC} is camber lift coefficient (also includes thickness effects)

$C_{L\beta}$ is flap lift-curve slope (= $\partial C_L/\partial\beta$)

C_H is moment coefficient (= moment/q $S\bar{c}$)

$C_{H\alpha}$ is foil moment-curve slope (= $\partial C_H/\partial\alpha$)

C_{HC} is camber moment coefficient

$C_{H\beta}$ is flap moment-curve slope (= $\partial C_H/\partial\beta$)

$\bar{c}$ is mean geometric chord based on foil planform extended to pod centerline

q is dynamic pressure (= $(1/2)\rho U^2$)

s is planform area of foil extended to pod centerline

U is free stream velocity

α is foil angle

β is flap angle

ρ is density of fluid

The data reported by Coder and Wisler[2] pertain to a flapped, freely-pivoting foil and are presented in the form of foil angle versus flap angle to maintain hydrodynamic-external bias moment equilibrium, i.e.,

in the form

$$\beta = m\alpha + b \qquad [3]$$

where m is the slope $(=\partial\beta/\partial\alpha)$

b is the intercept $(= (\beta)_{\alpha = 0})$

From these data alone, C_{HC} and $C_{H\beta}$ were calculated and are presented in that report. The present report also presents (in Appendix A) lift coefficient (C_L) versus foil angle (α) for that experiment. The slopes and intercepts of average straight-lines drawn through these data are presented in Table 1 together with pertinent data from Coder and Wisler.[2] From all these data, the coefficients in Equations [1] and [2] and centers of pressure (lines of action) for the various lift components may be determined. A schematic showing the analysis technique is shown in Figure 1 and will now be described.

LIFT COEFFICIENTS

If Equation [3] is used with Equation [1]

$$\begin{aligned} C_L &= C_{L\alpha}\alpha + C_{LC} + C_{L\beta}(m\alpha + b) \\ &= (C_{L\alpha} + m\,C_{L\beta})\alpha + (C_{LC} + bC_{L\beta}) \end{aligned} \qquad [4]$$

Thus we have

$$\begin{aligned} (C_L)_{\alpha = 0} &= C_{LC} + C_{L\beta}\,b \\ dC_L/d\alpha &= C_{L\alpha} + C_{L\beta}\,m \end{aligned} \qquad [5]$$

In Figure 2, $(C_L)_{\alpha = 0}$ from Table 1 is plotted versus b from Table 1 from which $C_{L\beta}$ and C_{LC} were determined as the slope and intercept, respectively and listed in Table 2. In Figure 3, $dC_L/d\alpha$ from Table 1 is plotted versus m from Table 1. As seen in the figure, it is impossible to

TABLE 1 - FITTED DATA FROM 1975 FLAP INCIDENCE CONTROL EXP.

Velocity (m/s)	h/c	M (N-M)	C_M	$m = \partial\beta/\partial\alpha$ (Deg/Deg)	$b = (\beta)_{\alpha=0}$ (Deg)	$\frac{\partial C_L}{\partial \delta}$ (1/Deg)	$(C_L)_{\alpha=0}$
7.31	0.578	0	0	0.681	-6.14	0.0467	0.0120
	1.156	0	0	0.665	-6.98	0.0527	-0.0050
	0.578	13.6	0.0160	0.594	-2.47	0.0503	0.0550
	1.156	13.6	0.0160	0.584	-3.70	0.0527	0.0450
	0.578	27.1	0.0319	0.699	0.76	0.0507	0.1050
	1.156	27.1	0.0319	0.647	-0.65	0.0547	0.0975
	0.578	40.7	0.0479	0.737	3.29	0.0513	0.1525
	1.156	40.7	0.0479	0.707	1.56	0.0550	0.1400
9.00	0.578	0	0	0.757	-5.76	0.0497	0.0120
	1.156	0	0	0.750	-7.16	0.0530	-0.0040
	0.578	13.6	0.0105	0.617	-4.09	0.0483	0.0320
	1.156	13.6	0.0105	0.611	-5.33	0.0517	0.0180
	0.578	27.1	0.0210	0.650	-2.78	0.0493	0.0530
	1.156	27.1	0.0210	0.611	-4.07	0.0523	0.0400
	0.578	40.7	0.0315	0.706	-0.81	0.0500	0.0860
	1.156	40.7	0.0315	0.667	-2.20	0.0577	0.0710
10.55	0.578	0	0	0.907	-6.01	0.0493	0.0080
	1.156	0	0	0.904	-7.62	0.0527	-0.0080
	0.578	13.6	0.0077	0.641	-4.73	0.0477	0.0210
	1.156	13.6	0.0077	0.733	-6.33	0.0523	0.0060
	0.578	27.1	0.0153	0.661	-4.12	0.0570	0.0330
	1.156	27.1	0.0153	0.610	-5.88	0.0533	0.0170
	0.578	40.7	0.0230	0.667	-2.79	0.0493	0.0520
	1.156	40.7	0.0230	0.654	-4.28	0.0547	0.0350
12.86	0.578	0	0	*	*	*	*
	1.156	0	0	*	*	*	*
	0.578	13.6	0.0052	*	*	*	*
	1.156	13.6	0.0052	*	*	*	*
	0.578	27.1	0.0103	0.736	-5.69	0.0497	0.0100
	1.156	27.1	0.0103	0.687	-6.90	0.0540	-0.0075
	0.578	40.7	0.0155	0.703	-4.88	0.0500	0.0200
	1.156	40.7	0.0155	0.680	-6.07	0.0540	0.0080

* NO DATA OBTAINED

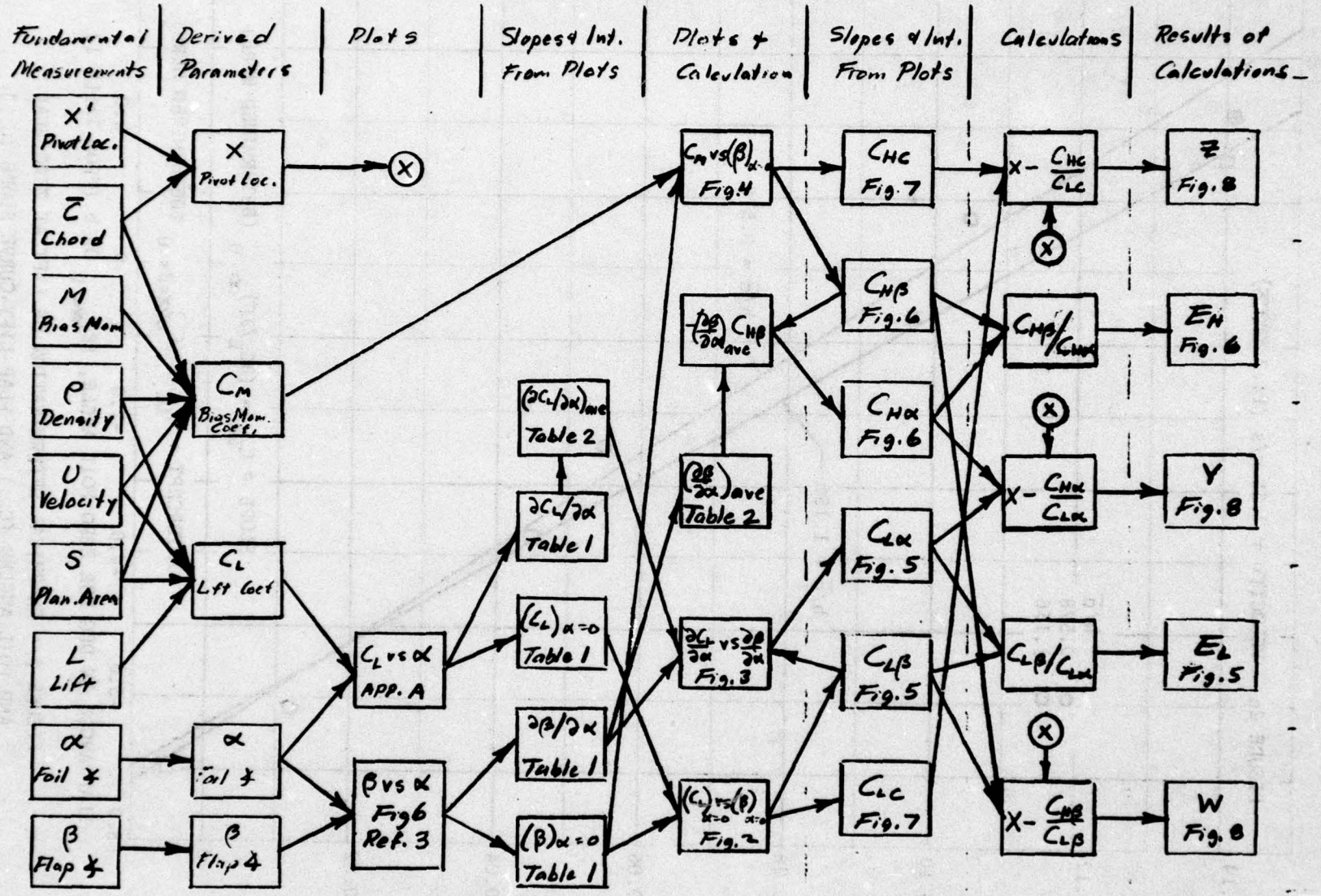

FIGURE 1 - SUMMARY OF "INDIRECT METHOD" ANALYSIS

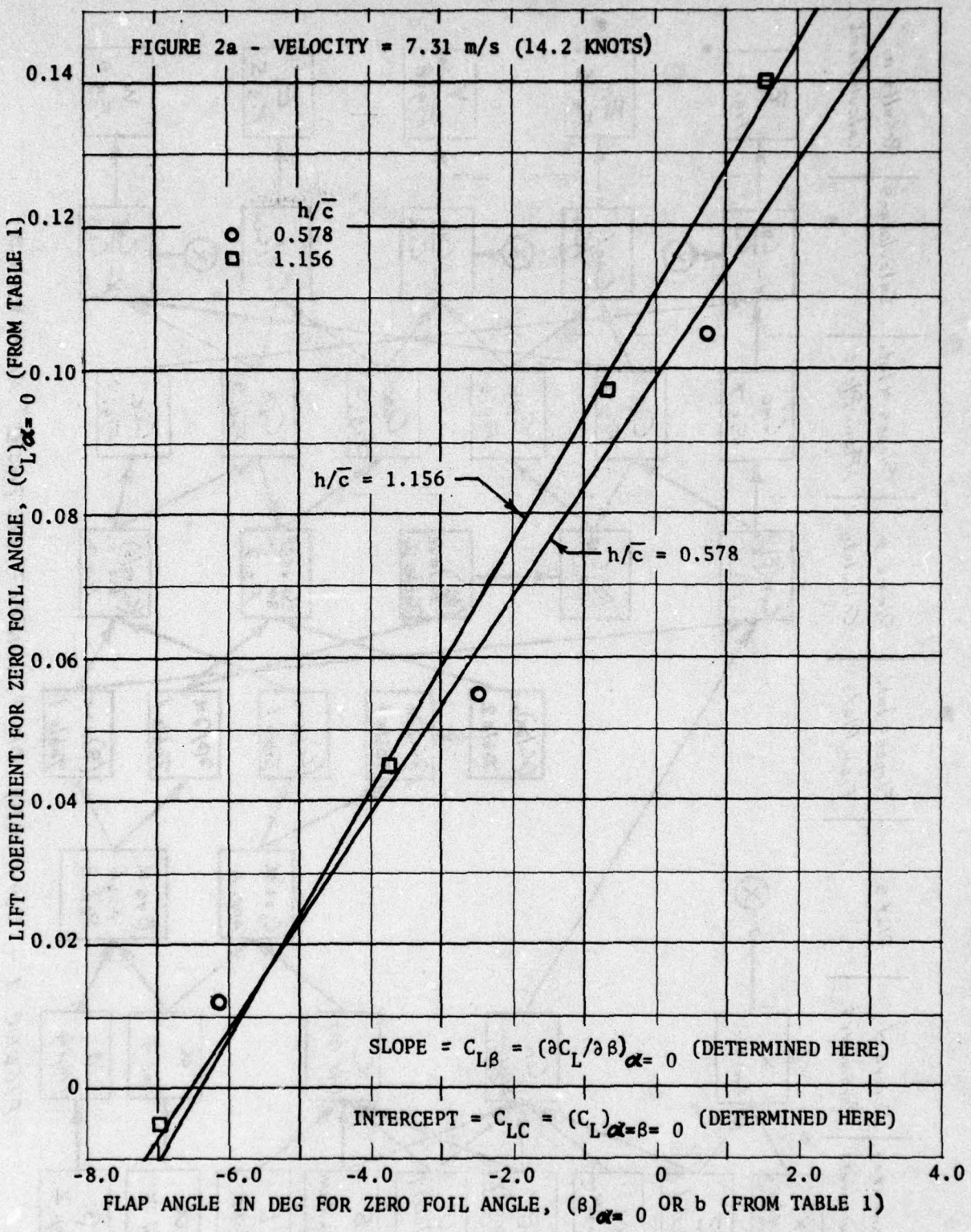

FIGURE 2 - GRAPHICAL DETERMINATION OF LIFT AT ZERO FLAP AND FOIL ANGLES (C_{LC}) AND FLAP-LIFT-CURVE SLOPE ($C_{L\beta}$)

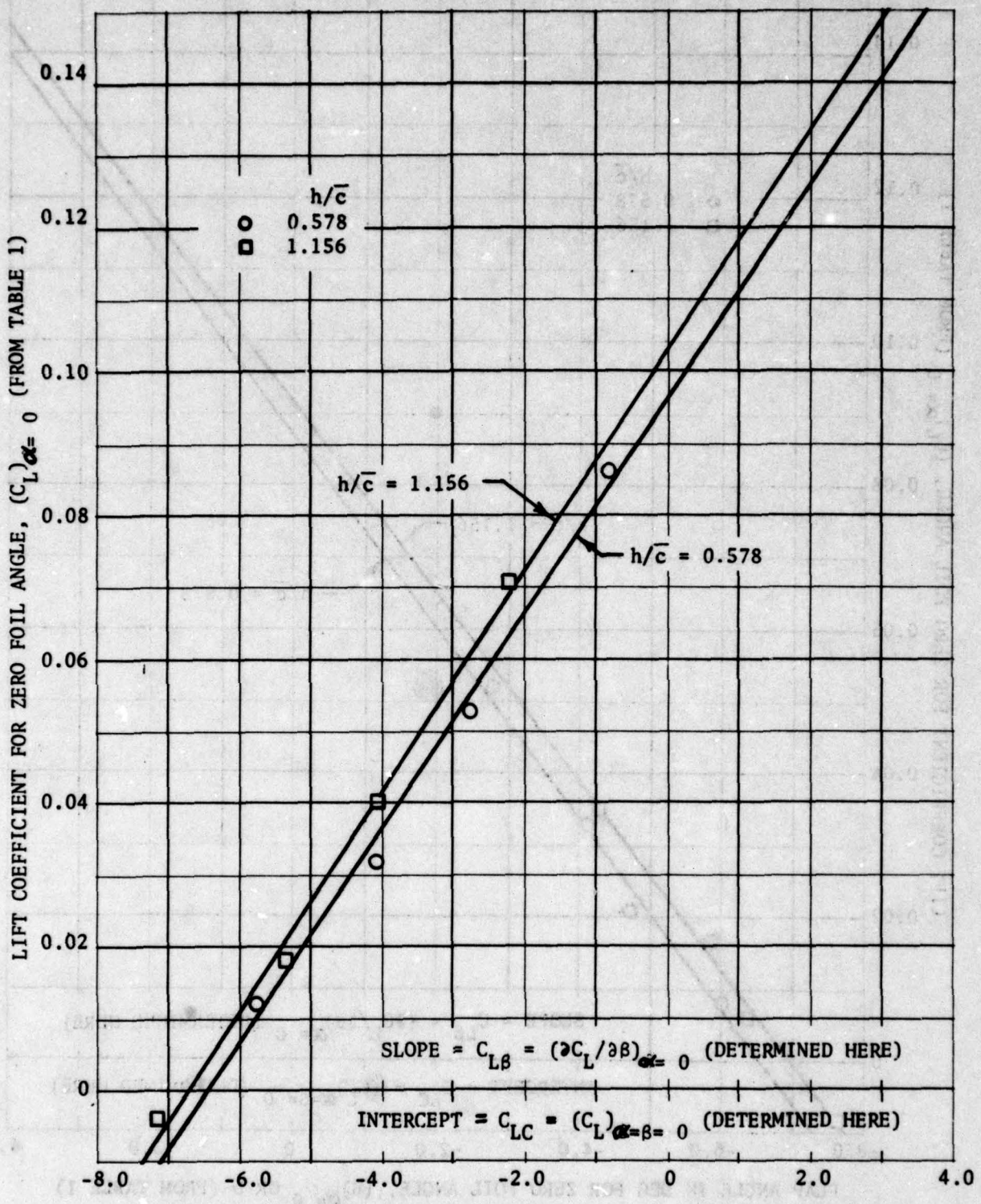

FIGURE 2b - VELOCITY = 9.00 m/s (17.5 KNOTS)

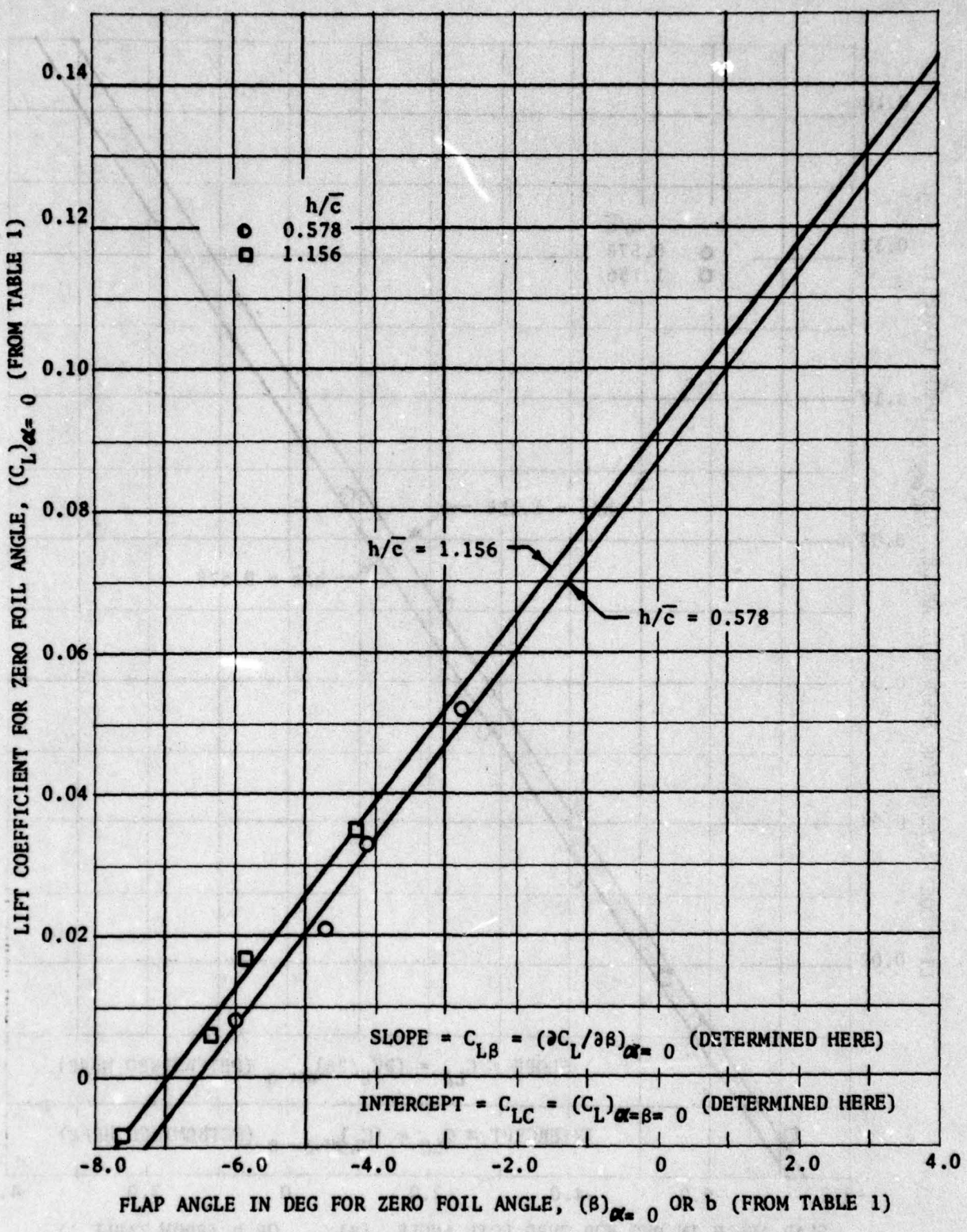

FIGURE 2c - VELOCITY = 10.55 m/s (20.5 KNOTS)

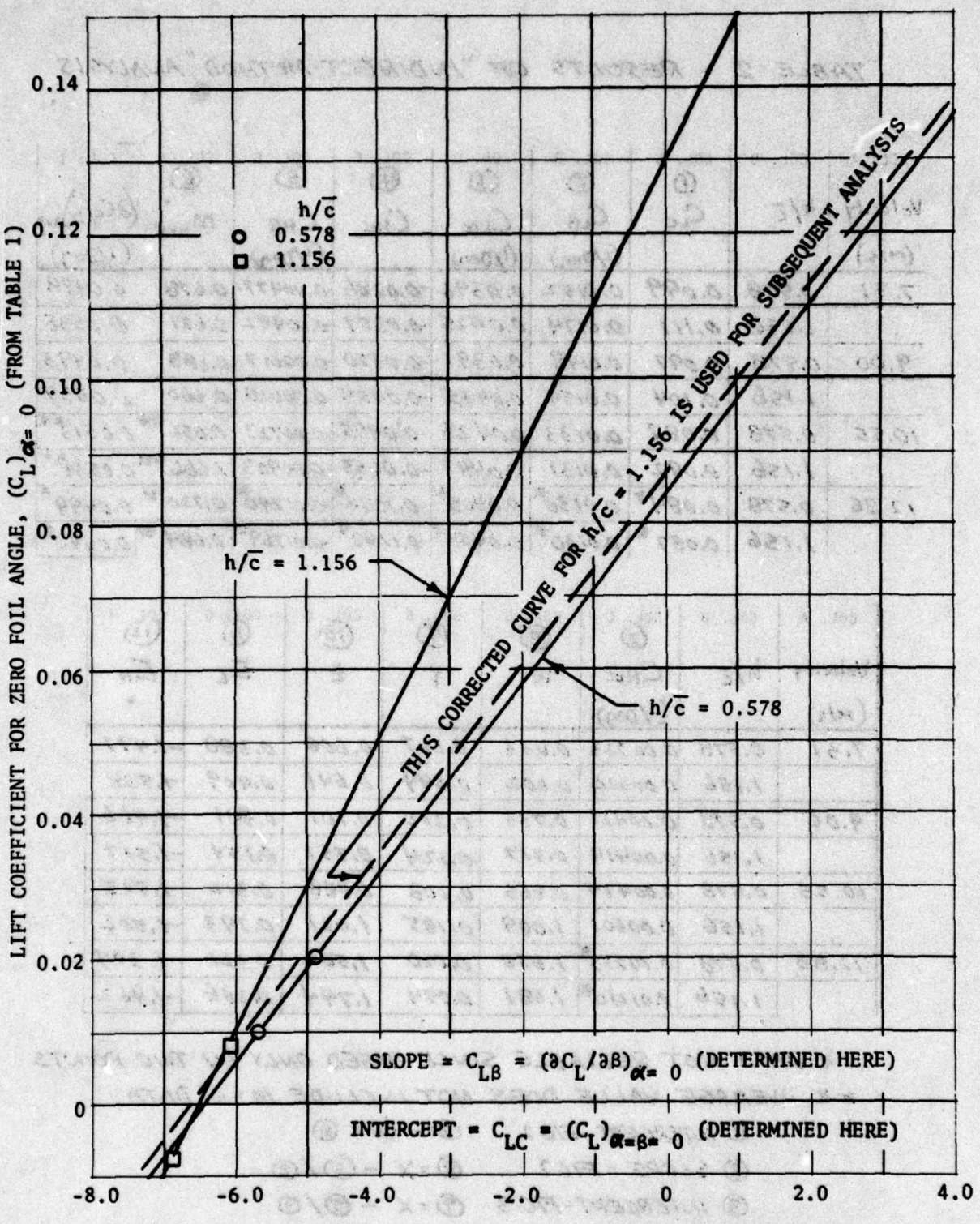

FIGURE 2d - VELOCITY = 12.86 m/s (25.0 KNOTS)

TABLE 2 - RESULTS OF "INDIRECT METHOD" ANALYSIS

COL. A	COL. B	COL. C	COL. D	COL. E	COL. F	COL. G	COL. H	COL. I
Velocity (m/s)	h/c̄	① C_{Lc}	② $C_{L\beta}$ (1/Deg)	③ $C_{L\alpha}$ (1/Deg)	④ C_{Hc}	⑤ $C_{H\beta}$ (1/Deg)	⑥ M_{ave}	$(\partial C_L/\partial \alpha)_{ave}$ (1/Deg)
7.31	0.578	0.099	0.0152	0.0392	-0.0286	-0.00477	0.678	0.0498
	1.156	0.111	0.0174	0.0425	-0.0357	-0.00492	0.651	0.0538
9.00	0.578	0.097	0.0149	0.0391	-0.0370	-0.00617	0.683	0.0493
	1.156	0.104	0.0154	0.0435	-0.0455	-0.00628	0.660	0.0537
10.55	0.578	0.087	0.0133	0.0426	-0.0495	-0.00723	0.656**	0.0513**
	1.156	0.092	0.0131	0.0447	-0.0653	-0.00903	0.666**	0.0534**
12.86	0.578	0.084*	0.0130*	0.0405*	-0.1044*	-0.01740*	0.720*	0.0499*
	1.156	0.087*	0.0130*	0.0455*	-0.1282*	-0.01769*	0.684**	0.0540*

COL. A	COL. B	COL. C	COL. D	COL. E	COL. F	COL. G	COL. H
Velocity (m/s)	h/c̄	⑦ $C_{H\alpha}$ (1/Deg)	⑧ W	⑨ Y	⑩ Z	⑪ E_L	⑫ E_H
7.31	0.578	0.00323	0.633	0.237	0.608	0.388	-1.477
	1.156	0.00320	0.602	0.244	0.641	0.409	-1.538
9.00	0.578	0.00421	0.733	0.212	0.701	0.381	-1.466
	1.156	0.00414	0.727	0.224	0.757	0.354	-1.517
10.55	0.578	0.00474	0.863	0.208	0.888	0.312	-1.525
	1.156	0.00601	1.009	0.185	1.031	0.293	-1.502
12.86	0.578	0.01253*	1.658	0.010	1.562	0.321	-1.389
	1.156	0.01240*	1.681	0.054	1.794	0.286	-1.462

* DATA NOT RELIABLE SINCE BASED ONLY ON TWO POINTS

** AVERAGE VALUE DOES NOT INCLUDE M=0 DATA

① INTERCEPT - FIG 2 ⑦ = - ⑤ × ⑥

② SLOPE - FIG 2 ⑧ = X - ⑤/②

③ INTERCEPT - FIG 3 ⑨ = X - ⑦/④

④ INTERCEPT - FIG 4 ⑩ = X - ④/①

⑤ - SLOPE - FIG 4 ⑪ = ②/③

⑥ AVE. FROM TABLE 1 ⑫ = ⑤/⑦

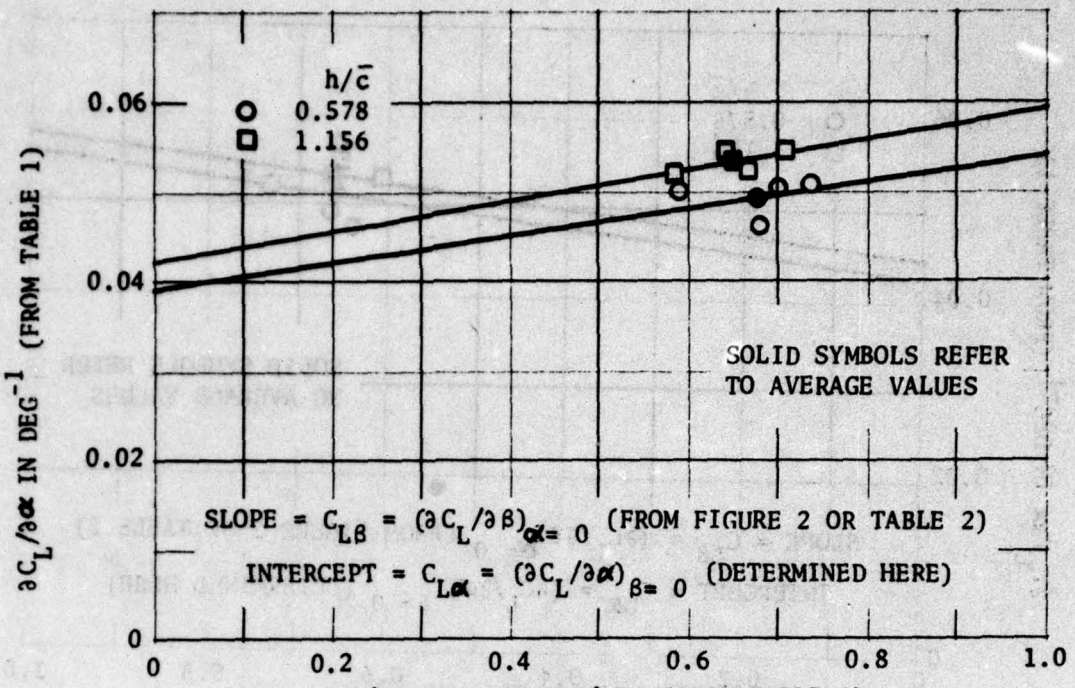

FIGURE 3a - VELOCITY = 7.31 m/s (14.2 KNOTS)

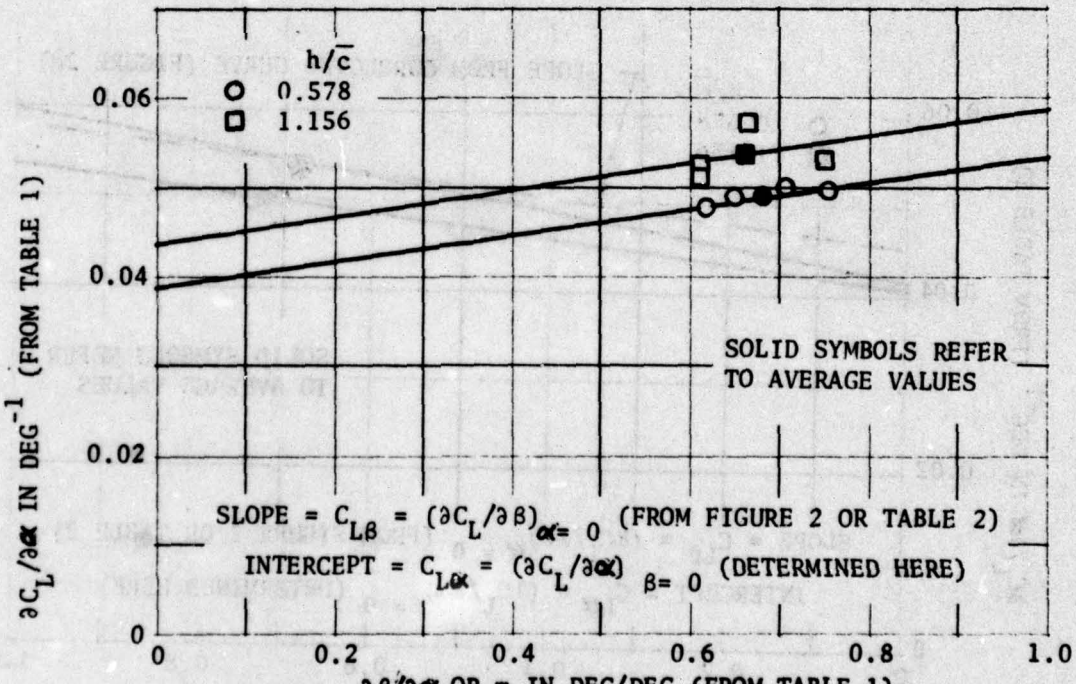

FIGURE 3b - VELOCITY = 9.00 m/s (17.5 KNOTS)

FIGURE 3 - GRAPHICAL DETERMINATION OF FOIL-LIFT-CURVE SLOPE ($C_{L\alpha}$)

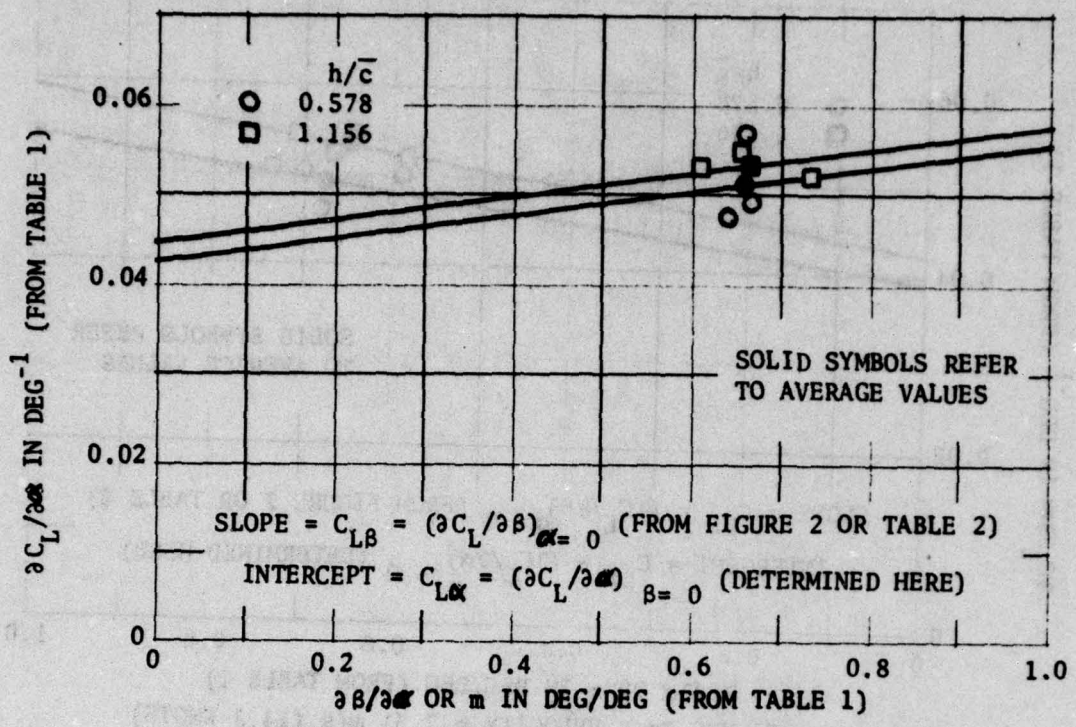

FIGURE 3c - VELOCITY = 10.55 m/s (20.5 KNOTS)

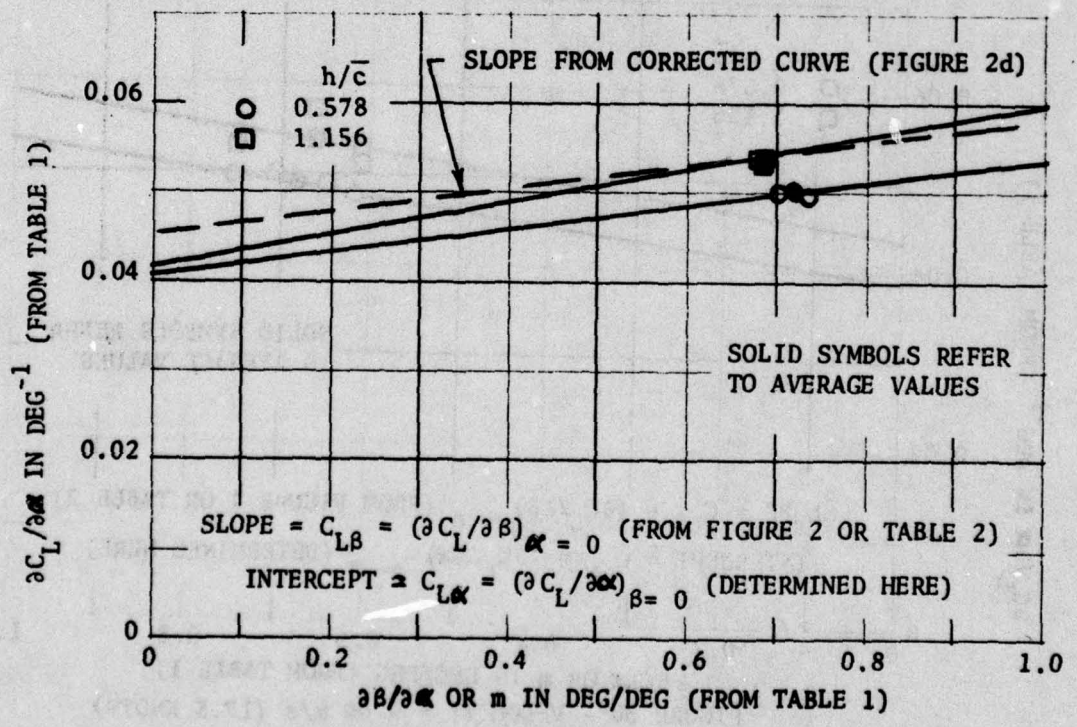

FIGURE 3d - VELOCITY = 12.86 m/s (25.0 KNOTS)

draw a straight line through the data so that an accurate value for $C_{L\beta}$ and $C_{L\alpha}$ could be obtained from the slope and intercept, respectively. However, since the appropriate slope for the straight line, $C_{L\beta}$, has already been determined from Figure 2, it was used to draw the straight line in Figure 3 so that the intercept, $C_{L\alpha}$, could be obtained. $C_{L\alpha}$ determined this way is also listed in Table 2.

MOMENT COEFFICIENTS

Since the hydrodynamic moment (C_H) and the bias moment (C_M) together are zero for a free foil,

$$C_H = -C_M$$

From Equation [2],

$$-C_M = C_{H\alpha}\alpha + C_{HC} + C_{H\beta}\beta$$

or

$$\beta = -[(C_M + C_{HC})/C_{H\beta}] - [C_{H\alpha}/C_{H\beta}]\alpha$$

From Equation [3] we have

$$\beta = m\alpha + b$$

so,

$$m = -(C_{H\alpha}/C_{H\beta})$$

$$b = -(C_M + C_{HC})/C_{H\beta}$$

or,

$$C_M = (-C_{HC}) + (-C_{H\beta})\, b$$

$$C_{H\alpha} = -m\, C_{H\beta}$$

By plotting C_M from Table 1 versus b from Table 1 in Figure 4, $-C_{H\beta}$ and $-C_{HC}$ were determined as the slope and intercept, respectively. Then using m averaged over the bias moments from Table 1 and $C_{H\beta}$ as determined

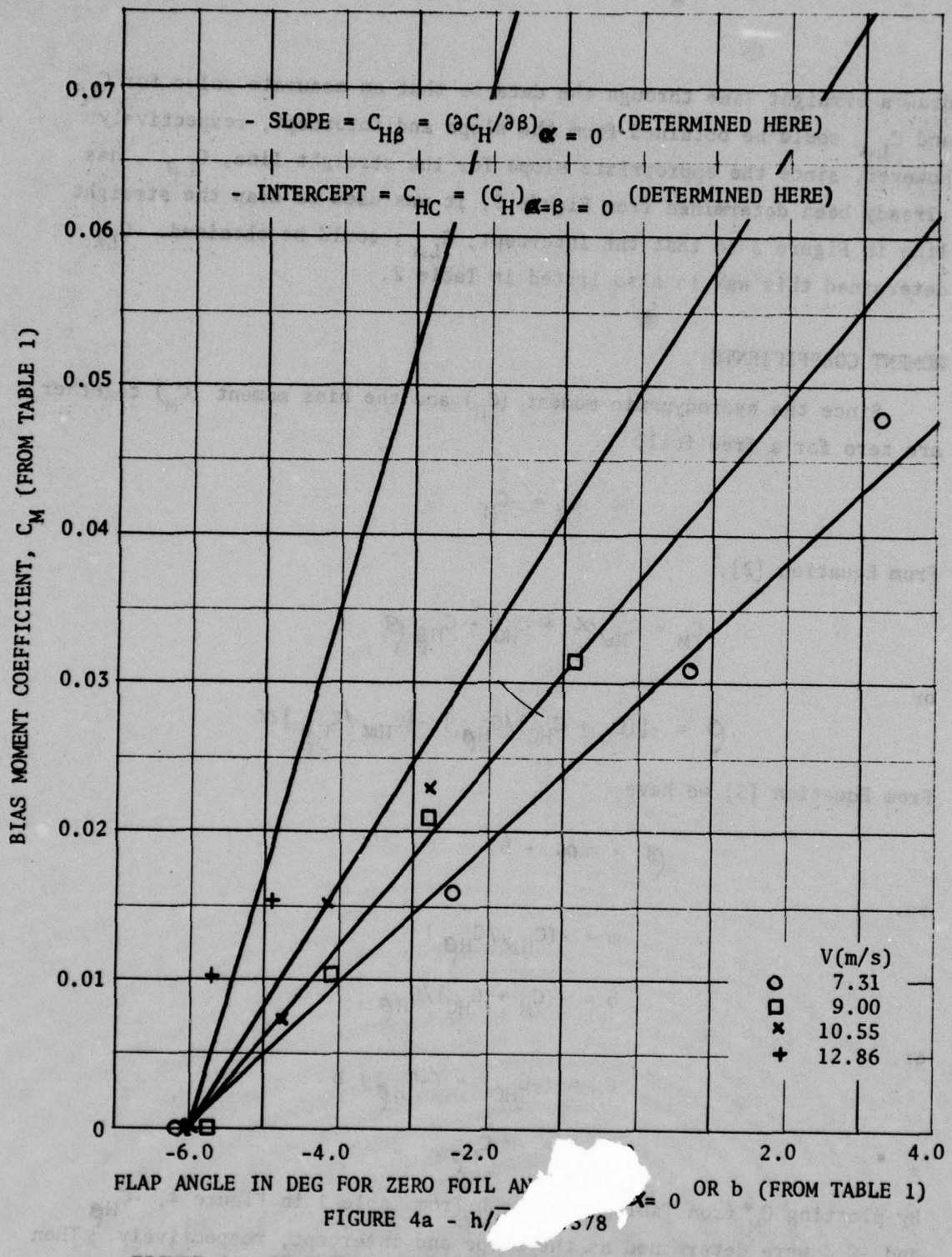

FIGURE 4a - h/

FIGURE 4 - GRAPHICAL DETERMINATION OF MOMENT AT ZERO FLAP AND FOIL ANGLES (C_{HC}) AND FLAP-MOMENT-CURVE SLOPE ($C_{H\beta}$)

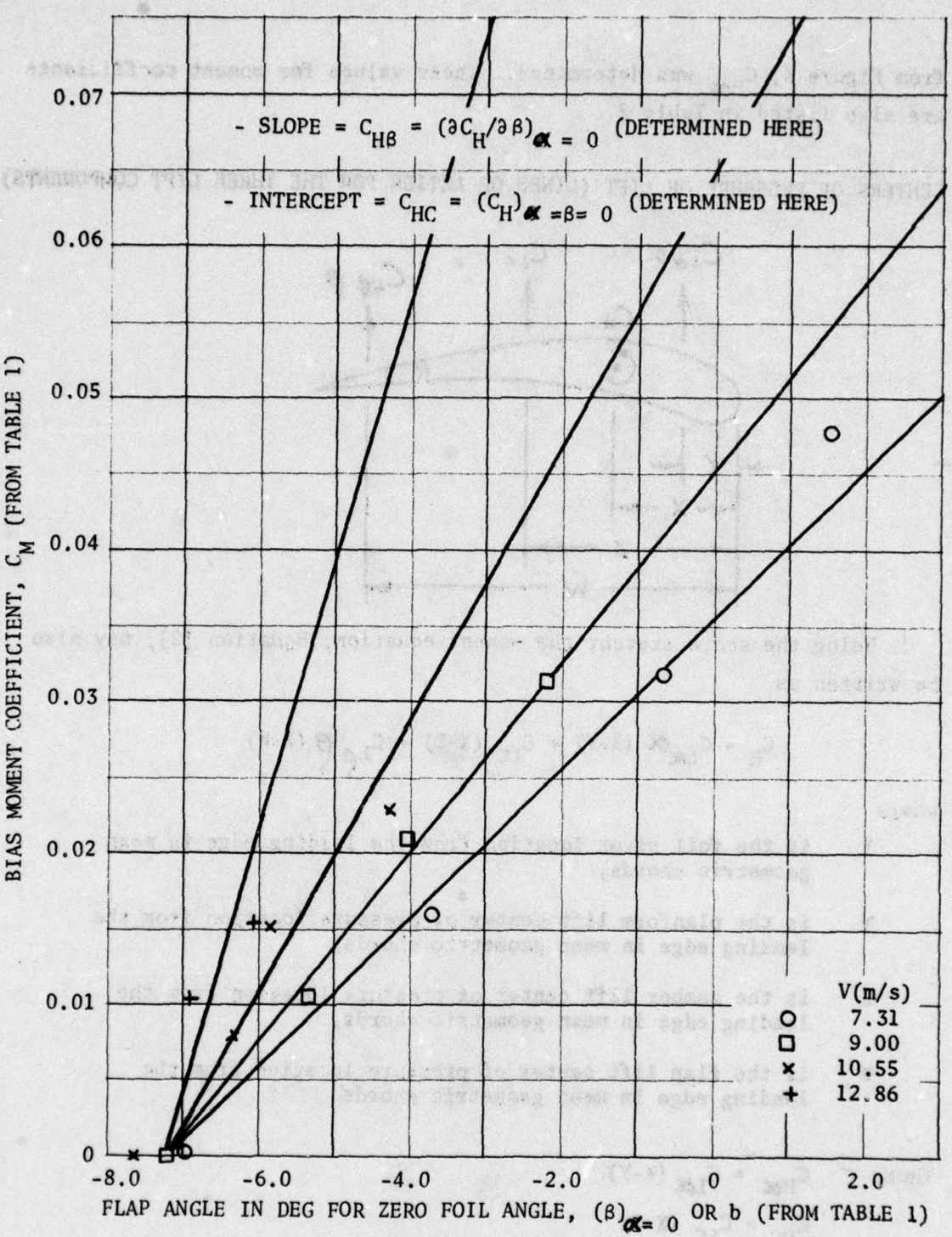

FIGURE 4b - $h/\bar{c} = 1.156$

from Figure 4, $C_{H\alpha}$ was determined. These values for moment coefficients are also listed in Table 2.

CENTERS OF PRESSURE OF LIFT (LINES OF ACTION FOR THE THREE LIFT COMPONENTS)

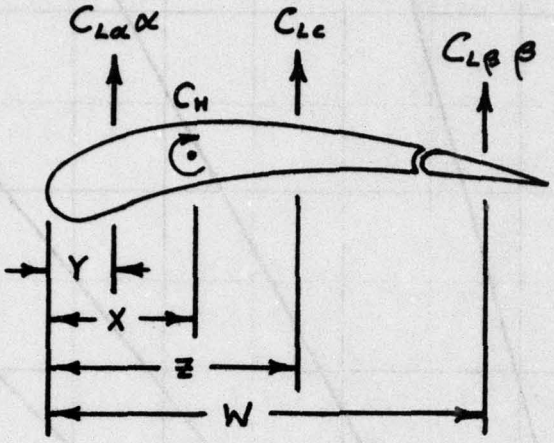

Using the above sketch, the moment equation, Equation [2], may also be written as

$$C_H = C_{L\alpha}\alpha\ (X-Y) + C_{LC}\ (X-Z) + C_{L\beta}\beta\ (X-W)$$

where

X is the foil pivot location from the leading edge in mean geometric chords,

Y is the planform lift center of pressure location from the leading edge in mean geometric chords,

Z is the camber lift center of pressure location from the leading edge in mean geometric chords,

W is the flap lift center of pressure location from the leading edge in mean geometric chords

Thus, $C_{H\alpha} = C_{L\alpha}\ (X-Y)$

$C_{HC} = C_{LC}\ (X-Z)$

$C_{H\beta} = C_{L\beta}\ (X-W)$

or,

$$Y = X - C_{H\alpha}/C_{L\alpha}$$

$$Z = X - C_{HC}/C_{LC}$$

$$W = X - C_{H\beta}/C_{L\beta}$$

Thus, the location of these centers of pressure of lift (or lines of action for the three lift components) were calculated from the hydrodynamic coefficients and are listed in Table 2.

FLAP EFFECTIVENESS

The flap lift and moment effectiveness, respectively are defined as

$$E_L = C_{L\beta}/C_{L\alpha}$$

$$E_H = C_{H\beta}/C_{H\alpha}$$

These were also calculated from the coefficients and are listed in Table 2.

RESULTS

When viewing the results of the analysis presented in Figures 5 through 8, it should be noted that the analyzed results for 12.86 m/s are not reliable since data for only two bias moments (instead of four) were obtained and analyzed. For this reason, the hand-faired curves through the analyzed results in the figures are dashed when extending the results from 10.55 m/s to 12.86 m/s. For most cases, these results for 12.86 m/s, do however, follow the general trends established from the lower velocities.

As shown in Figure 5, over the range of model depths and velocities, the flap lift-curve slope ($C_{L\beta}$) increases slightly with increasing depth and decreases slightly with increasing velocity. The foil lift-curve slope ($C_{L\alpha}$) increases with increasing depth and increasing velocity.

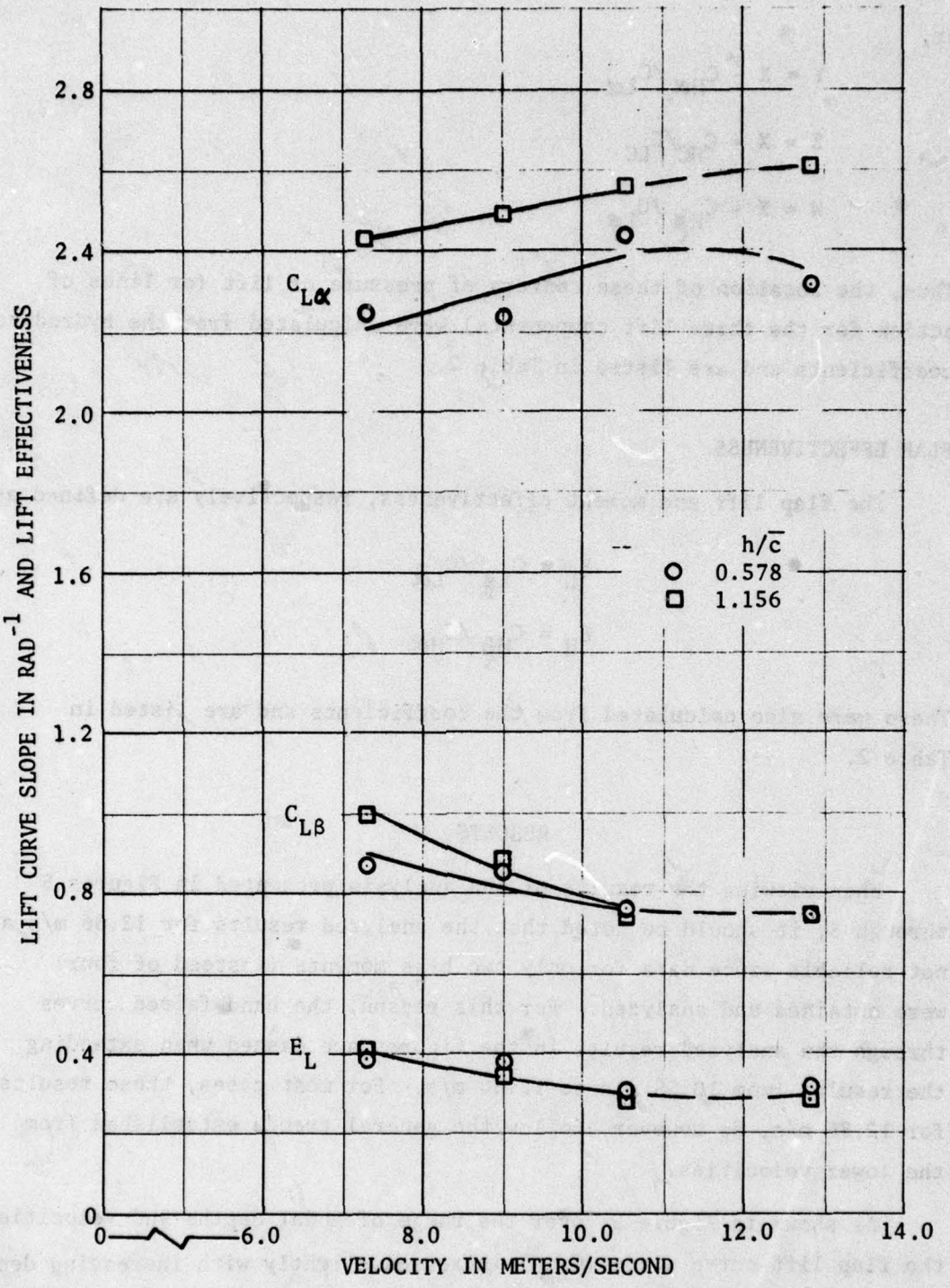

FIGURE 5 - LIFT CURVE SLOPES AND FLAP LIFT EFFECTIVENESS VERSUS VELOCITY

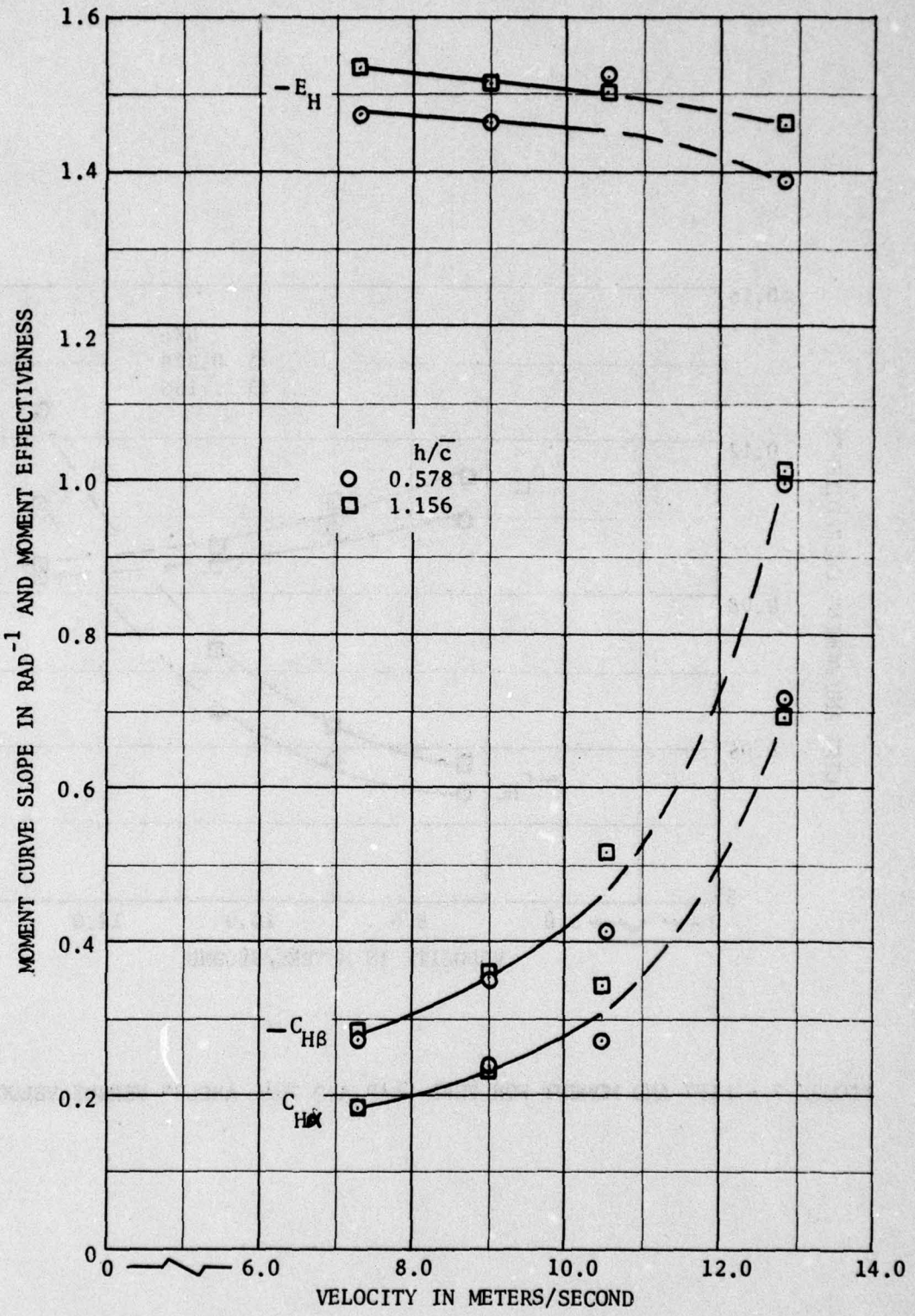

FIGURE 6 - MOMENT CURVE SLOPES AND FLAP MOMENT EFFECTIVENESS VERSUS VELOCITY

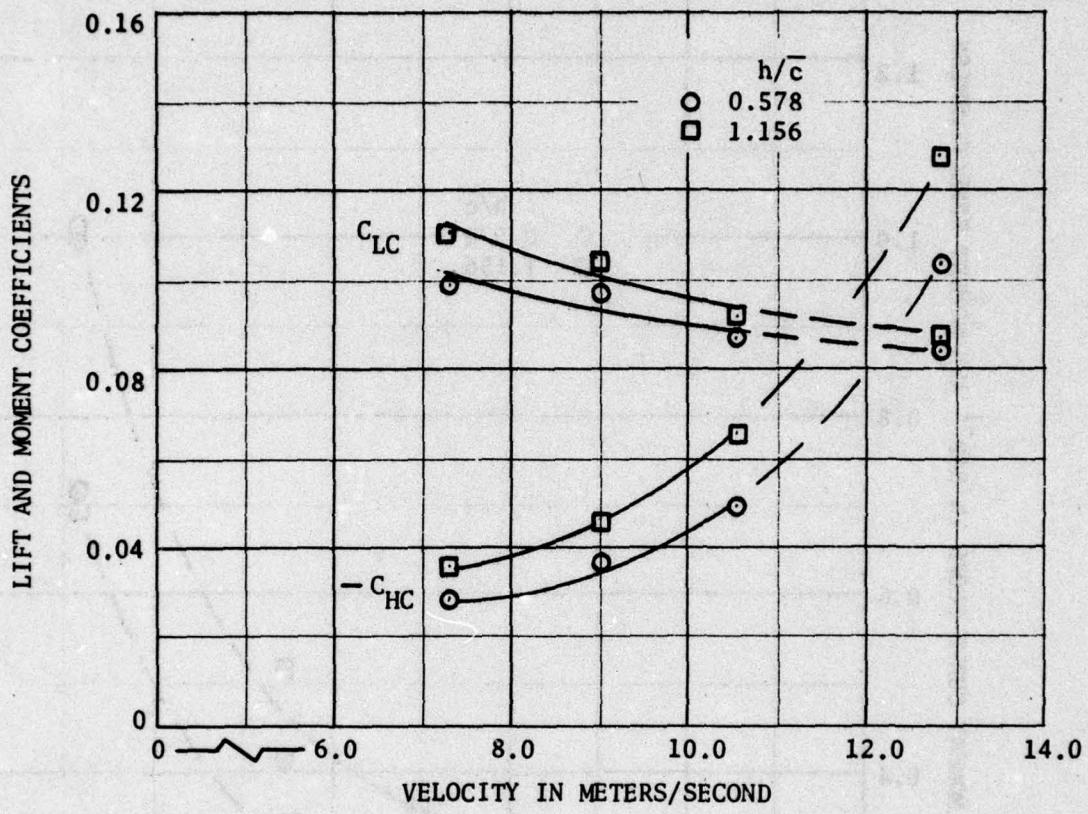

FIGURE 7 - LIFT AND MOMENT FOR ZERO FLAP AND FOIL ANGLES VERSUS VELOCITY

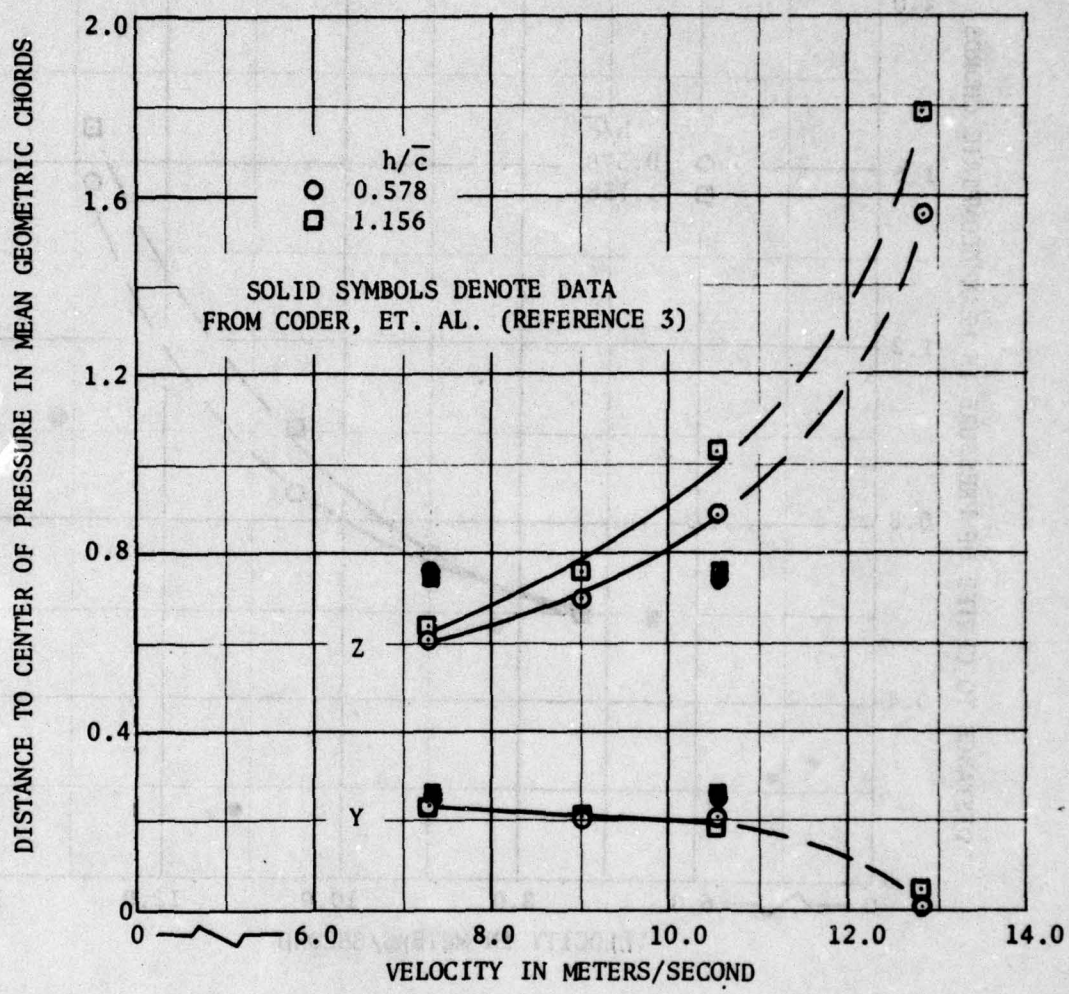

FIGURE 8a - DUE TO PLANFORM (Y) AND CAMBER (Z)

FIGURE 8 - CENTER OF PRESSURE OF LIFT DUE TO PLANFORM (Y), CAMBER (Z), AND FLAP (W)

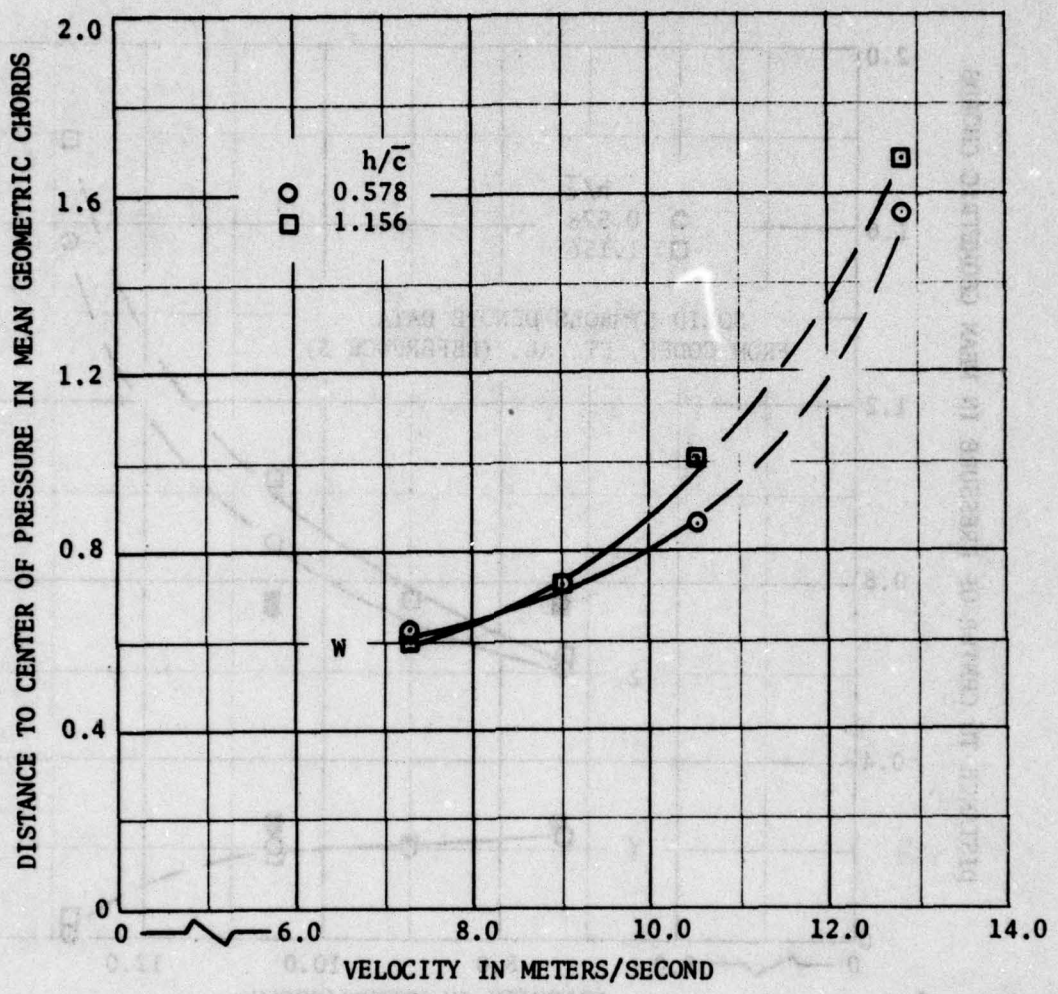

FIGURE 8b - DUE TO FLAP (W)

The resulting flap lift effectiveness ($E_L = C_{L\beta}/C_{L\alpha}$) shows no depth dependence but a slight decrease with increasing velocity.

In Figure 6, depth has a very small effect on the flap moment-curve slope ($C_{H\beta}$) and the foil moment-curve slope ($C_{H\alpha}$). Both $-C_{H\beta}$ and $C_{H\alpha}$ increase significantly with increasing velocity. When the flap moment effectiveness ($E_H = C_{H\beta}/C_{H\alpha}$) is calculated, the effect of depth is more easily discernible -- its magnitude is larger for larger depths. The magnitude of E_H decreases slightly with increasing velocity.

The lift and moment coefficients for zero flap and foil angles are shown in Figure 7. The magnitudes of the coefficients are larger for the larger depth. The lift coefficient for zero flap and foil angles (C_{LC}) decreases somewhat and the negative of the moment coefficient for zero flap and foil angle ($-C_{HC}$) increases significantly with increasing velocity. This large increase in the magnitude of this moment coefficient is due to the aft movement of the center of pressure of lift due to camber ($Z = X - C_{HC}/C_{LC}$) as shown in Figure 8. This center of pressure is slightly more aft for the larger depth.

The center of pressure of lift due to planform ($Y = X - C_{H\alpha}/C_{L\alpha}$) moves slightly forward with velocity up to 10.55 m/s and approaches the leading edge (near zero) for 12.86 m/s. The center of pressure of lift due to flap ($W = X - C_{H\beta}/C_{L\beta}$) is slightly more aft at the larger depth and moves aft with increasing velocity. Thus, it is seen that the two centers of pressure Z and W shift with velocity such as to cause a larger negative moment (pitching leading edge downward) with increasing velocity and Y shifts slightly more forward to cause a larger positive moment.

DISCUSSION

The foregoing analysis and results show that it is possible to obtain the six hydrodynamic lift and moment coefficients from a foil that is freely pivoting, has a controllable flap with suitable feedback control system, and has provision for externally applied bias moments.

The coefficients such obtained are not as accurate as those that might be obtained by direct measurement. For example, the flap lift curve slope could be obtained more accurately by fixing the foil at a set angle (say zero) and measuring the lift while varying the flap angle. The present method does, however, provide a simple determination of the coefficients from a relatively small body of data. When using this method, it would be best to ensure that for every condition (velocity and depth) data were obtained for at least three bias moments and preferably four.

The most significant result of the analyzed results is the drastic shift in centers of pressure due to velocity (shown in Figure 8). For a similar foil (but without a flap) at the lower velocities (7.31 and 10.55 m/s), it was determined by Coder, et al[3] that Y (Planform Center) was near the quarter chord and Z (Camber Center) was at about the three-quarter chord with no apparent effect of velocity. These results are shown on Figure 8a for a comparison with the present data. The present data shows a greater dependence on velocity. It is thought that the effect of velocity on the centers of pressure of the data analyzed here might well be due to small amounts of water and/or air leaking out of the pod into the flow. The experiment described in Reference 4 had one push-rod passing vertically through the strut which was a possible path for atmospheric air leakage to the pod and foil. An attempt was made to seal the strut to prevent this source of leakage. Whenever this was done, it was found that the resulting hydrodynamic coefficients became constant for the two velocities. In the present experiment, discussed in Reference 2, it was more difficult to seal the strut because two linkages passed vertically through the strut and it was imperative that the sealing technique not increase friction in the linkages. Little, if any, air was observed during testing. However, it is apparent now that there might have been enough leakage to influence the results.

The large shifts in centers of pressure at the higher velocities (10.55 and 12.86 m/s) may be partly due to the license used in drawing the straight line fits through the data during the analysis procedure. For example, the straight lines drawn on Figure 4 were drawn through the

average of $(\rho)_{\alpha = 0}$ for $C_M = 0$ of the three lower velocities. It is seen that the resulting lines drawn for the larger velocities of 10.55 and 12.86 m/s are steeper and have larger intercepts than those that might be drawn through the actual data points for the particular velocity alone. This would result in a larger $-C_{H\beta}$, $-C_{HC}$ and $C_{H\alpha}$ (since this is determined as $-m\ C_{H\rho}$) than what ordinarily might be determined. Thus, Y, Z, W, and E_H are affected by this interpretation -- Y might be too small, and Z, W, and $-E_H$ too large. This would tend to make the results show a weaker dependence on velocity.

A detailed error analysis is performed in Appendix B. Estimated maximum errors in the fundamental experimental measurements were determined and followed through the analysis step by step. Error bands for the hydrodynamic coefficients, centers of pressure, and effectiveness were thus obtained. This error analysis shows that there could be considerable errors apparently resulting mainly from the inaccuracy of the flap angle measurement. Improvement in this measurement and perhaps foil angle and bias moment could improve the results considerably.

CONCLUSIONS

1. The technique developed in this report permits determination of the hydrodynamic loading coefficients characteristics on a freely pivoting foil with controllable flap, a suitable control system, and external applied bias moments. Measurement of lift, foil angle, and flap angle must be made and the bias moment known.

2. To use this technique effectively, data for several values of bias moment are required. At least three values, and preferably four, for each velocity and depth should be used.

3. A critical step in the analysis is drawing the straight line fits. Varying the approach can alter the results.

4. Error bands for the hydrodynamic coefficient, centers of pressure, and effectivenesses could be considerably improved by an improvement in the flap angle measurement. Lesser amounts of improvement could be obtained by improving the foil angle and bias moment measurements.

5. The data of Reference 2 is not a good representation of the full-scale AGEH system. The present analysis suggests that there was air/water leaking down the strut and out of the pod into the flow.

RECOMMENDATIONS

1. In future experiments employing the present technique, data for four values of bias moment should be obtained for each velocity and depth.

2. In future experiments to determine hydrodynamic coefficients, etc., by the "indirect method", the flap angle measurement should definitely be improved. Also further improvement of the results could be obtained by improving the foil angle and bias moment measurements.

3. The experiment should be extended into the region of cavitating condition to see what effect cavitation has on the hydrodynamic characteristics and the "indirect method" analysis technique.

ACKNOWLEDGEMENTS

The authors of this report wish to acknowledge that the data they analyzed here came from experimental work in which Mr. Lester B. Moore, Mr. Michael F. Jeffers, and Mr. Bejamin B. Wisler were instrumental.

APPENDIX A

LIFT COEFFICIENT VERSUS FOIL ANGLE FROM THE 1975 FLAP INCIDENCE CONTROL EXPERIMENT

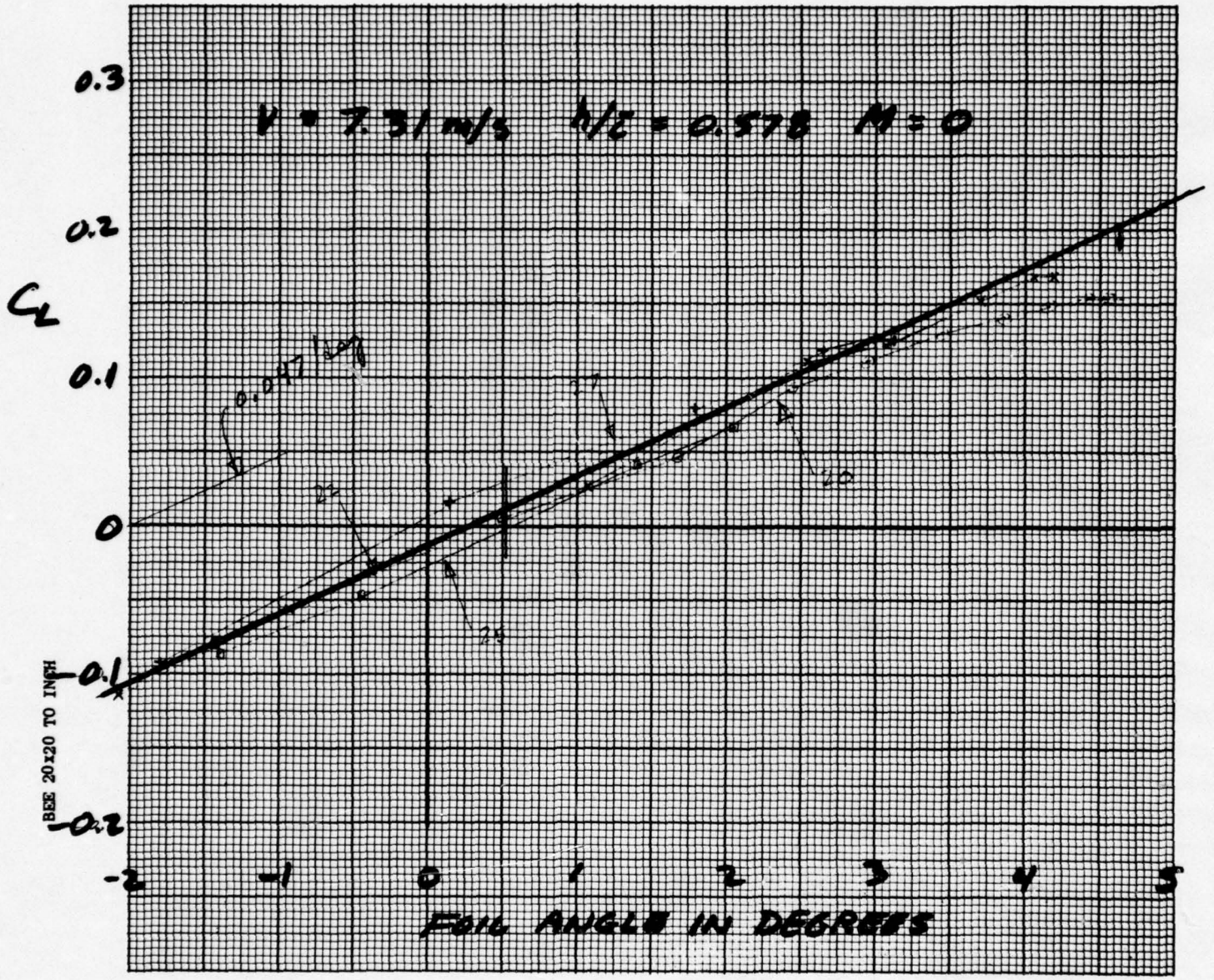
V = 7.31 m/s h/c = 0.578 N = 0
0.3
0.2
C_L
0.1
0
-0.1
-0.2
-2
-1
0
1
2
3
4
5
FOIL ANGLE IN DEGREES
0.047
BEE 20120 TO INCH

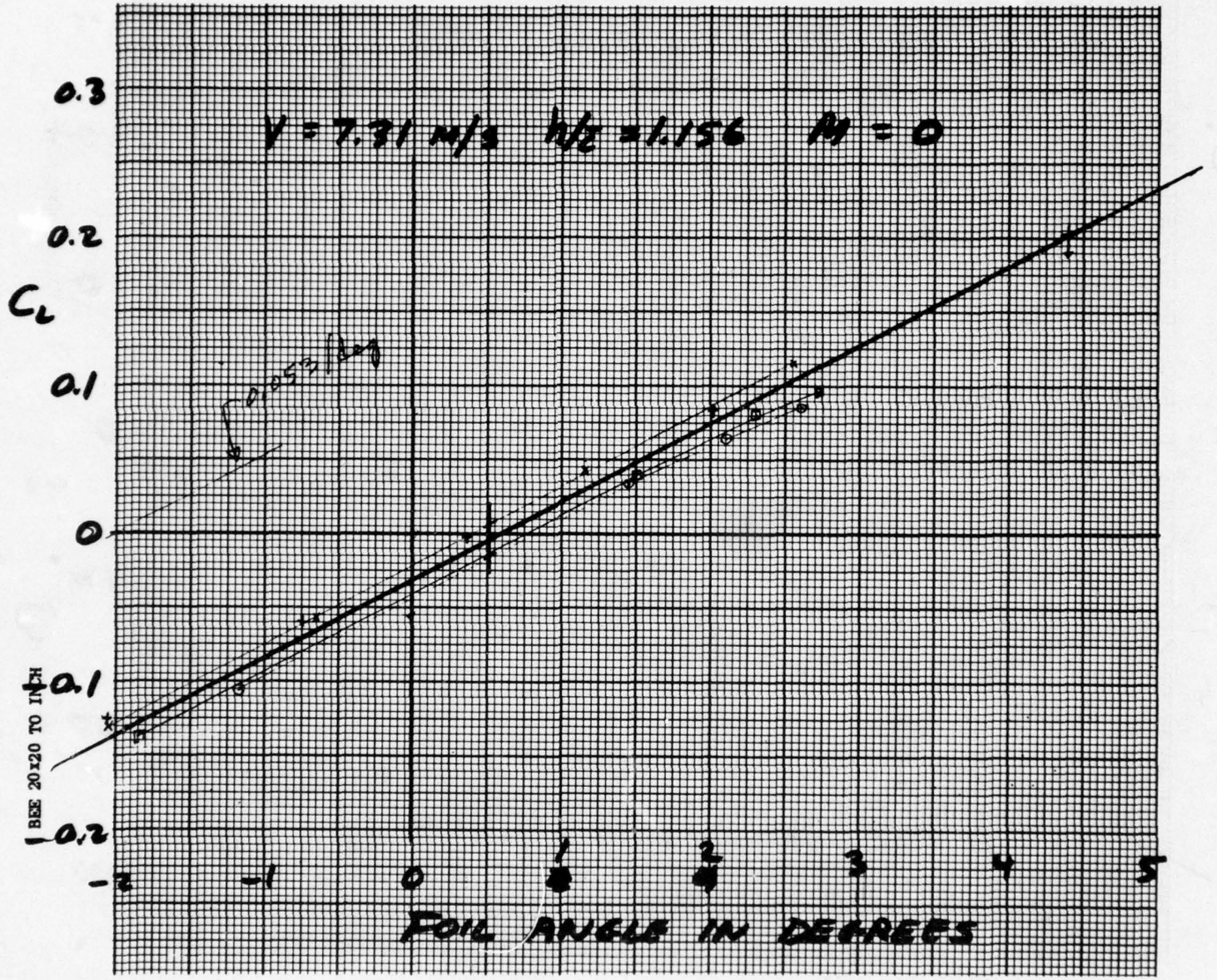
V = 7.31 m/s h/c = 1.156 M = 0
0.3
0.2
C_L
0.1
0
-0.1
-0.2
-2
-1
0
1
2
3
4
5
FOIL ANGLE IN DEGREES
0.05
BEE 20x20 TO INCH

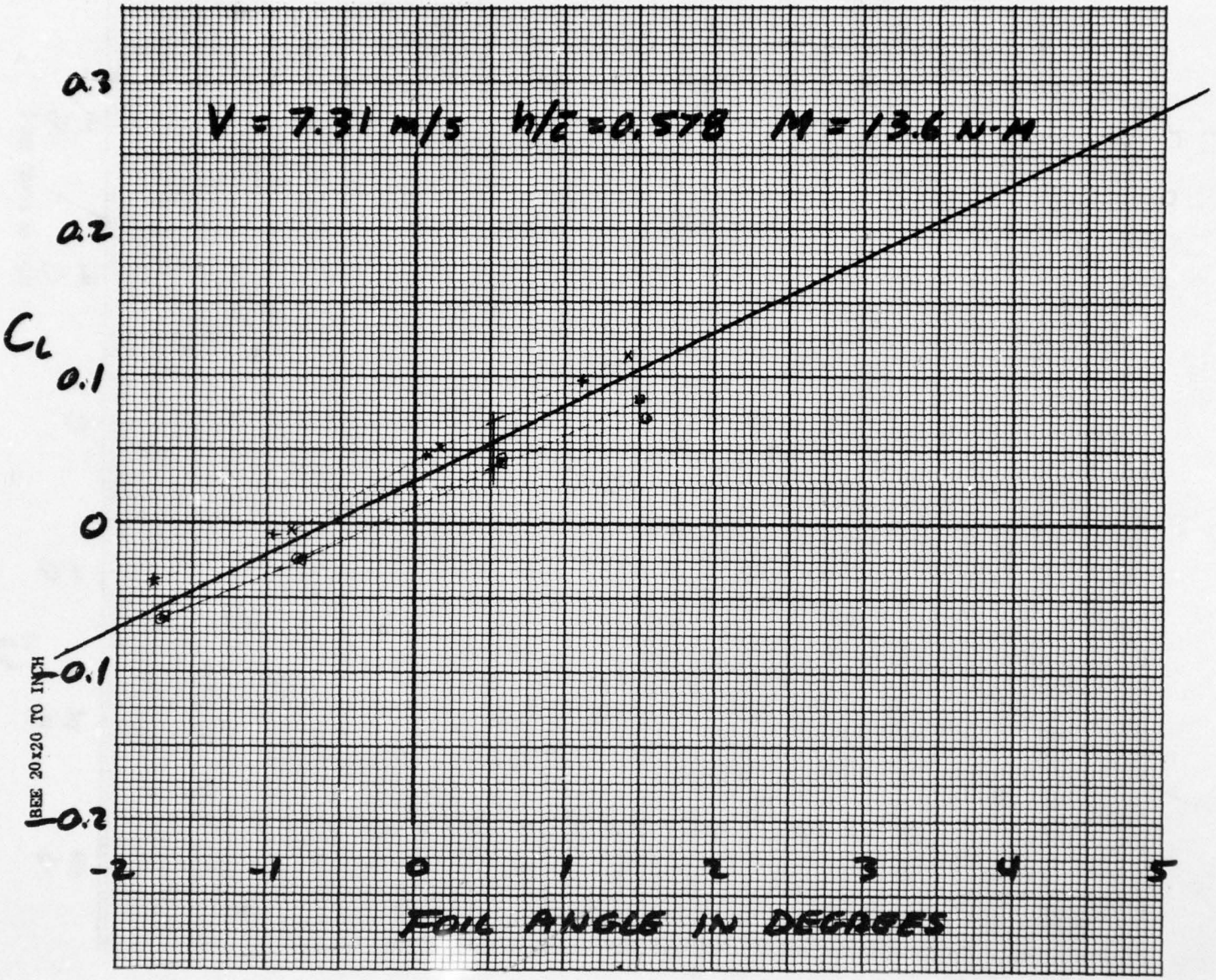
V = 7.31 m/s h/c = 0.578 M = 13.6 N-M
0.3
0.2
C_L
0.1
0
-0.1
-0.2
-2
-1
0
1
2
3
4
5
FOIL ANGLE IN DEGREES
KEE 20x20 TO INCH

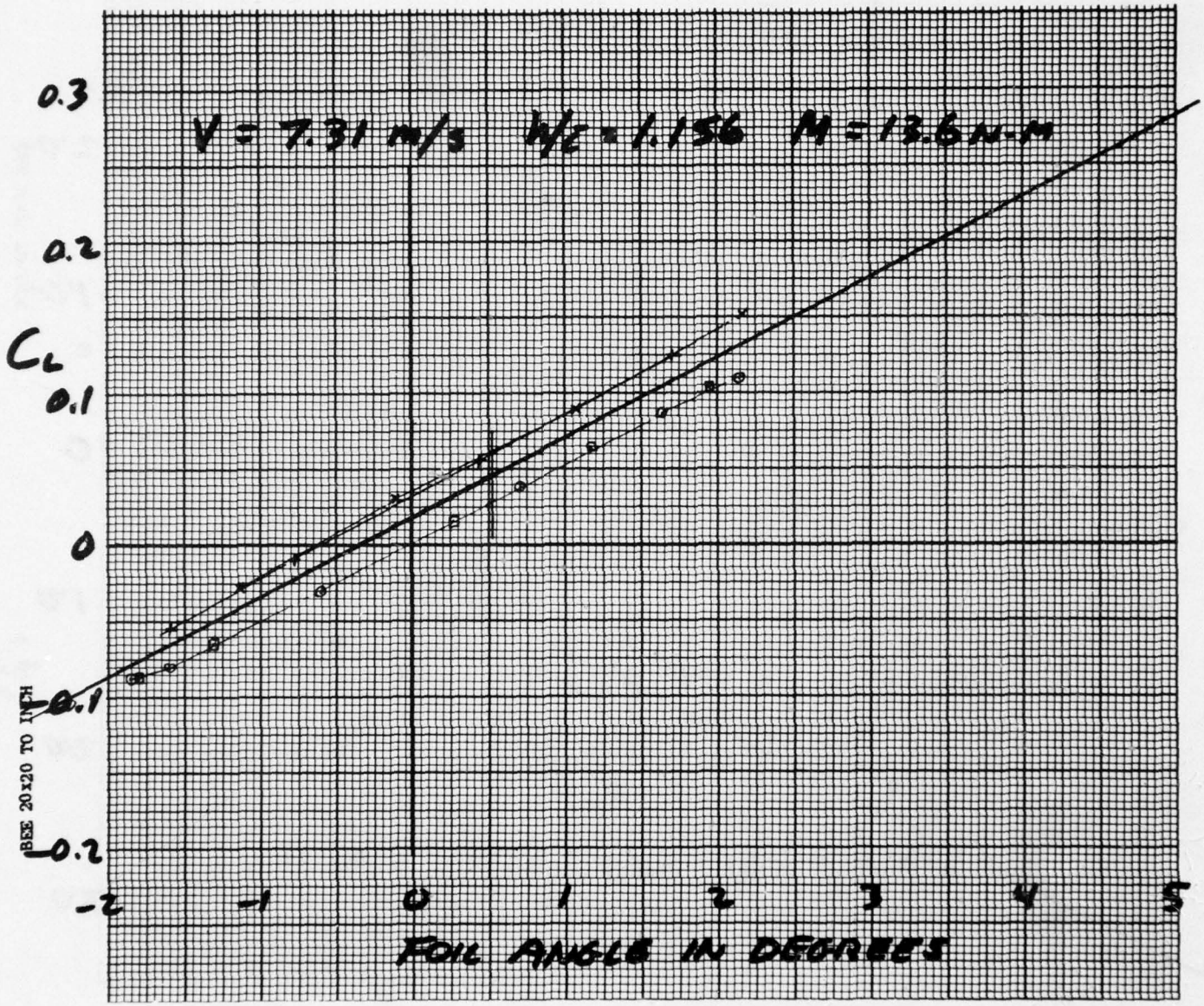
V = 7.31 m/s W/L = 1.156 M = 13.6 N-m
0.3
0.2
C_L
0.1
0
-0.1
-0.2
-2
-1
0
1
2
3
4
5
FOIL ANGLE IN DEGREES
KEUFFEL & ESSER CO. MADE IN U.S.A.
46 8520 TO INCH

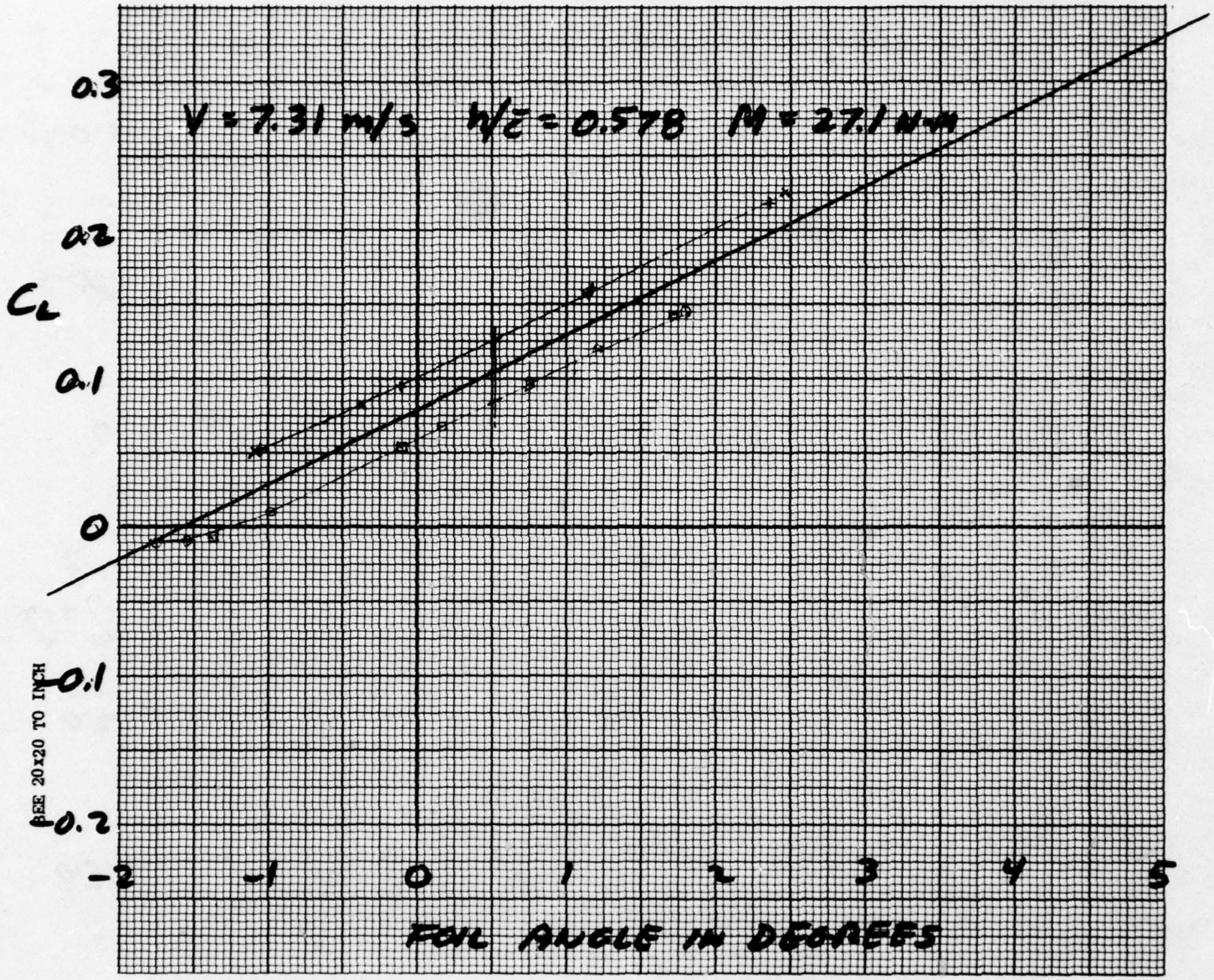
V = 7.31 m/s h/c = 0.578 M = 27.1 N-m
0.3
0.2
C_L
0.1
0
-0.1
-0.2
-2
-1
0
1
2
3
4
5
FOIL ANGLE IN DEGREES
KEUFFEL & ESSER CO. 20x20 TO INCH

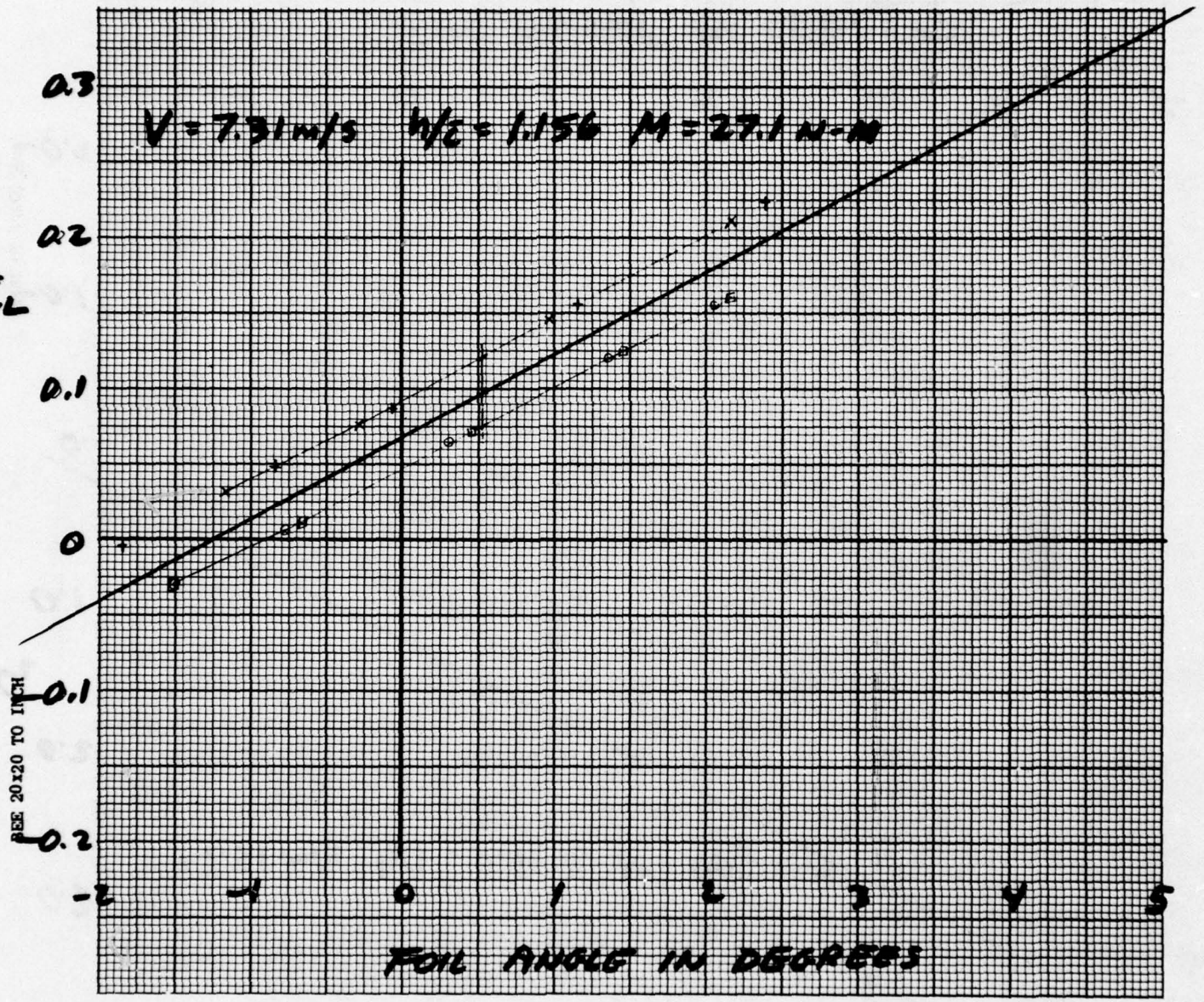
V = 7.31 m/s h/c = 1.156 M = 27.1 N-M
0.3
0.2
C_L
0.1
0
-0.1
-0.2
SEE 20x20 TO INCH
-2
-1
0
1
2
3
4
5
FOIL ANGLE IN DEGREES

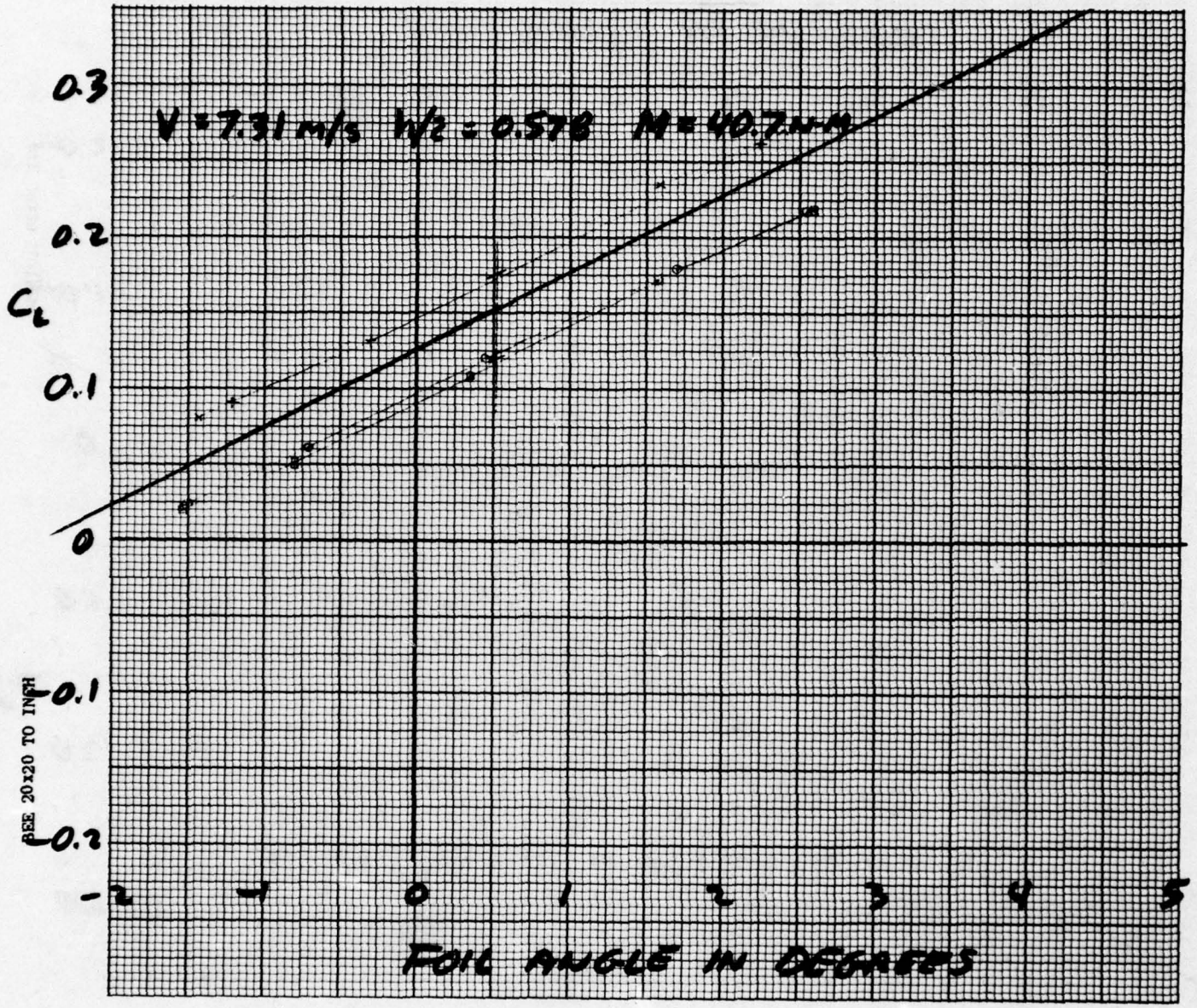
V = 7.31 m/s W/2 = 0.578 M = 40.7 N-m
0.3
0.2
C_L
0.1
0
-0.1
-0.2
-2
-1
0
1
2
3
4
5
FOIL ANGLE IN DEGREES
SEE 20x20 TO INCH

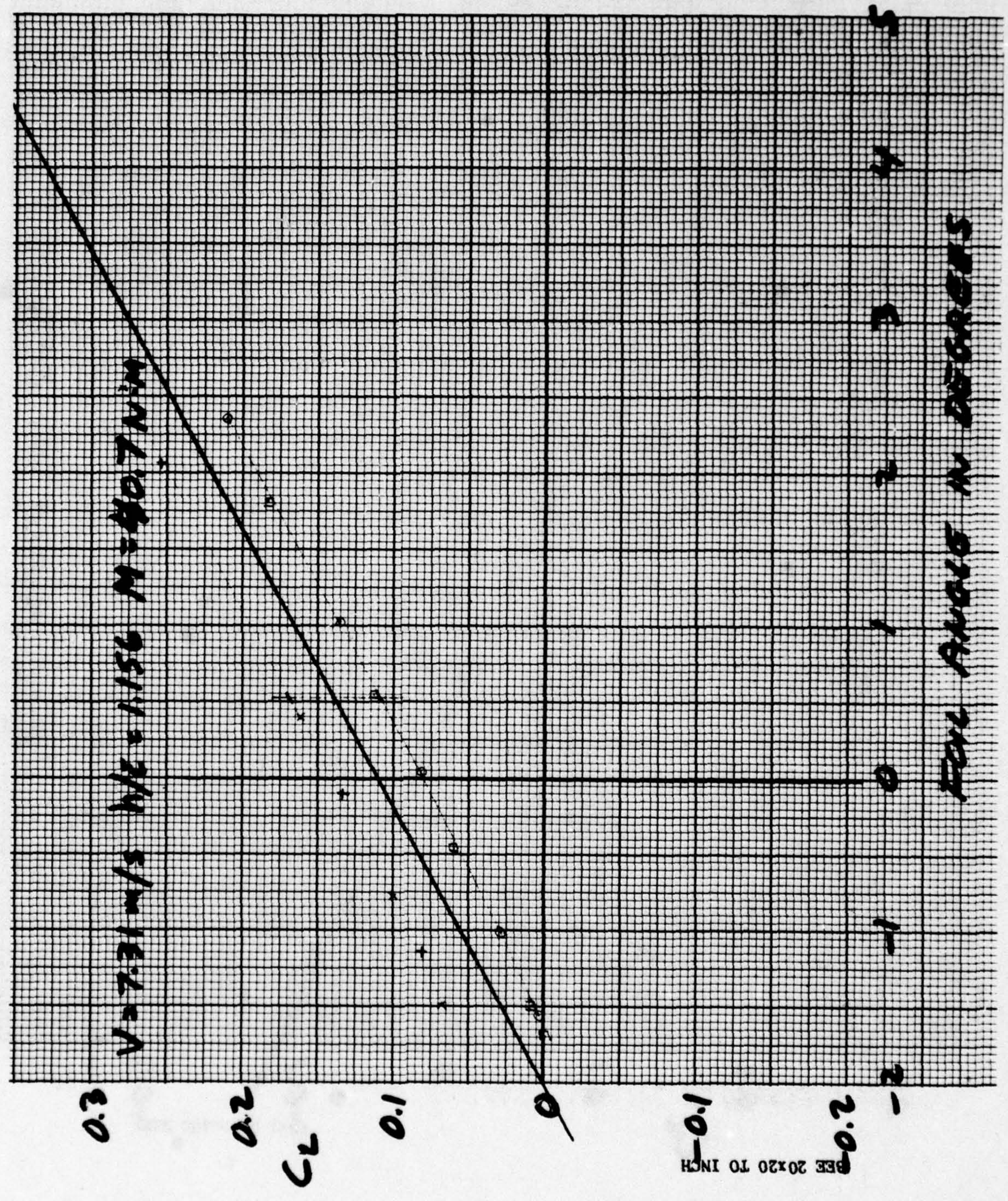
V=7.31 m/s h/c=1.156 M=40.7 N·m
C_L
FOIL ANGLE IN DEGREES
0.3
0.2
0.1
0
-0.1
-0.2
-2
-1
0
1
2
3
4
5
SEE 20x20 TO INCH

V = 9.00 m/s M/L = 0.579 M = 0
C_L
0.3
0.2
0.1
0
-0.1
-0.2
-2
-1
0
1
2
3
4
5
Pitch Angle in Degrees
SEE 20x20 TO INCH

V = 9.00 m/s M = 0.026
0.3
0.2
0.1
0
-0.1
-0.2
C_L
-2
0
2
4
6
Alpha, angle in degrees
SEE 20x20 TO INCH

V = 9.00 m/s M/2 = 0.529 M = 13.6 mm
0.3
0.2
0.1
0
-0.1
-0.2
C_L
-2
-1
0
1
2
3
Pot. Aug. in degrees
BEE 20x20 TO INCH

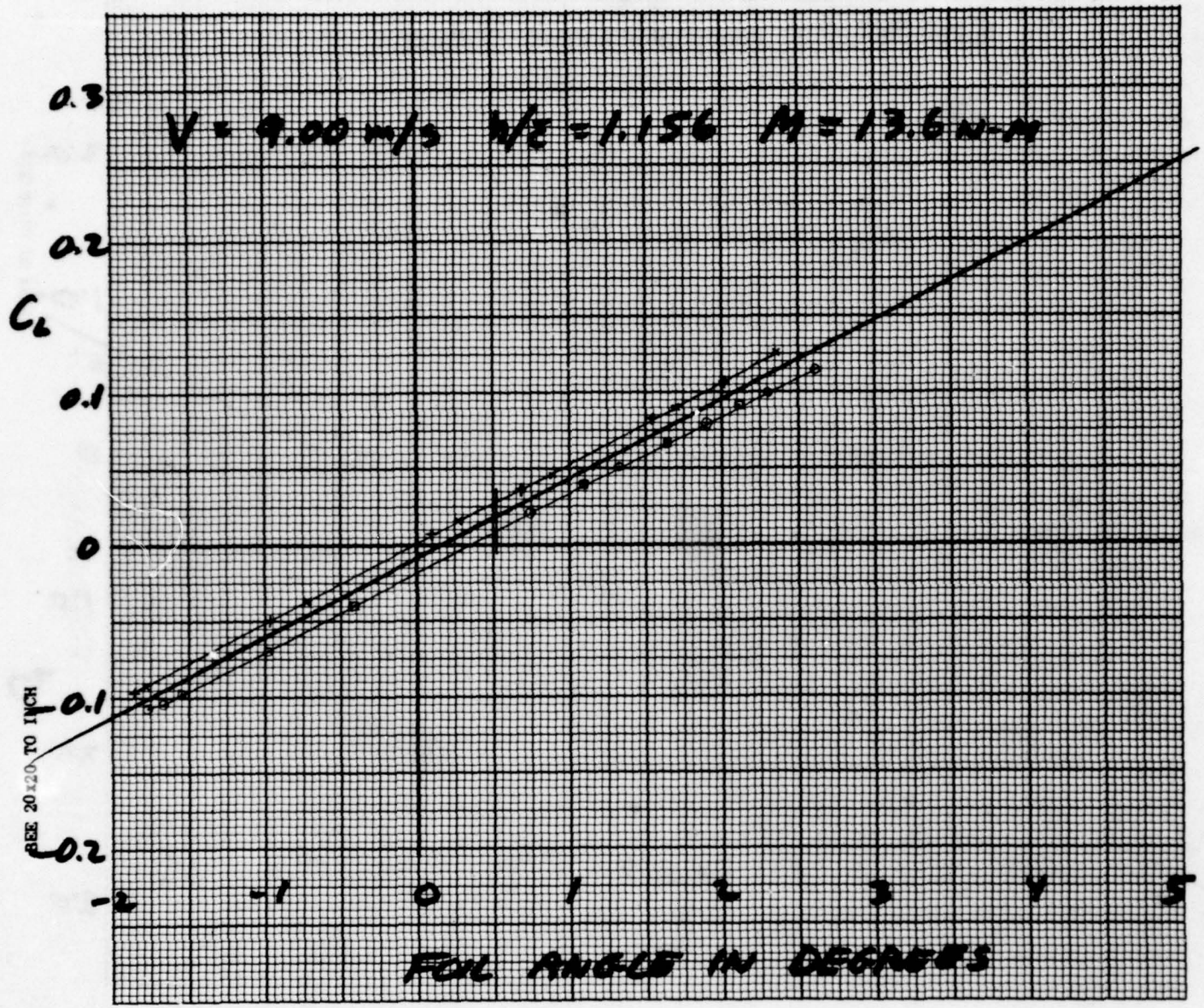
V = 9.00 m/s W/L = 1.156 M = 13.6 N-M
0.3
0.2
C_L
0.1
0
-0.1
-0.2
-2
-1
0
1
2
3
4
5
FOR ANGLE IN DEGREES
SEE 20 x 20 TO INCH

V = 9.00 m/s M/2 = 0.029 M = 2.7 M-M
0.3
0.2
C_L 0.1
0
-0.1
-0.2
-2
0
2
4
6
ROLL ANGLE IN DEGREES
SEE 20x20 TO INCH

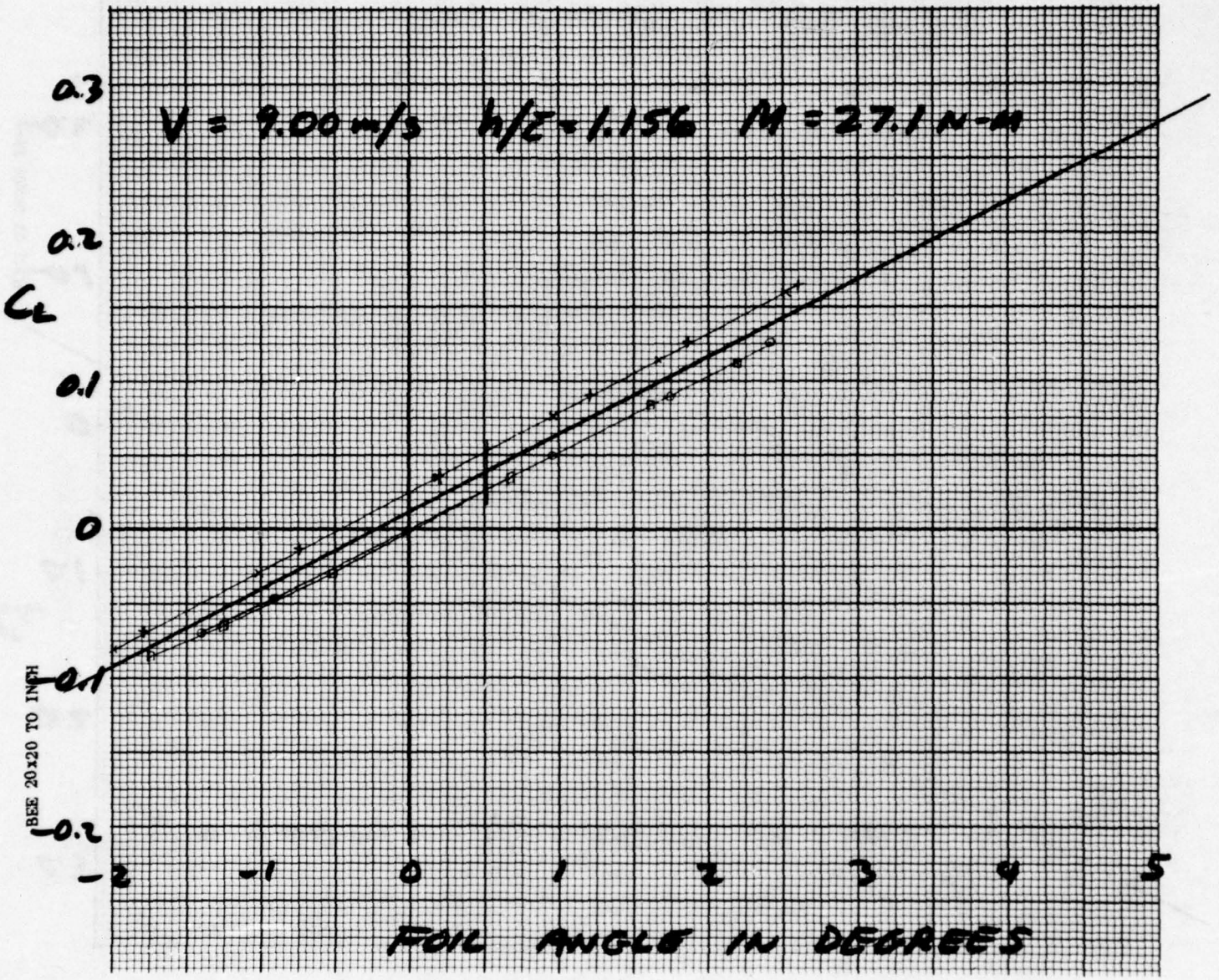
V = 9.00 m/s h/c = 1.156 M = 27.1 N-m
0.3
0.2
C_L
0.1
0
-0.1
-0.2
-2
-1
0
1
2
3
4
5
FOIL ANGLE IN DEGREES
KEUFFEL & ESSER CO. MADE IN U.S.A.
46 1320 20 x 20 TO INCH

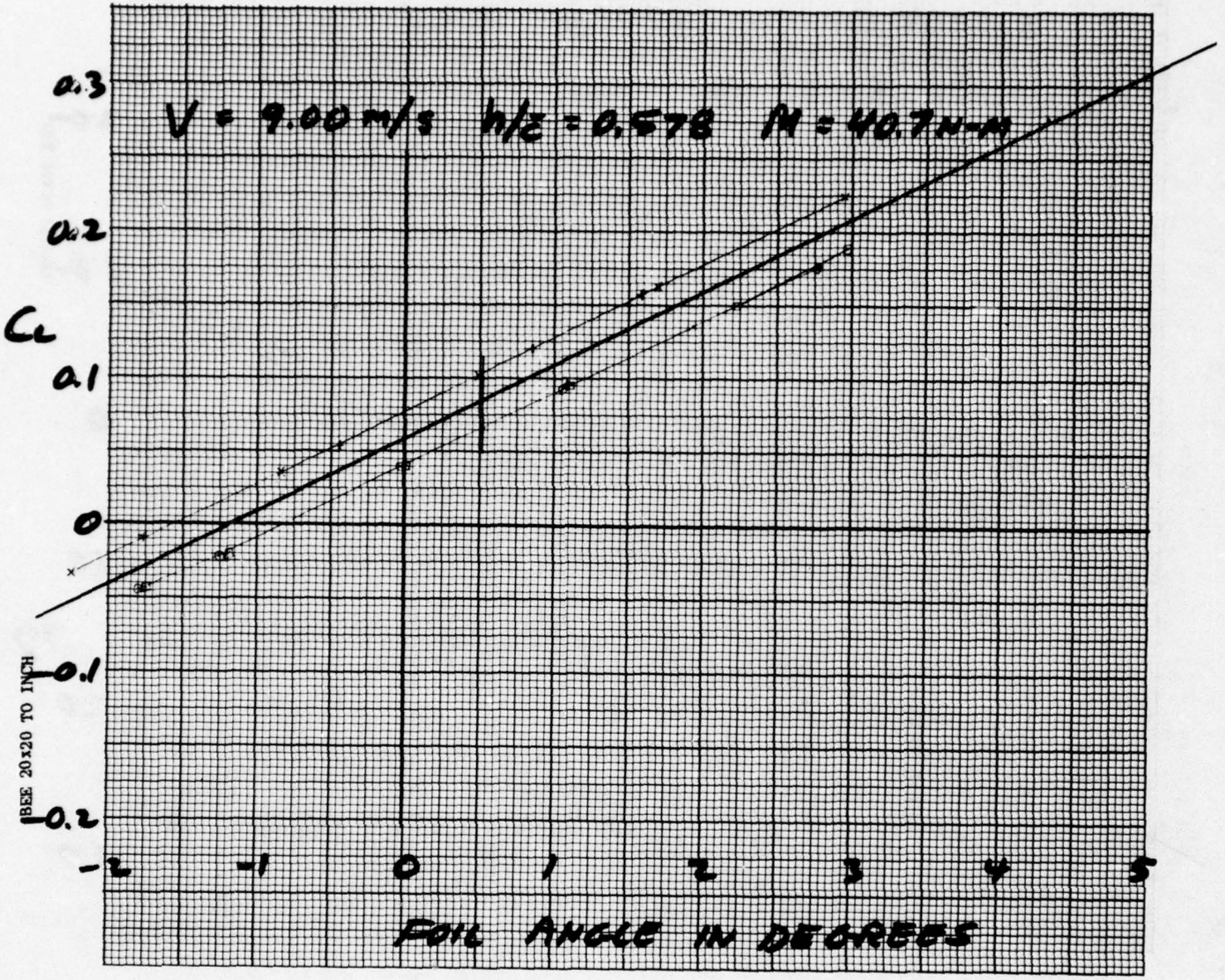
V = 9.00 m/s h/c = 0.578 N = 40.7 N-m
0.3
0.2
C_L
0.1
0
-0.1
-0.2
-2
-1
0
1
2
3
4
5
FOIL ANGLE IN DEGREES
KEUFFEL & ESSER CO. 20x20 TO INCH

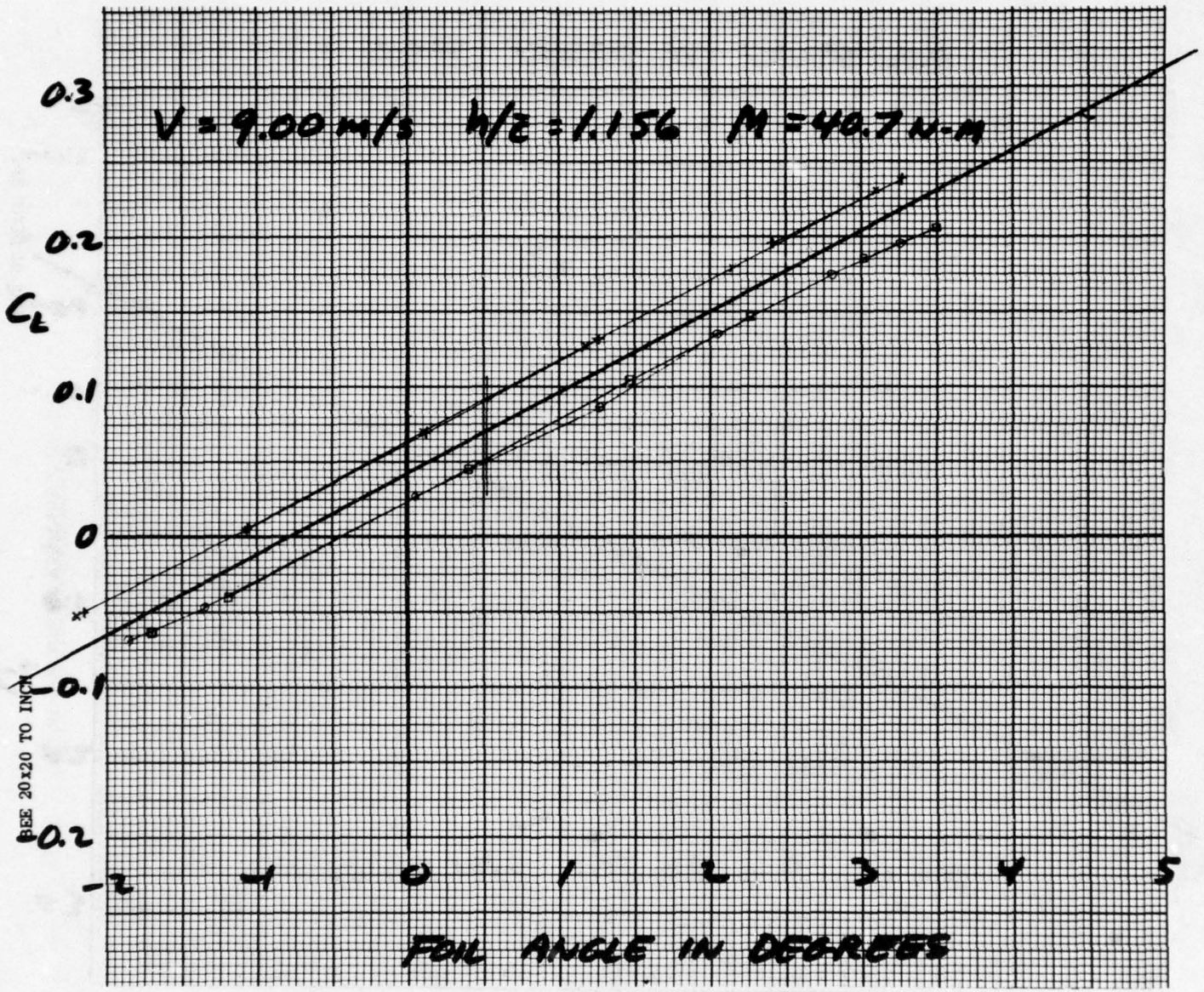
V = 9.00 m/s h/c = 1.156 M = 40.7 N-M
0.3
0.2
C_L
0.1
0
-0.1
-0.2
-2
-1
0
1
2
3
4
5
FOIL ANGLE IN DEGREES
KEUFFEL & ESSER CO. MADE IN U.S.A.
KEE 20x20 TO INCH

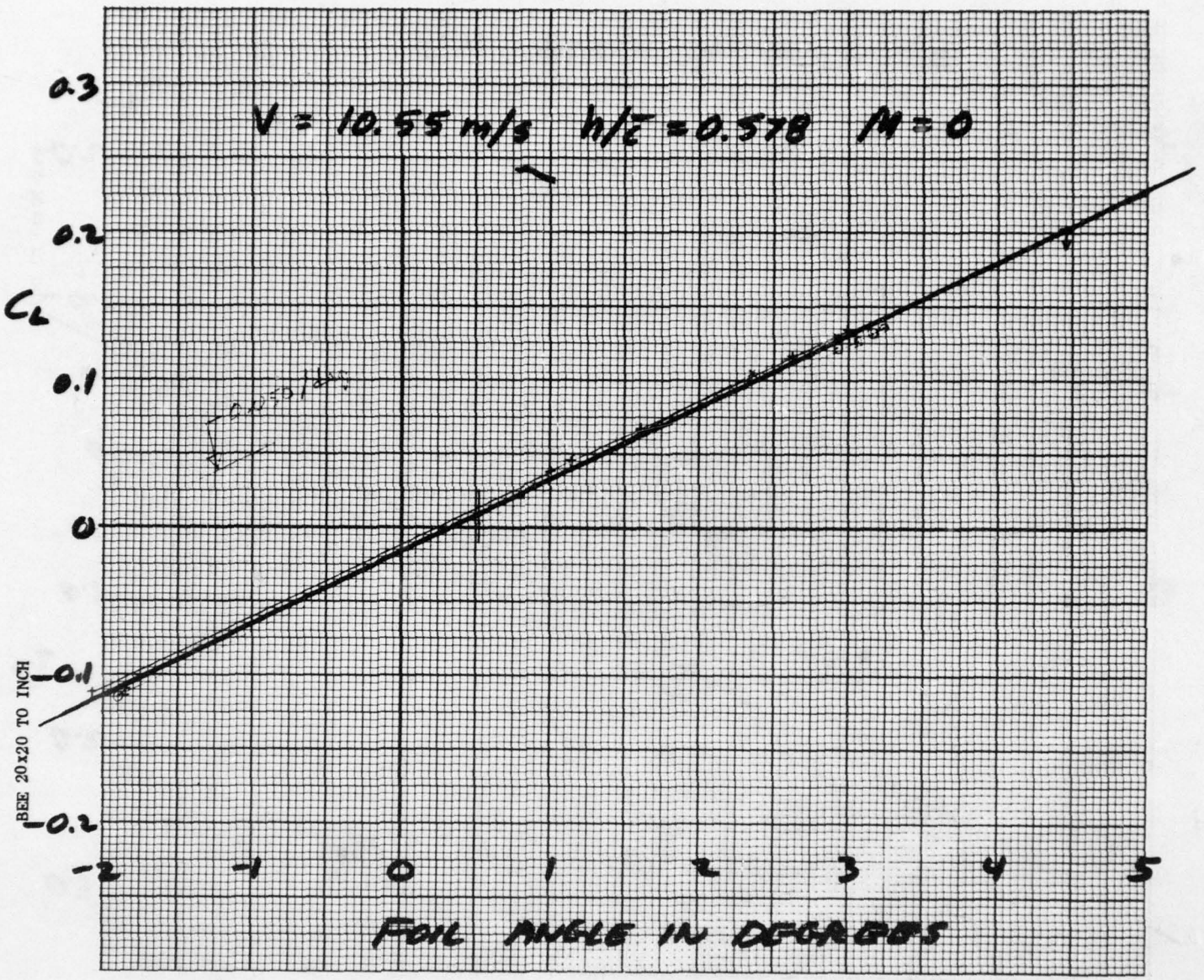
V = 10.55 m/s h/c = 0.578 N = 0
0.3
0.2
C_L
0.1
0
-0.1
-0.2
-2
-1
0
1
2
3
4
5
FOIL ANGLE IN DEGREES
BEE 20x20 TO INCH

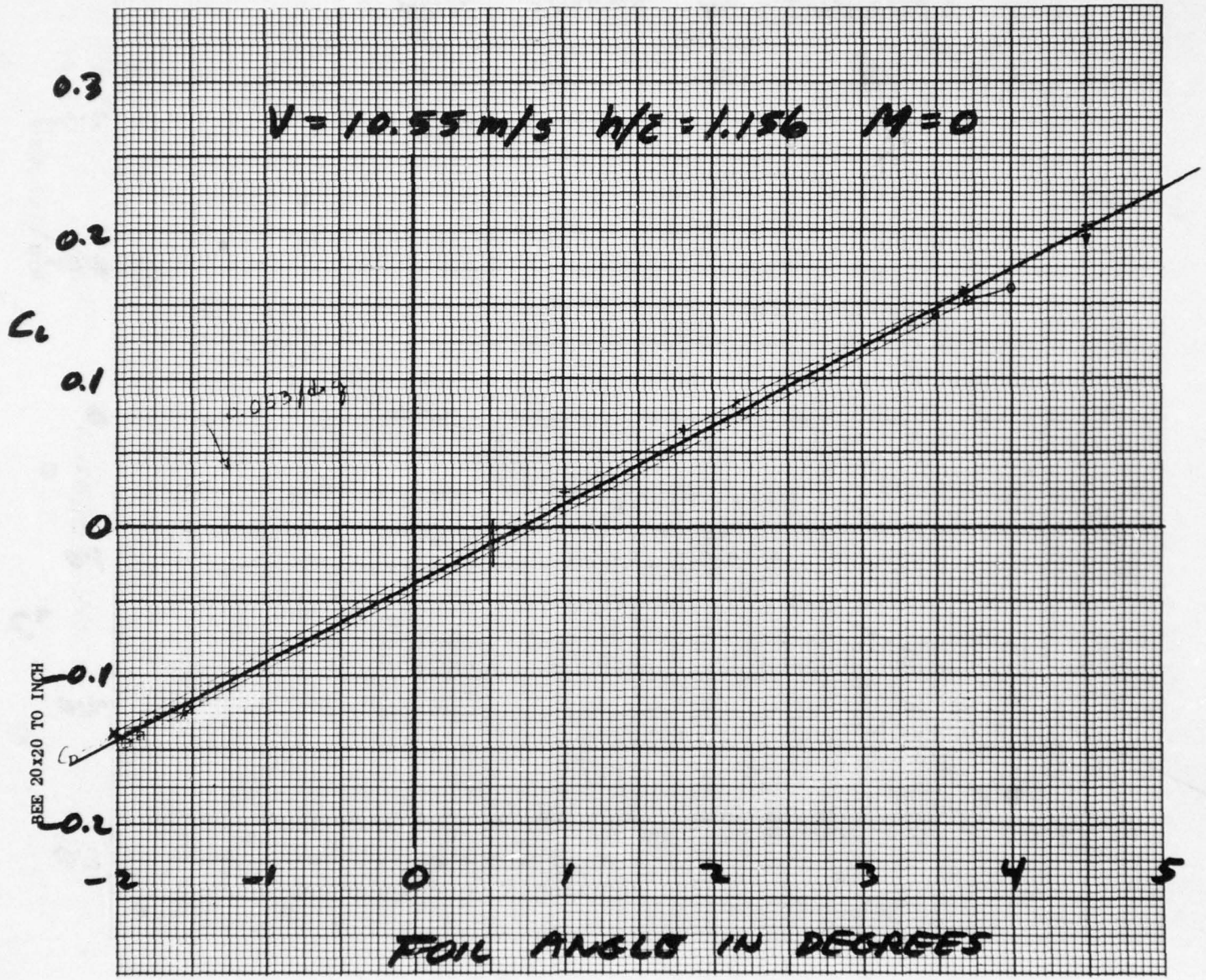
V = 10.55 m/s h/c = 1.156 M = 0
0.3
0.2
C_L
0.1
0
-0.1
-0.2
-2
-1
0
1
2
3
4
5
FOIL ANGLE IN DEGREES
KEUFFEL & ESSER CO. MADE IN U.S.A.
KEE 20X20 TO INCH

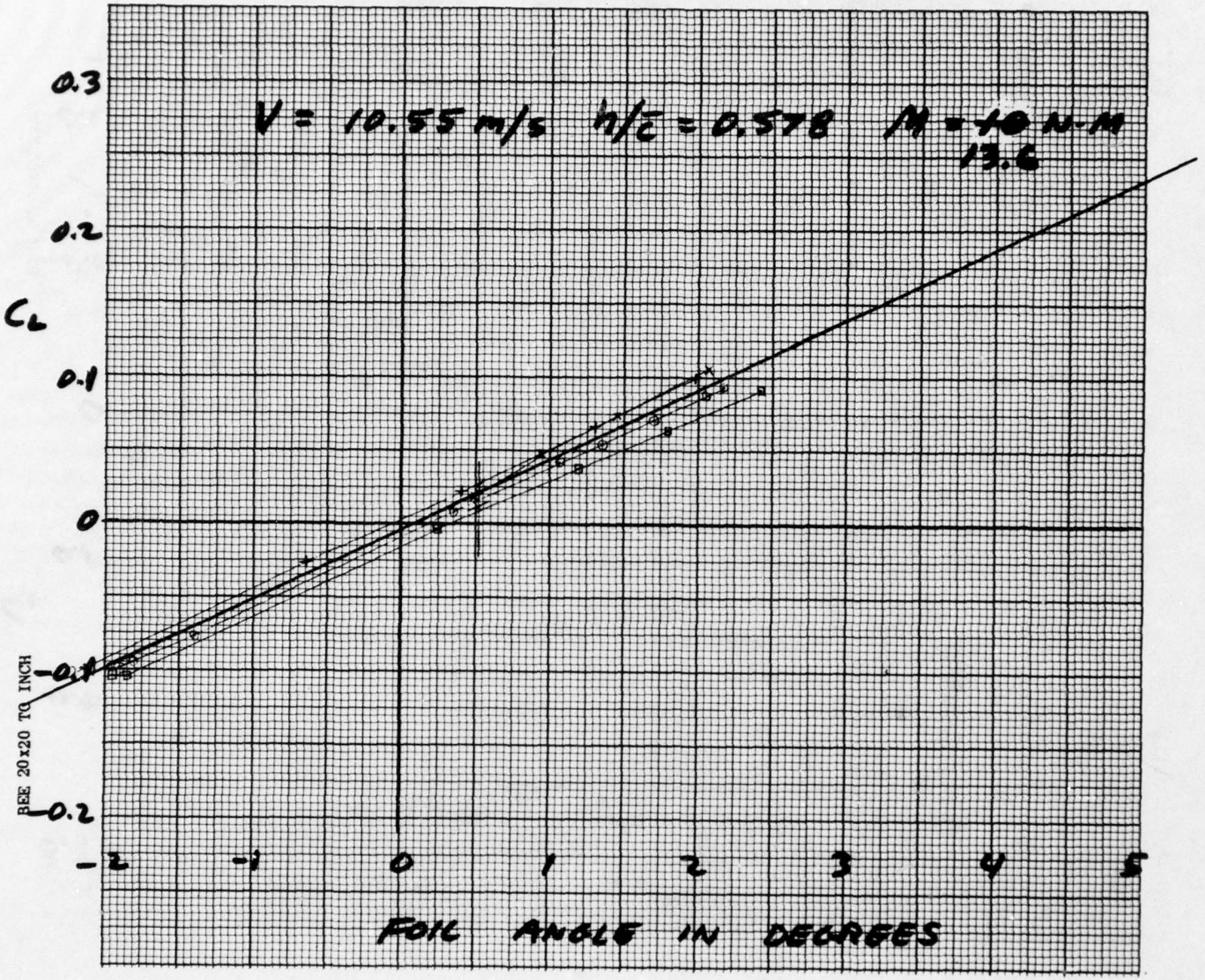
V = 10.55 m/s h/c = 0.578 M = 10 N-M
13.6
0.3
0.2
C_L
0.1
0
-0.1
-0.2
-2
-1
0
1
2
3
4
5
FOIL ANGLE IN DEGREES
KEE 20x20 TO INCH

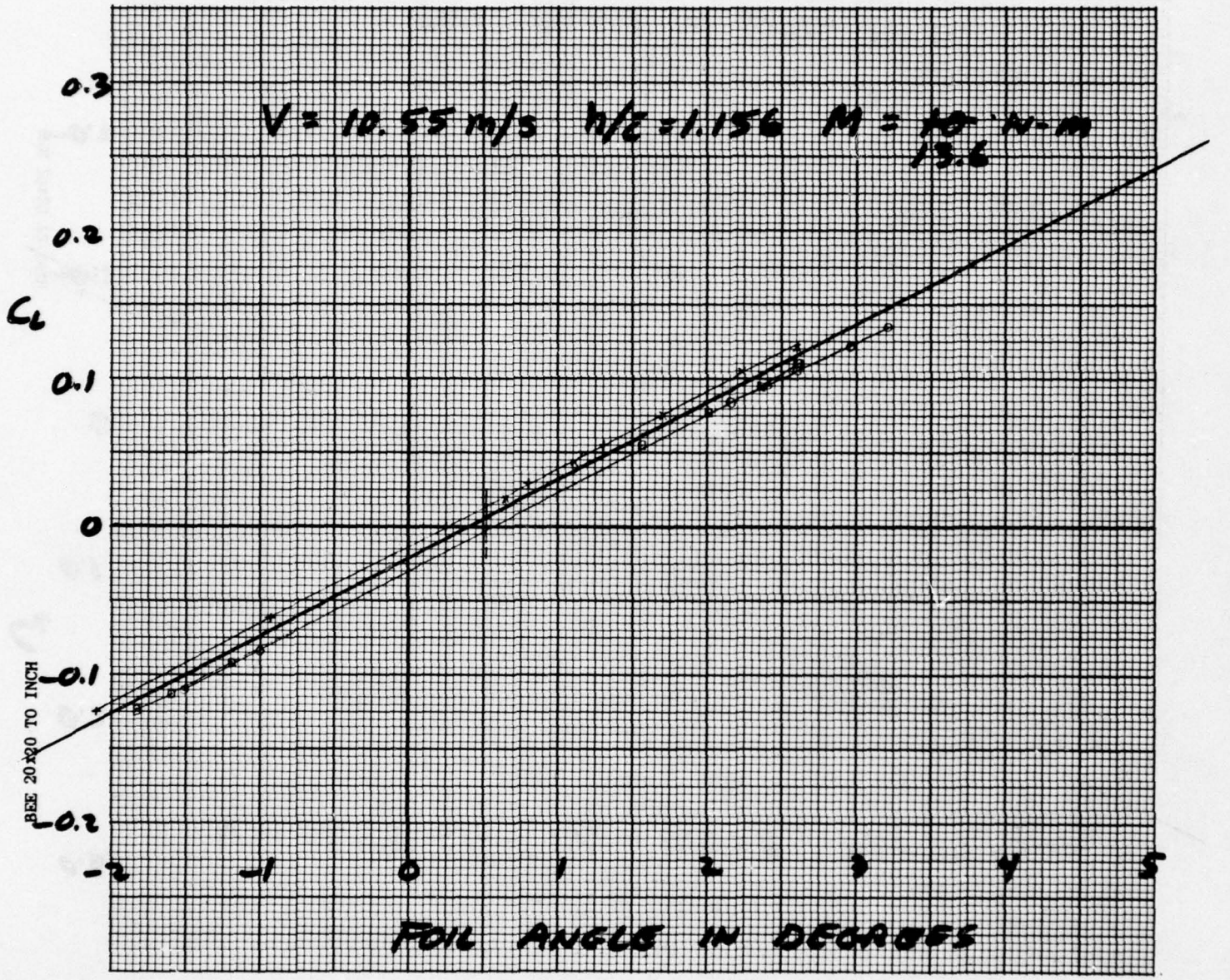
V = 10.55 m/s h/c = 1.156 M = 10 N-m
13.6
0.3
0.2
C_L
0.1
0
-0.1
-0.2
-2
-1
0
1
2
3
4
5
FOIL ANGLE IN DEGREES
BEE 20 X 20 TO INCH

V = 10.55 m/s, M/L = 0.578, M = 27.1 N·m
0.3
0.2
0.1
0
-0.1
-0.2
C_L
-2
-1
0
1
2
3
4
5
ANGLE OF ATTACK IN DEGREES
DEE 20x20 TO INCH

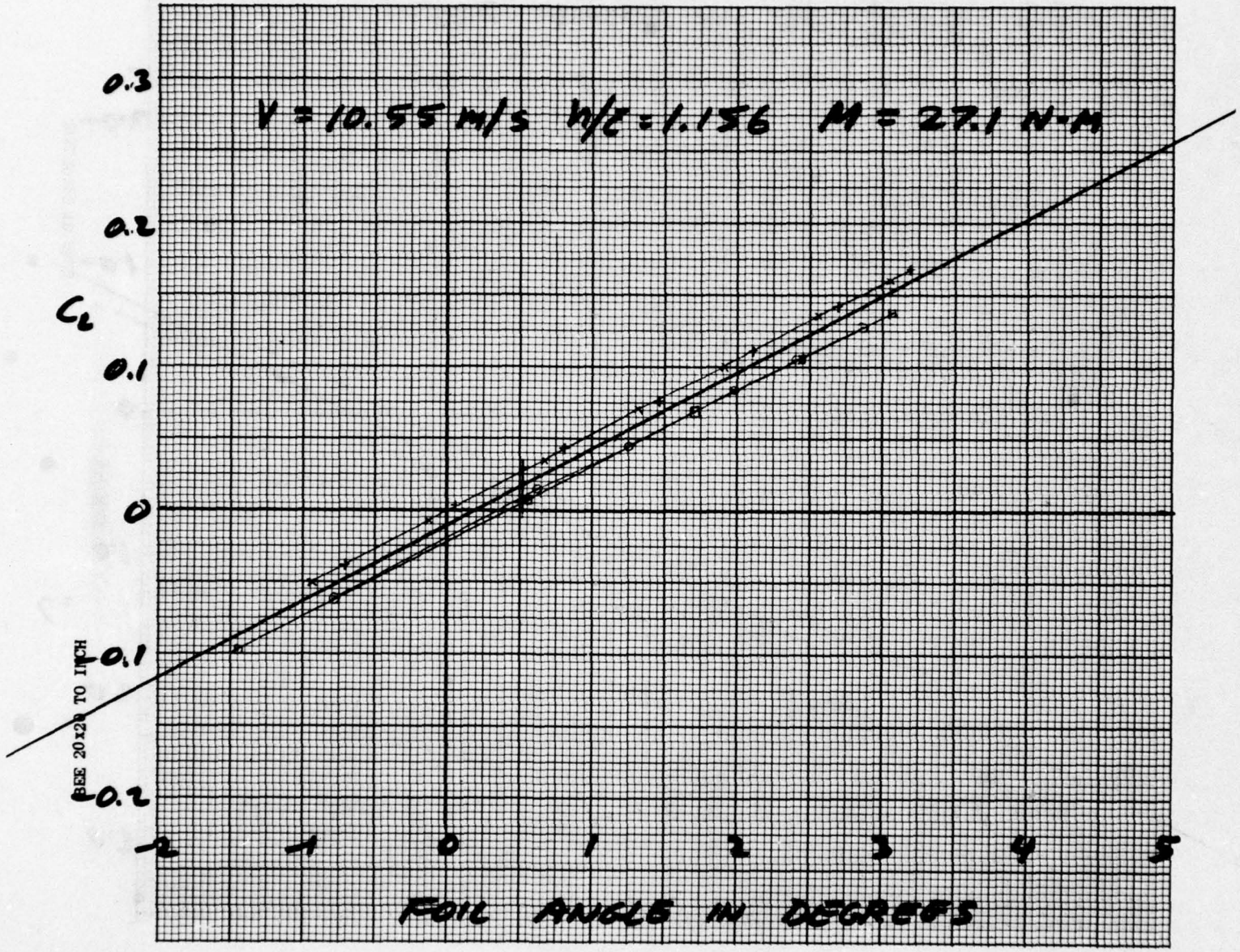
V = 10.55 m/s h/c = 1.156 M = 27.1 N-M
0.3
0.2
C_L
0.1
0
-0.1
-0.2
-2
-1
0
1
2
3
4
5
FOIL ANGLE IN DEGREES
SEE 20x20 TO INCH

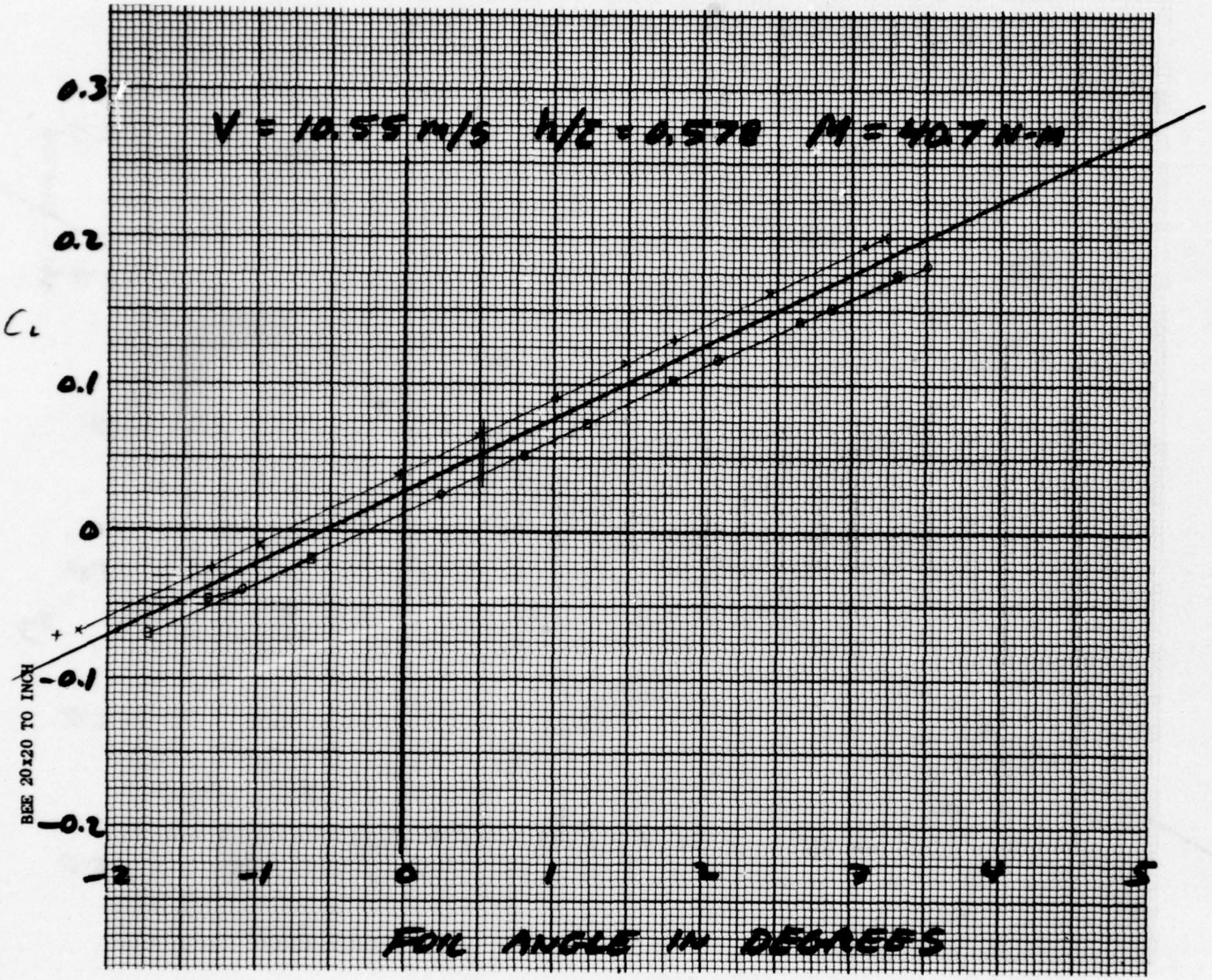
V = 10.55 m/s h/c = 0.578 M = 4047 N-m
0.3
0.2
C_L
0.1
0
-0.1
-0.2
-2
-1
0
1
2
3
4
5
FOR ANGLE IN DEGREES
BEE 20x20 TO INCH

V = 10.55 m/s M = 0.031
M = 0.047
0.3
0.2
0.1
0
-0.1
-0.2
C_l
5
4
3
2
1
0
-1
-2
ROLL ANGLE IN DEGREES
BEE 20x20 TO INCH

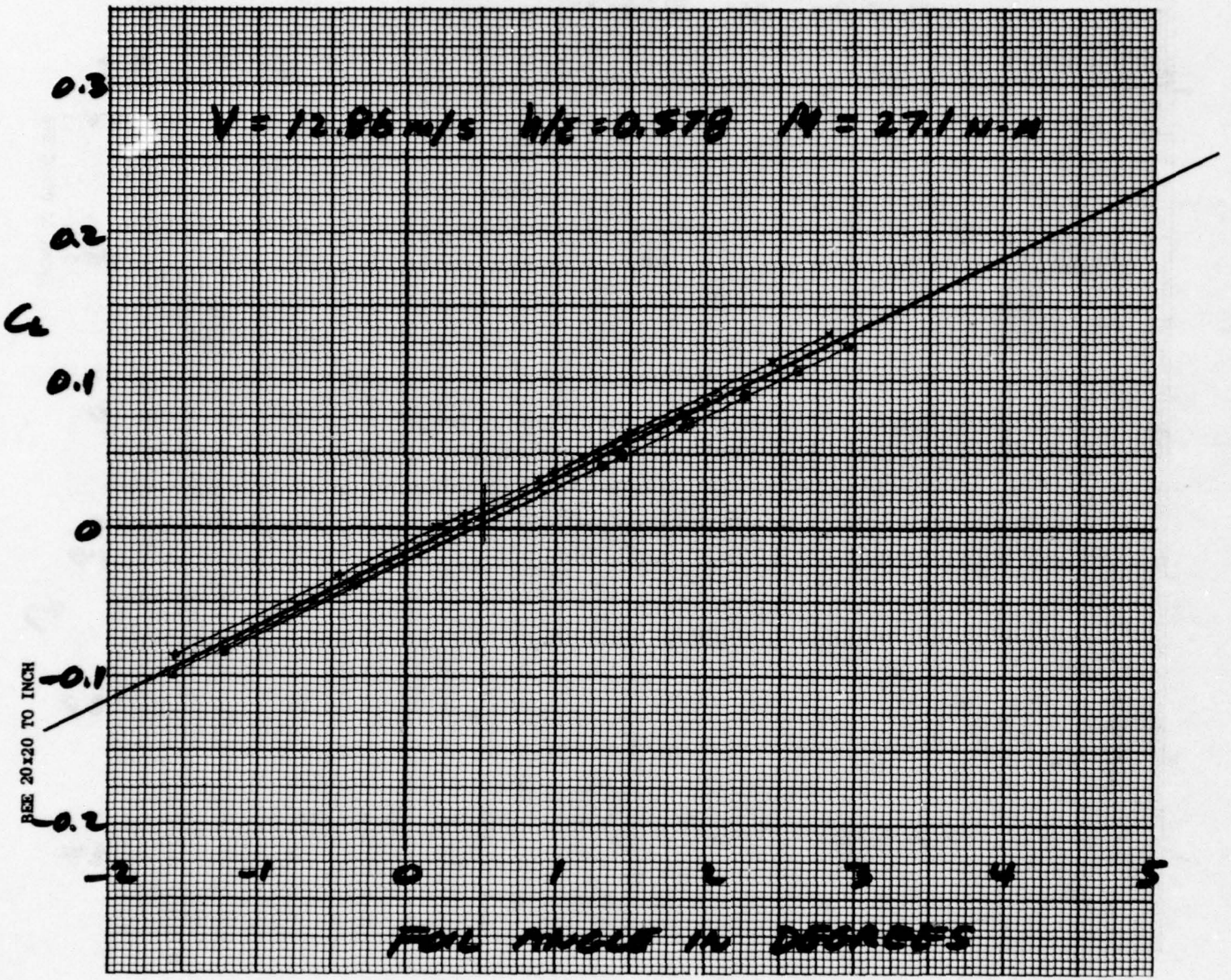
V = 12.86 m/s h/c = 0.578 N = 27.1 N-M
0.3
0.2
C_L
0.1
0
-0.1
-0.2
-2
-1
0
1
2
3
4
5
FOIL ANGLE IN DEGREES
KEE 20x20 TO INCH

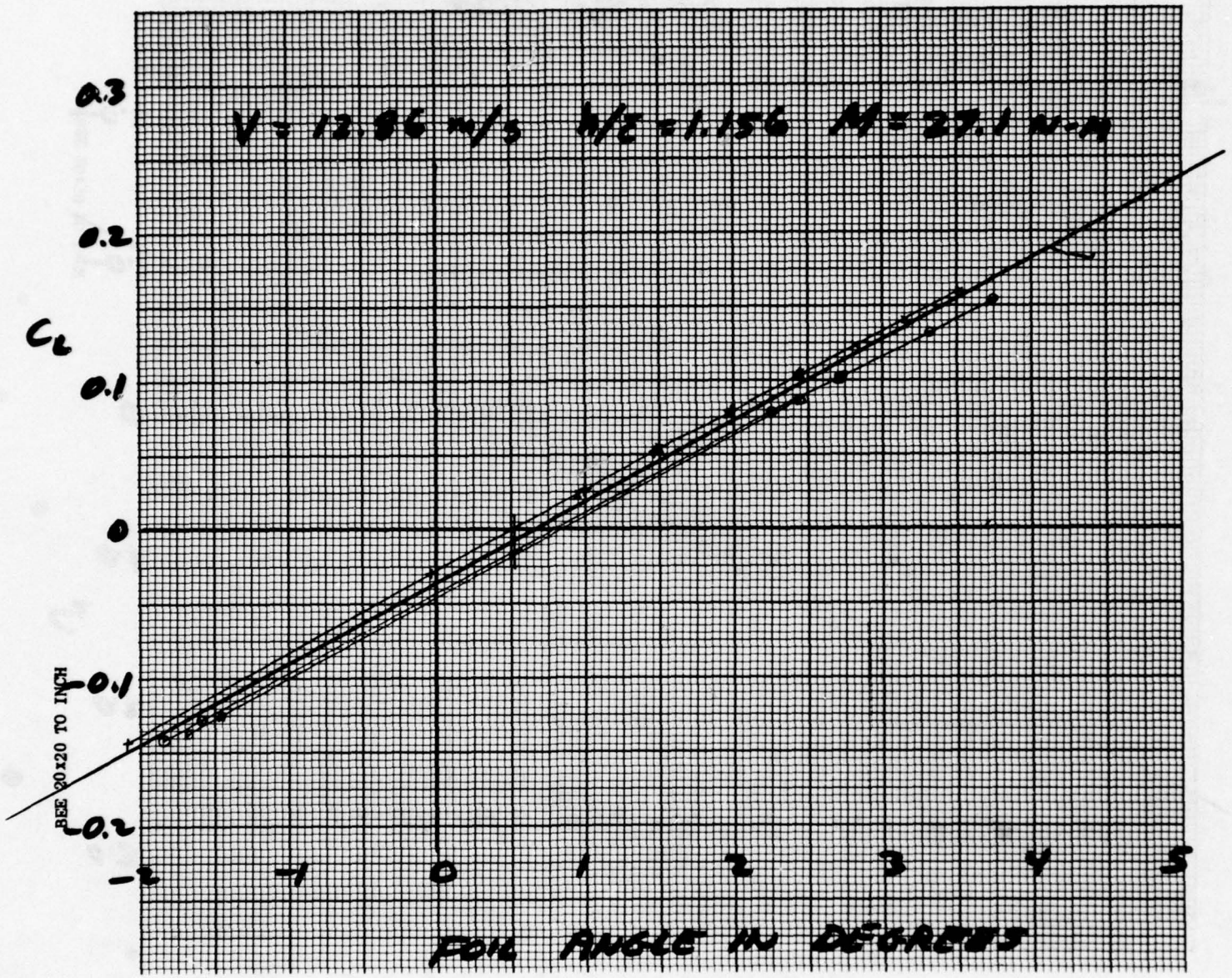
V = 12.86 m/s h/c = 1.156 M = 27.1 m-N
0.3
0.2
C_L
0.1
0
-0.1
-0.2
-2
-1
0
1
2
3
4
5
FOIL ANGLE IN DEGREES
KEE 20x20 TO INCH

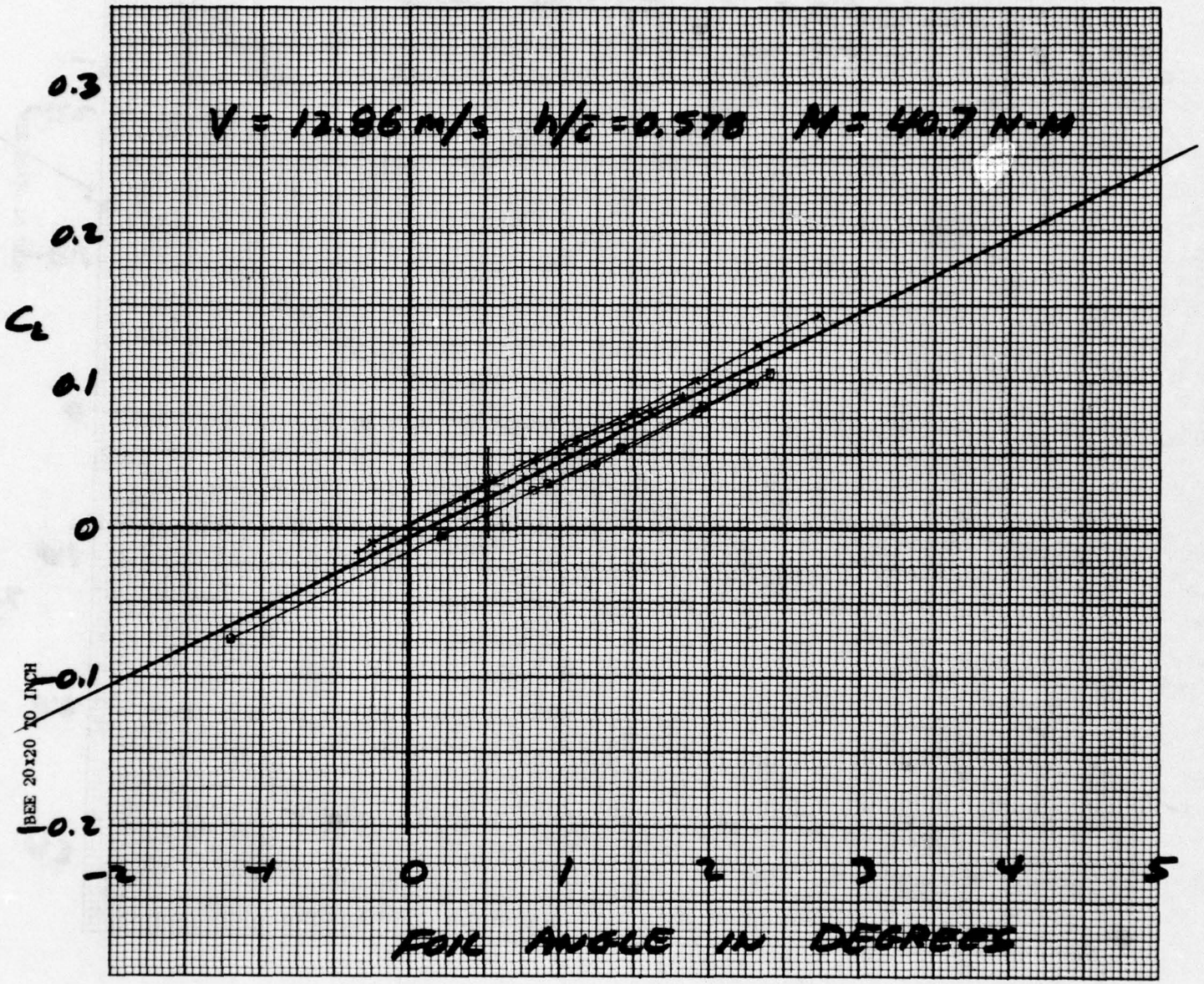
V = 12.86 m/s h/c = 0.570 M = 46.7 N-M
0.3
0.2
C_L
0.1
0
-0.1
-0.2
-2
-1
0
1
2
3
4
5
FOIL ANGLE IN DEGREES
BEE 20x20 TO INCH

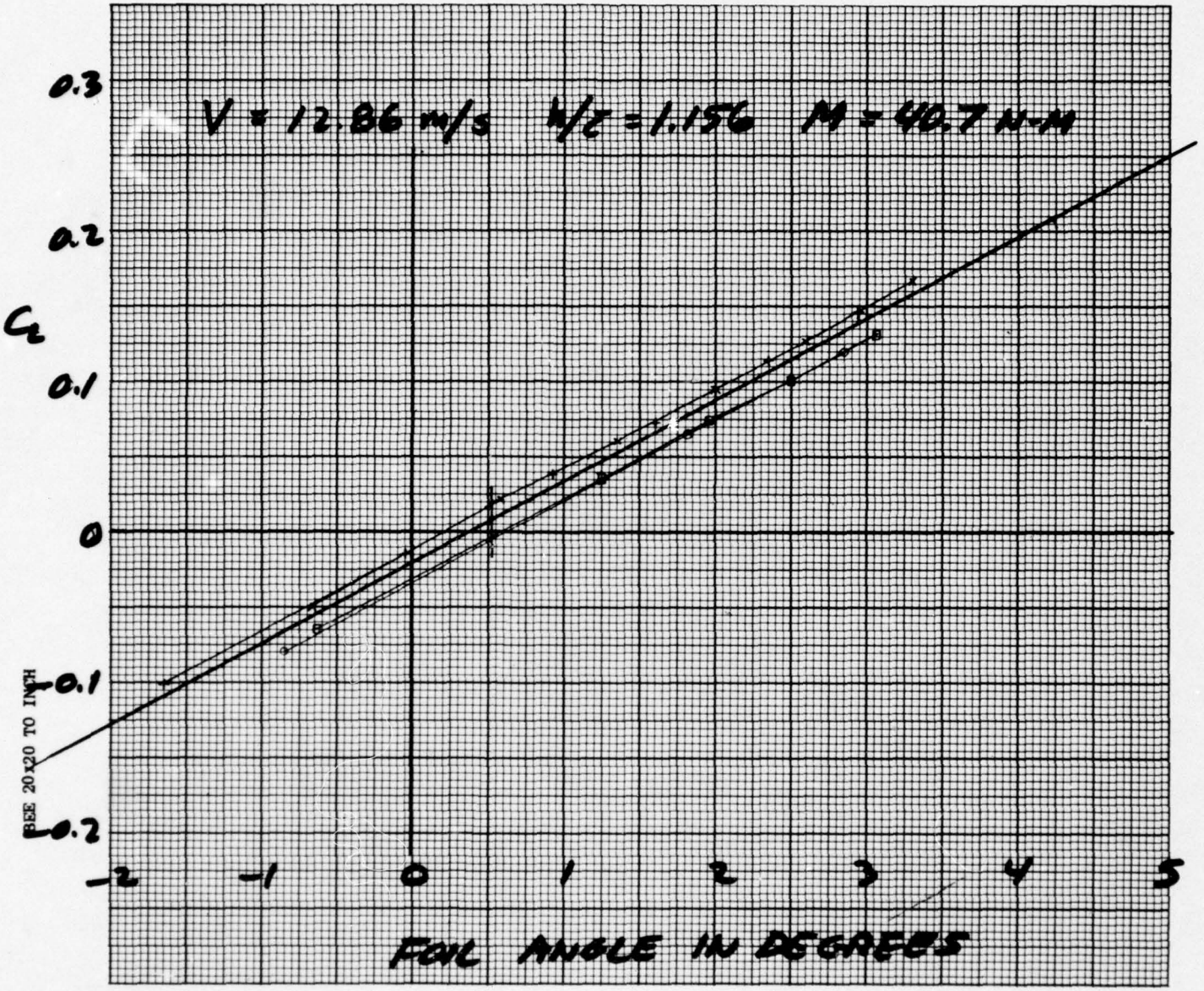
V = 12.86 m/s
b/2 = 1.156
M = 40.7 N-M
0.3
0.2
C_L
0.1
0
-0.1
-0.2
-2
-1
0
1
2
3
4
5
FOIL ANGLE IN DEGREES
KEUFFEL & ESSER CO. MADE IN U.S.A.

APPENDIX B

ERROR ANALYSIS OF "INDIRECT METHOD"

The "indirect method" of determining the hydrodynamic coefficients, lift- and moment-curve slopes, centers of pressure, and flap effectiveness is shown in Figure B1 (also shown as Figure 1 of main report). This analysis is based on the linear equations developed in the report (Equations [1] through [3]). No attempt is made here to determine the errors introduced by the basic assumptions of those equations, but rather to follow the errors due to measurement of the fundamental experimental parameters through the analysis procedure.

The estimated maximum errors* in the fundamental experimental measurements are listed in Table B1. Based on these errors, the estimated maximum errors in the derived parameter may be determined as follows:

1. LOCATION OF PIVOT POINT (X)

$$X = (X\bar{c})/\bar{c}$$

$$dx/x = d(x\bar{c})/(x\bar{c}) - d\bar{c}/\bar{c}$$

$$\left|dx/x\right| \leq \left|d(x\bar{c})/(x\bar{c})\right| + \left|d\bar{c}/\bar{c}\right|$$

From Table B1,

$$\left|dx/x\right| \leq 0.00036 + 0.00012 = 0.00048$$

Thus, maximum percent error in X is about 0.05 percent.

---

* These estimated maximum errors include both accuracy and precision errors.

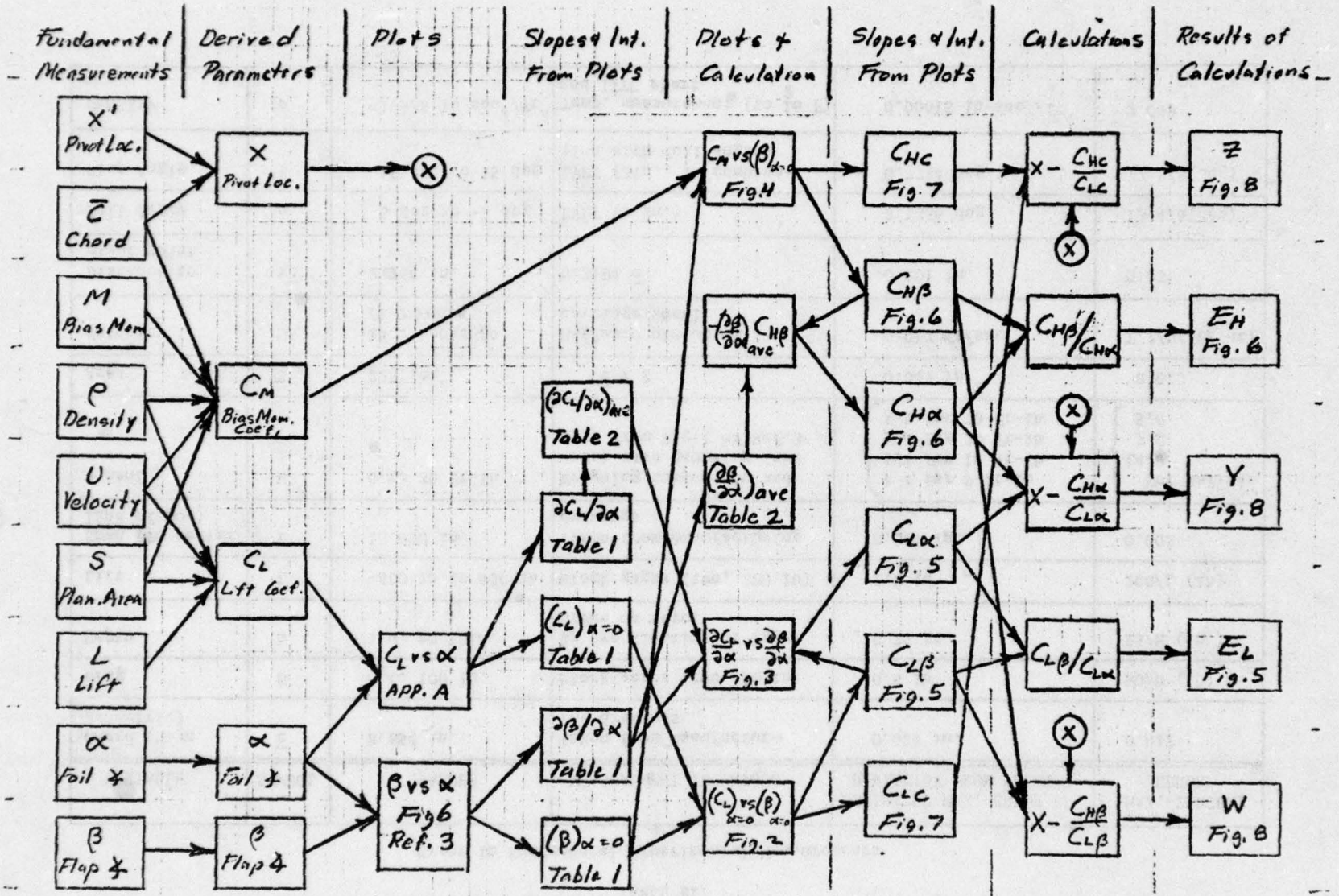

FIGURE B1 - SUMMARY OF "INDIRECT METHOD" ANALYSIS

TABLE B1

Error in Fundamental Experimental Measurements

VARIABLE	SYMBOL	VALUES	MEASUREMENT TECHNIQUE	ESTIMATED MAX. ERROR OR DEVIATION FROM VALUE	MAX. PERCENT ERROR
Chord (Mean geometric)	$\bar{c}$	8.654 in.	Taken from manufacturing drawings	0.001 in.	0.012
Drag	D	0 to 100 lb.	Block gages (two, 50 lb)	0.5 lb	50/D (lb)
Depth	h	5in. to 10in.	By eye sighting of lines drawn on strut	0.25 in.	25/h (in.)
Lift	L	-400 lb to 400 lb	Block gages (two, 200 lb)	2.0 lb	200/L (lb)
Span (To centerline of pod)	ℓ	13.000 in.	Taken from manufacturing drawings	0.001 in.	0.008
Moment	M	0 to 30 ft-lb	Weighing components and worst case geometry (α=5 deg) from Fig.1 of Ref.3	1.4 for 0 ft-lb 1.4 for 10 ft-lb 1.4 for 20 ft-lb 1.5 for 30 ft-lb	Not defined 14.0 7.0 5.0
Area	S	225 in.^{2}	$\bar{c} \times \ell$	0.047 in.^{2}	0.020
Velocity	U	14.2 knots to 25.0 knots	Magnetic pickup on carriage wheel	0.017 ft/sec	1.7/U(ft/sec)
Distance to pivot point	$x\bar{c}$	2.764 in.	0.3194 $\bar{c}$	0.001 in.	0.036
Foil Angle	α	-5 deg to +5 deg	LVDT (1 in.)	0.1336 deg	13.4/α(deg)
Flap Angle	β	-15 deg to 15 deg.	LVDT (3in., in combination with foil angle)	0.7784 deg	77.8/β(deg)
Density	ρ	$\sim$1.935 lb-sec^2/ft^4	Temp. measurement (to $\frac{1}{2}$o F) and ITTC chart	0.00015 lb-sec^2/ft^4	0.008

2. BIAS MOMENT COEFFICIENT (C_M)

$$C_M = M/(1/2\rho U^2 S\bar{c})$$

$$dC_M/C_M = dM/M - d\rho/\rho - 2dU/U - dS/S - d\bar{c}/\bar{c}$$

$$\left|dC_M/C_M\right| \leq \left|dM/M\right| + \left|d\rho/\rho\right| + 2\left|dU/U\right| + \left|dS/S\right| + \left|d\bar{c}/\bar{c}\right|$$

From Table B1,

$$\left|dC_M/C_M\right| \leq \begin{cases} \text{Not Defined for } M = 0 \text{ ft-lb} \\ 0.14 \quad \text{for } M = 10 \text{ ft-lb} \\ 0.07 \quad \text{for } M = 20 \text{ ft-lb} \\ 0.05 \quad \text{for } M = 30 \text{ ft-lb} \end{cases}$$

$$+ 0.00008 + 2 \begin{cases} 0.0007 \text{ for } U = 14.2 \text{ Kts} \\ 0.0006 \text{ for } U = 17.5 \text{ Kts} \\ 0.0005 \text{ for } U = 20.5 \text{ Kts} \\ 0.0004 \text{ for } U = 25 \text{ Kts} \end{cases}$$

$$+ 0.00020 + 0.00012$$

All other terms on the right side of the equation are negligible compared to the first term, so

$$\left|dC_M\right| \leq \left|dM/M\right| \times \left|C_M\right| = \left|dM/(1/2\rho U^2 S\bar{c})\right|$$

The maximum error in C_M is calculated* as a function of M and U and is shown in Table B2.

* Using $1/2\rho S\bar{c} = 1.090$ lb-sec^2/ft

TABLE B2

ESTIMATED MAXIMUM ERROR IN BIAS MOMENT COEFFICIENT (C_M)

U (kts) \ M (ft-lb)	0	10	20	30
14.2	0.0022	0.0023	0.0022	0.0025
17.5	0.0015	0.0015	0.0015	0.00o6
20.5	0.0011	0.0011	0.0011	0.0012
25.0	0.0007	0.0007	0.0007	0.0008

3. LIFT COEFFICIENT (C_L)

$$C_L = L/(1/2\rho U^2 S)$$

$$dC_L/C_L = dL/L - d\rho/\rho - 2dU/U - dS/S$$

$$\left|dC_L/C_L\right| \leq \left|dL/L\right| + \left|d\rho/\rho\right| + 2\left|dU/U\right| + \left|dS/S\right|$$

From Table B1,

$$\left|dC_L/C_L\right| \leq 2/L \text{ (lbs)} + 0.00008$$

$$+ 2 \begin{cases} 0.0007 \text{ for } U = 14.2 \text{ Kts} \\ 0.0006 \text{ for } U = 17.5 \text{ Kts} \\ 0.0005 \text{ for } U = 20.5 \text{ Kts} \\ 0.0004 \text{ for } U = 25.0 \text{ Kts} \end{cases}$$

$$+ 0.0002$$

The range for lift is $0 \leq L \leq 400$ lbs, so the first term on the right is

$$0.005 \leq 2/L \leq \infty$$

All other terms are small compared to this one so we may write

$$\left|dC_L/C_L\right| \leq \left|dL/L\right|$$

$$\left|dC_L\right| \leq \left|dL/L\right| \times \left|C_L\right| = \left|dL/(1/2\,\rho\, U^2 S)\right|$$

The maximum error in C_L is calculated* for the various velocities as

---

* Using $1/2\,\rho S = 1.512$ lb-sec^2/ft^2

$$\left|dC_L\right| = 2/(1.512\ U^2(\text{ft/sec})^2)$$

$$= \begin{cases} 0.0021 \text{ for } U = 14.2 \text{ Kts} \\ 0.0015 \text{ for } U = 17.0 \text{ Kts} \\ 0.0011 \text{ for } U = 20.5 \text{ Kts} \\ 0.0007 \text{ for } U = 25.0 \text{ Kts} \end{cases}$$

4. FOIL ANGLE (α)

The estimated maximum error in foil angle from Table B1 is 0.13 deg.

5. FLAP ANGLE (β)

The estimated maximum error in flap angle from Table B1 is 0.78 deg.

From the derived parameters onward, the analysis technique involves various calculations and plots as shown in Figure B1. The errors in the slopes and intercepts obtained from the plots are determined as followed. For example, take the general case of a plot of one variable (F) versus another variable (G) as shown in Figure B2a. A "best" straight line is drawn by hand. From this line, "best" values for slope and intercept are determined. These are the values listed in the report. Since the variables F and G may have error, the data points may be represented by error boxes as shown in Figure B2b. An infinite number of straight lines may be drawn through all of the boxes. The lines with the maximum and minimum slopes are shown in Figure B2c and the maximum and minimum intercepts are shown in Figure B2d. Thus, the maximum and minimum for the slope and intercept are determined from these four lines. These "bands" of error are carried along through the rest of the analysis by using them in the next calculation or plot.

The types of calculations that are made in the analysis are of the form:

$$F_{ave} = (1/4) \sum_{n=1}^{4} F_n \qquad [B1]$$

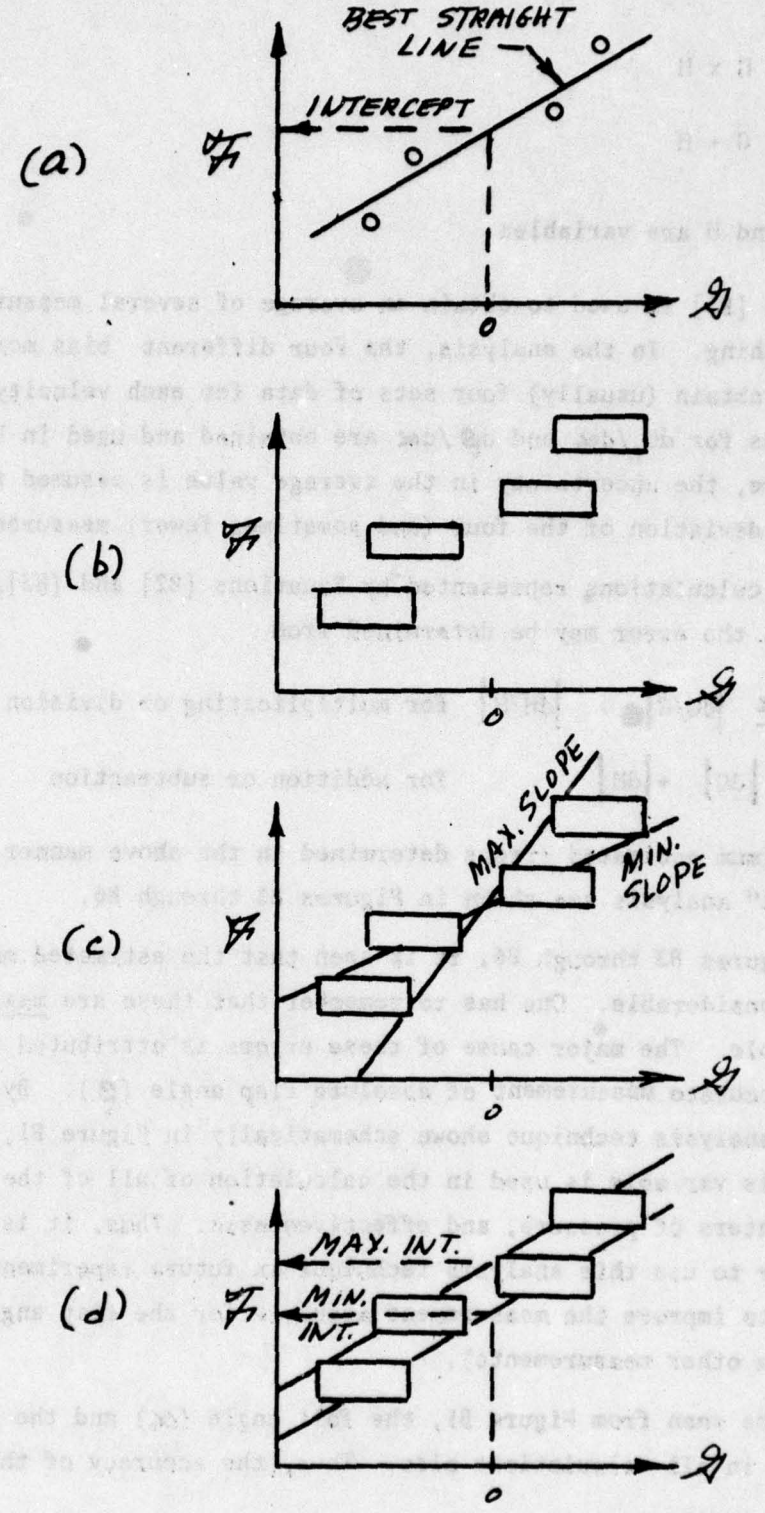

FIGURE B2 - DETERMINATION OF MAXIMUM AND MINIMUM SLOPES AND INTERCEPTS FROM PLOTS

$$F = G \times H \qquad [B2]$$

$$F = G + H \qquad [B3]$$

where F, G, and H are variables.

Equation [B1] is used to obtain an average of several measurements of the same thing. In the analysis, the four different bias moments were used to obtain (usually) four sets of data for each velocity. Average values for $dC_L/d\alpha$ and $d\beta/d\alpha$ are obtained and used in Figure 3. In that figure, the uncertainty in the average value is assumed to be the standard deviation of the four (and sometimes fewer) measurements.

For the calculations represented by Equations [B2] and [B3], respectively, the error may be determined from

$$\left|dF/F\right| \leq \left|dG/G\right| + \left|dH/H\right| \quad \text{for multiplicating or division}$$

$$\left|dF\right| \leq \left|dG\right| + \left|dH\right| \quad \text{for addition or subtraction}$$

The maximum estimated errors determined in the above manner for the "indirect" analysis are shown in Figures B3 through B6.

From Figures B3 through B6, it is seen that the estimated maximum errors are considerable. One has to remember that these are <u>maximum</u> errors possible. The major cause of these errors is attributed to the somewhat inaccurate measurement of absolute flap angle (β). By tracing through the analysis technique shown schematically in Figure B1, it is seen that this variable is used in the calculation of all of the coefficients, centers of pressure, and effectivenesses. Thus, it is concluded that in order to use this analysis technique in future experiments, it is imperative to improve the measurement accuracy for the flap angle (while not degrading other measurements).

As can be seen from Figure B1, the foil angle (α) and the velocity (U) are used in all calculations also. Thus, the accuracy of these

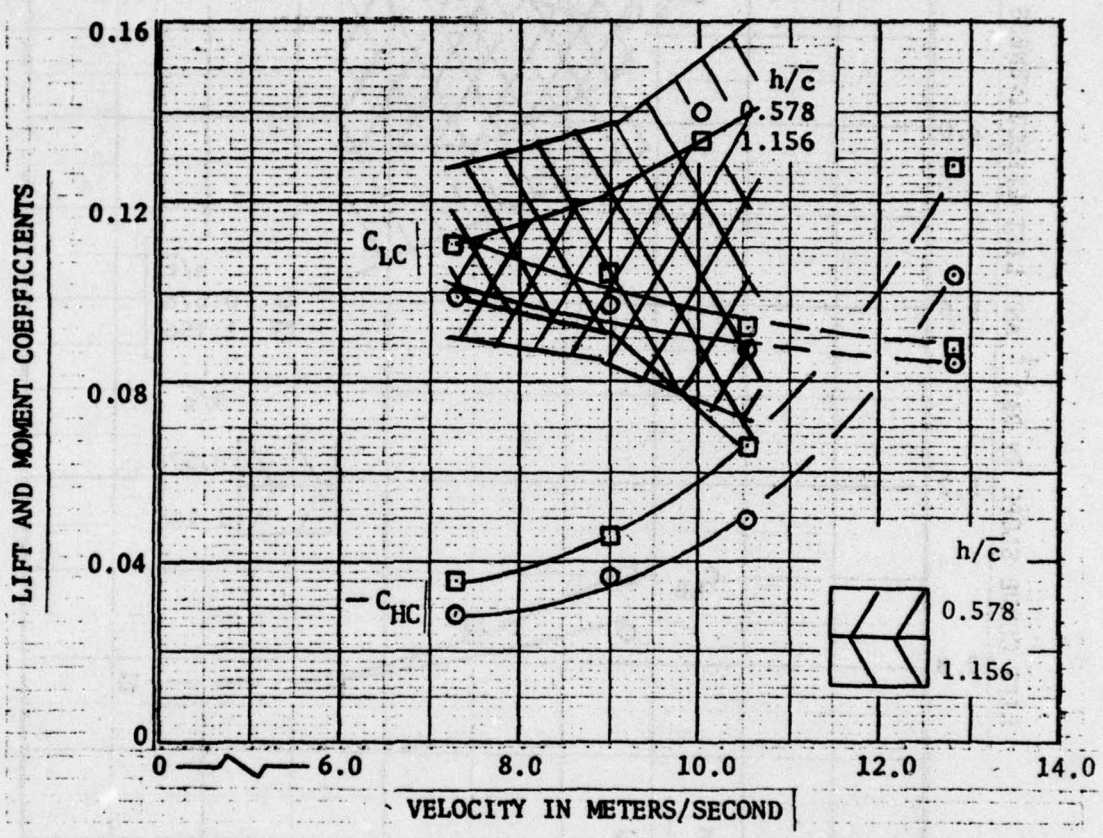

FIGURE B3a - ESTIMATED MAXIMUM ERROR IN C_{LC}

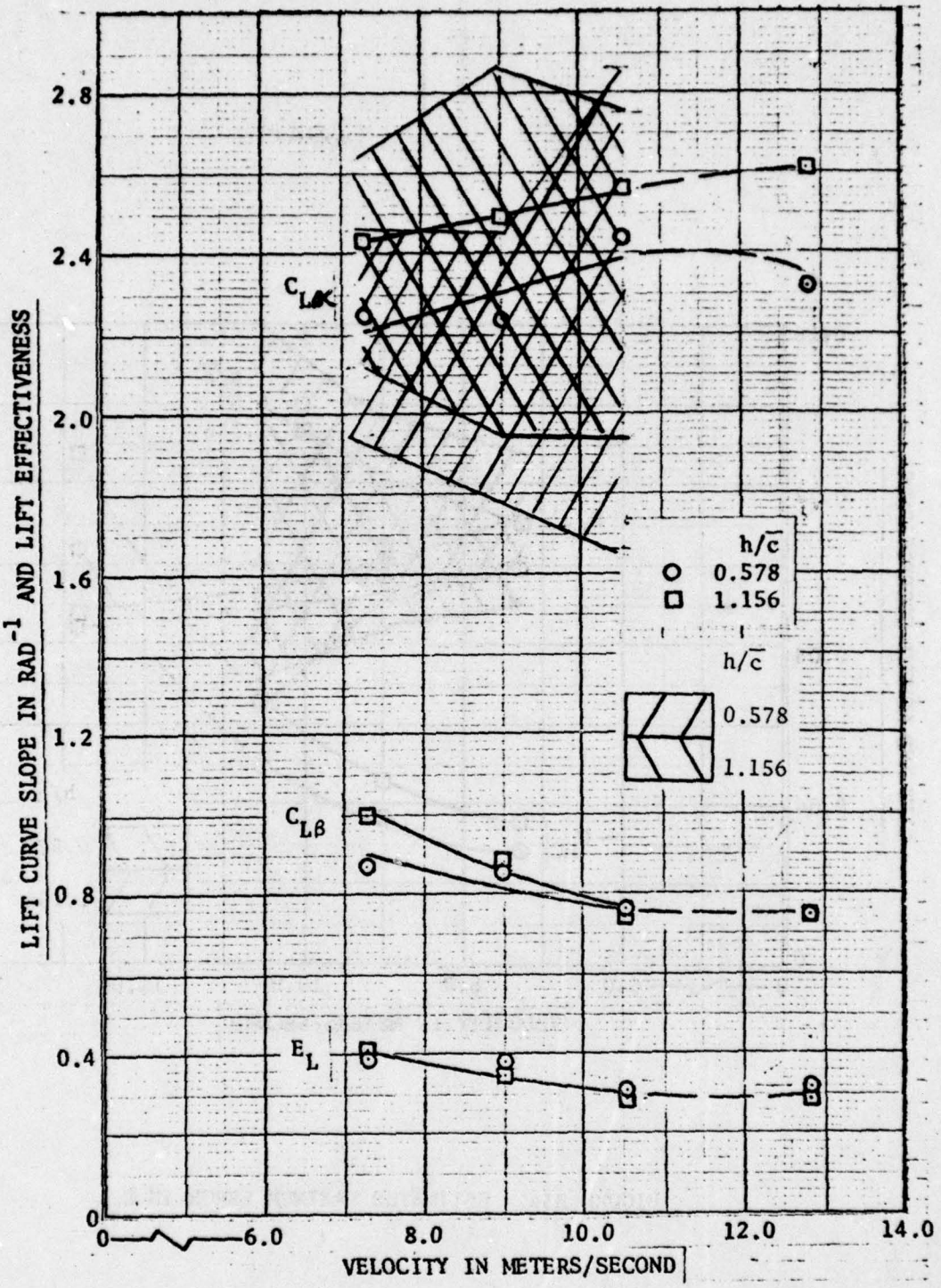

FIGURE B3b - ESTIMATED MAXIMUM ERROR IN $C_{L\alpha}$

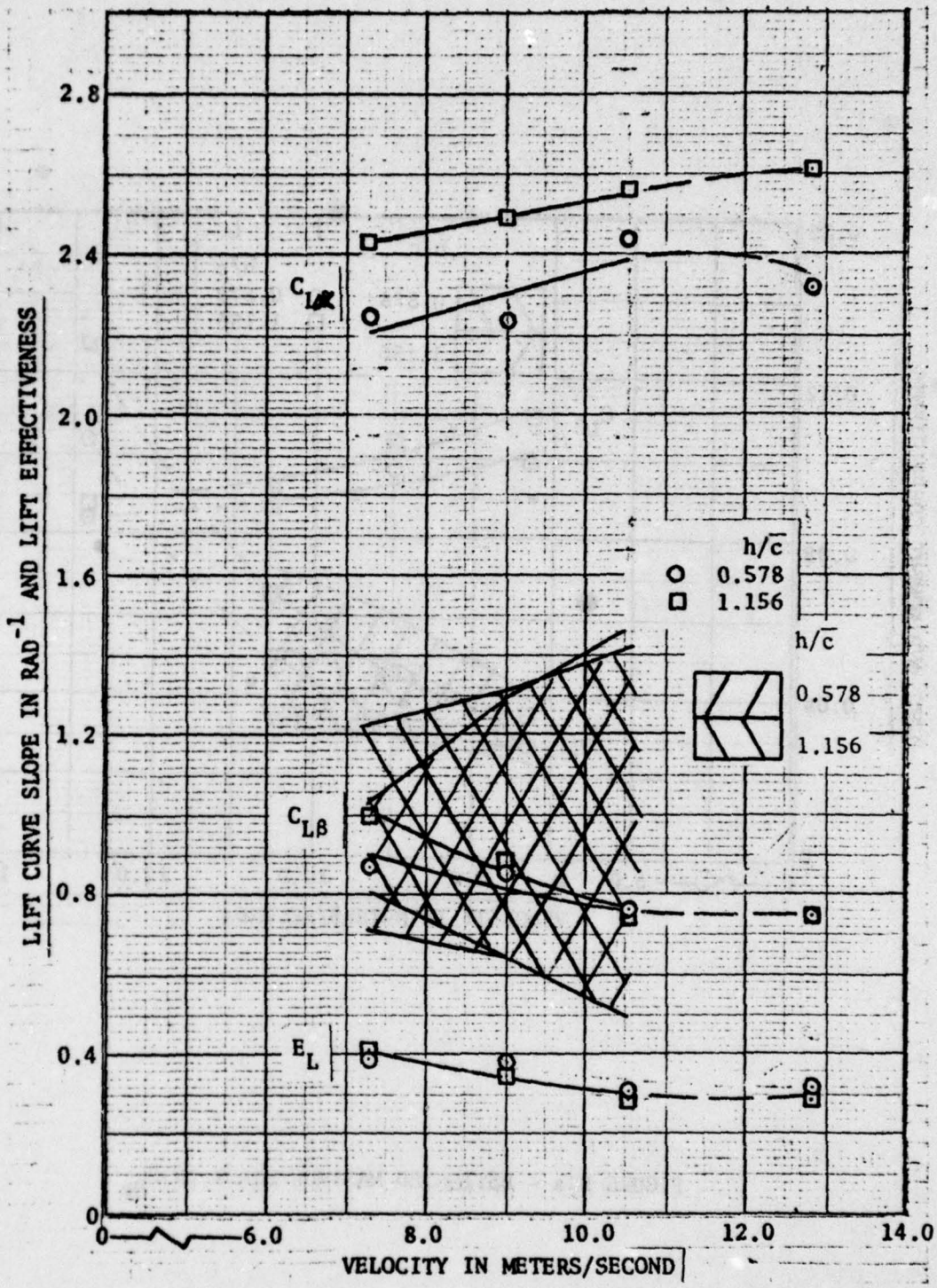

FIGURE B3c - ESTIMATED MAXIMUM ERROR IN $C_{L\beta}$

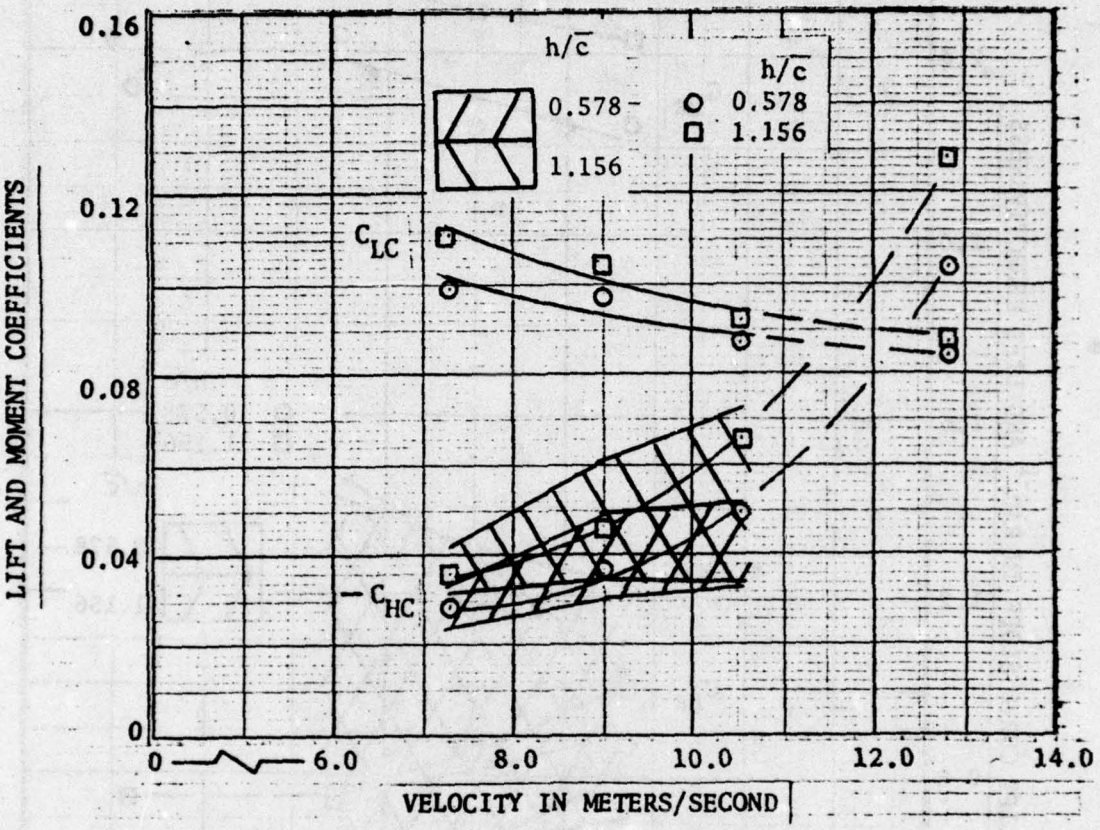

FIGURE B4a - ESTIMATED MAXIMUM ERROR IN C_{Hc}

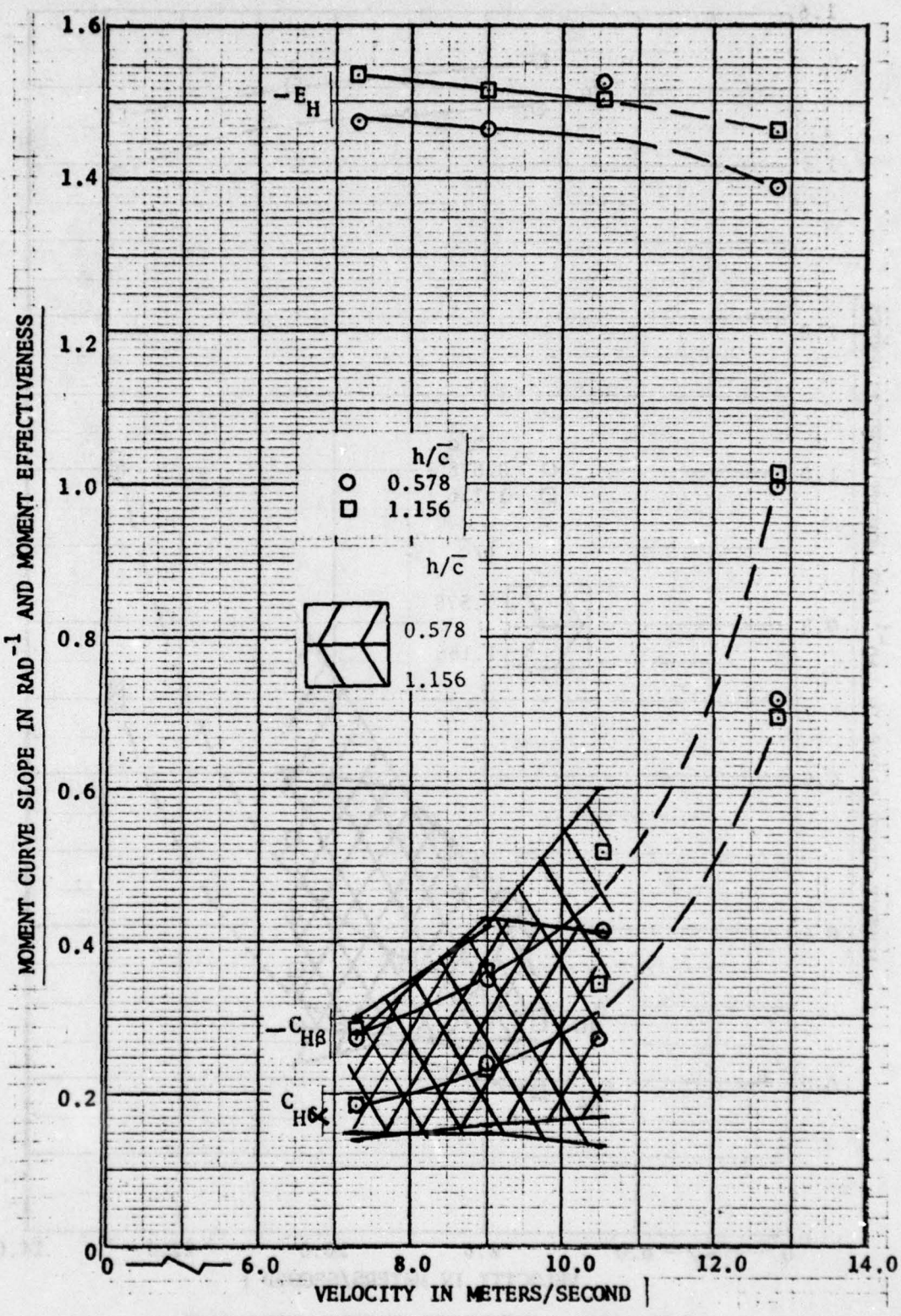

FIGURE B4b - ESTIMATED MAXIMUM ERROR IN $C_{H\alpha}$

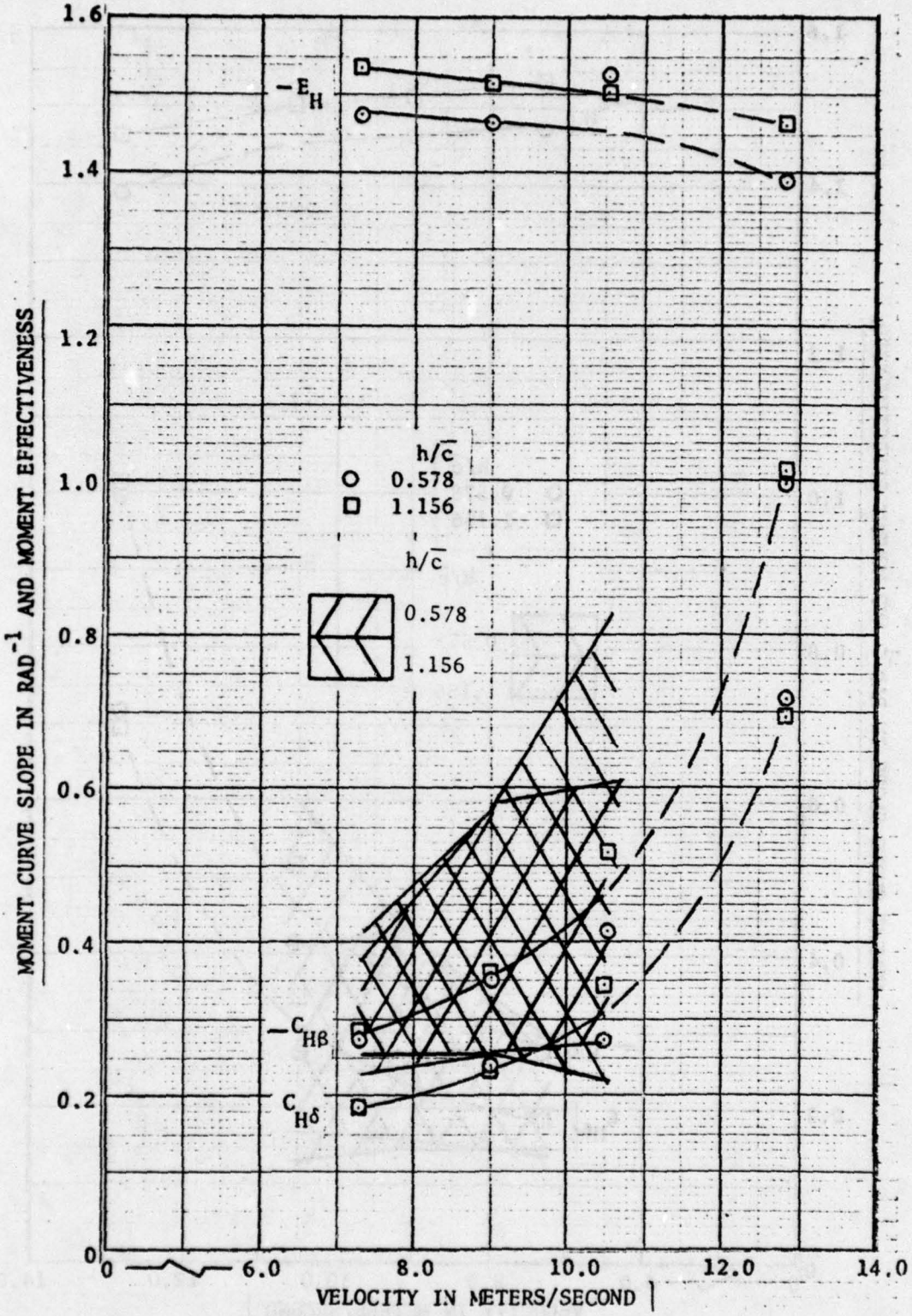

FIGURE B4c - ESTIMATED MAXIMUM ERROR IN C_{H_β}

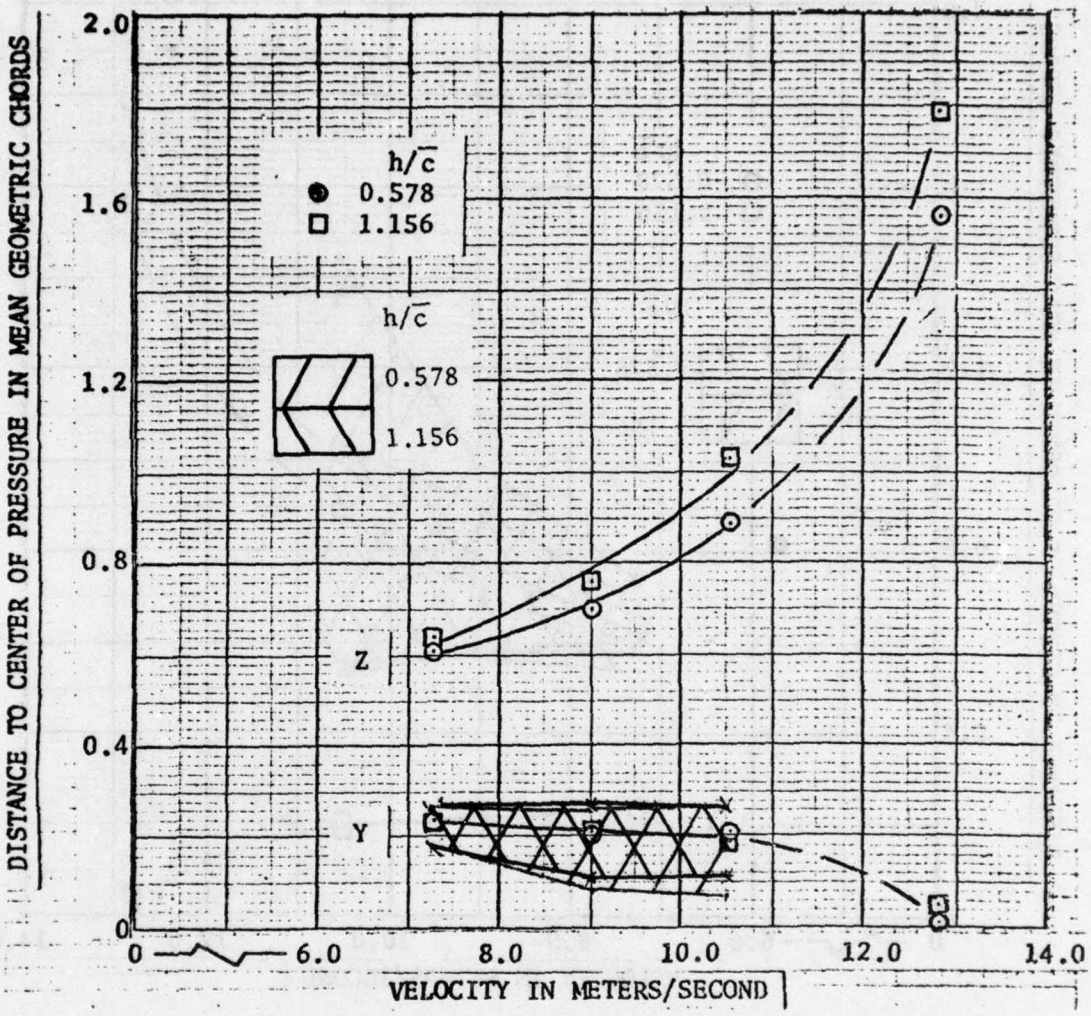

FIGURE B5a - ESTIMATED MAXIMUM ERROR IN Y

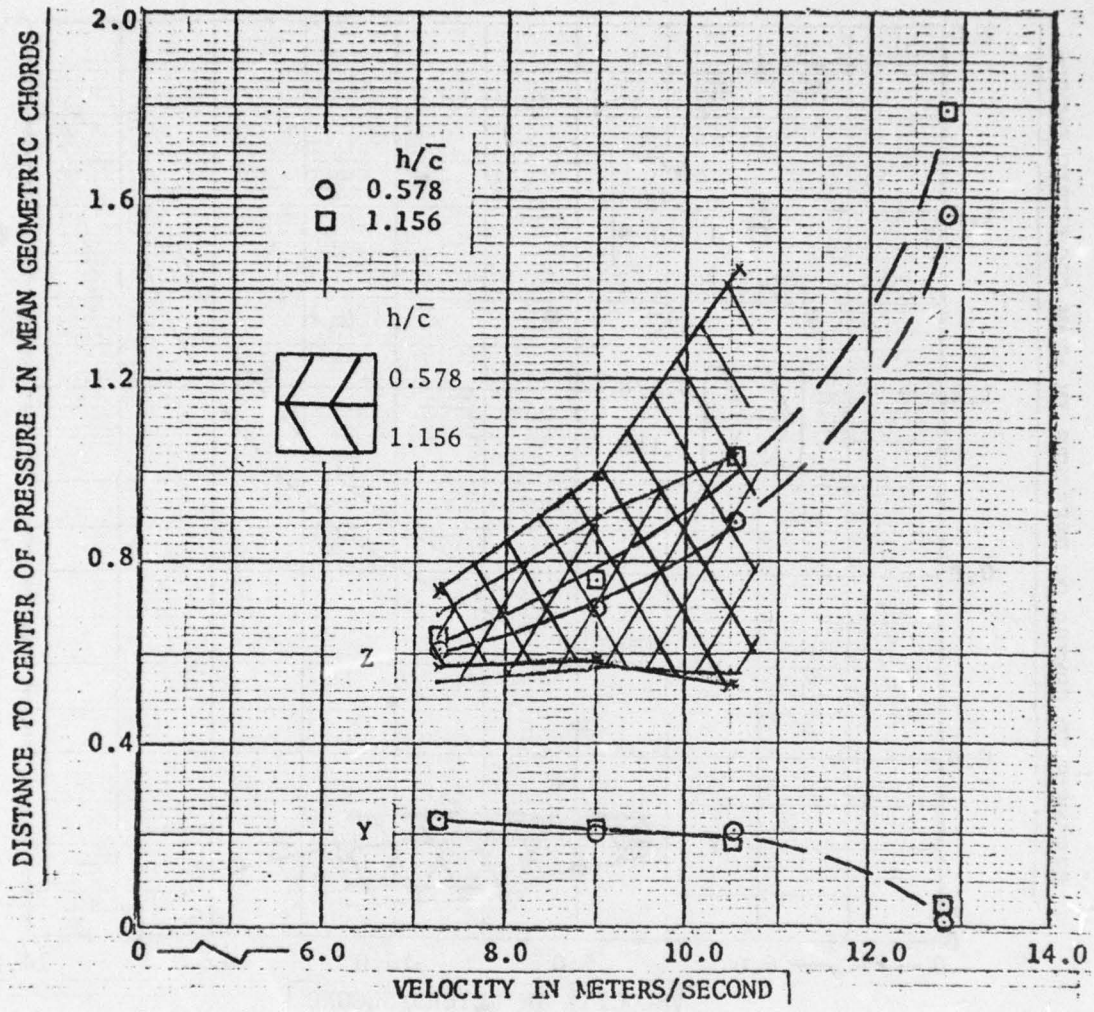

FIGURE B5b - ESTIMATED MAXIMUM ERROR IN z

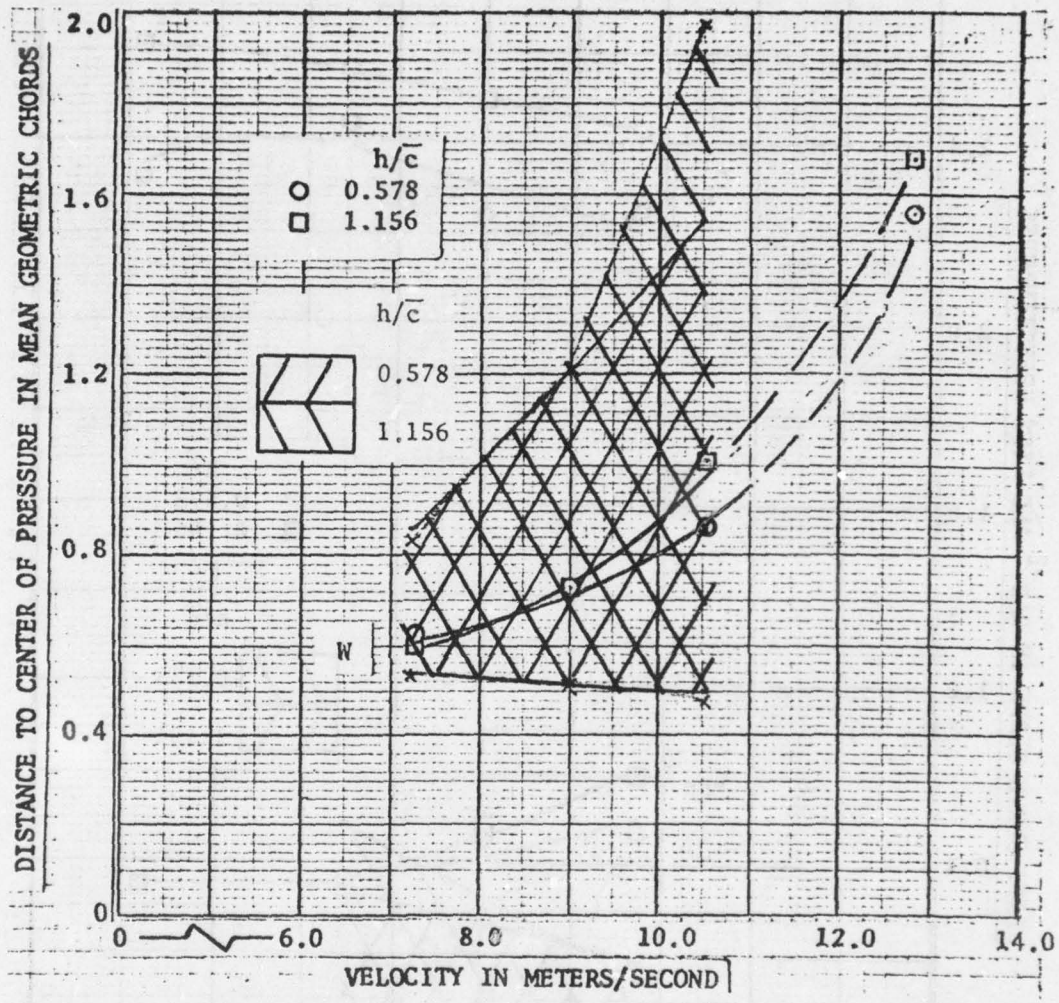

FIGURE B5c - ESTIMATED MAXIMUM ERROR IN W

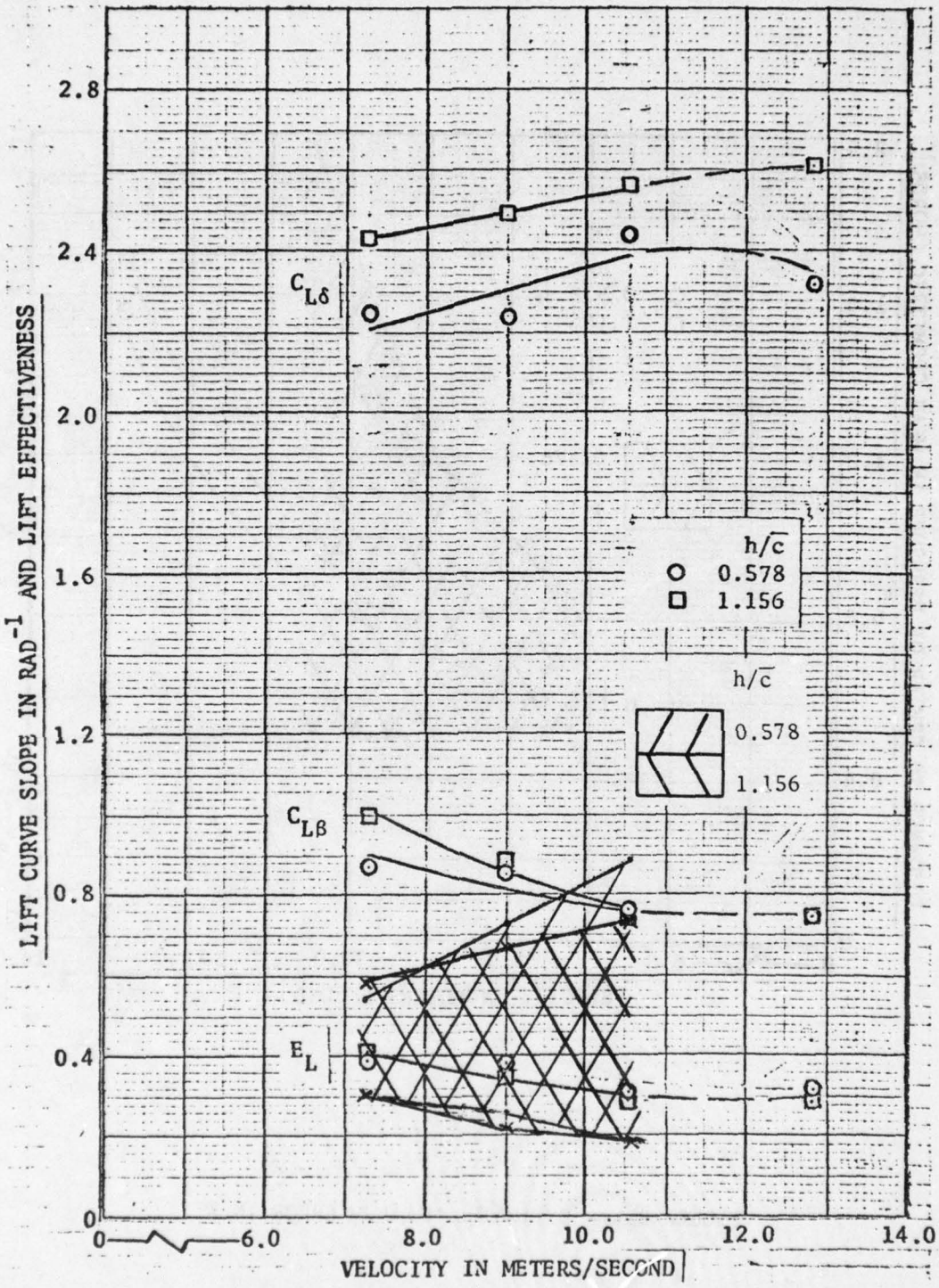

FIGURE B6a - ESTIMATED MAXIMUM ERROR IN E_L

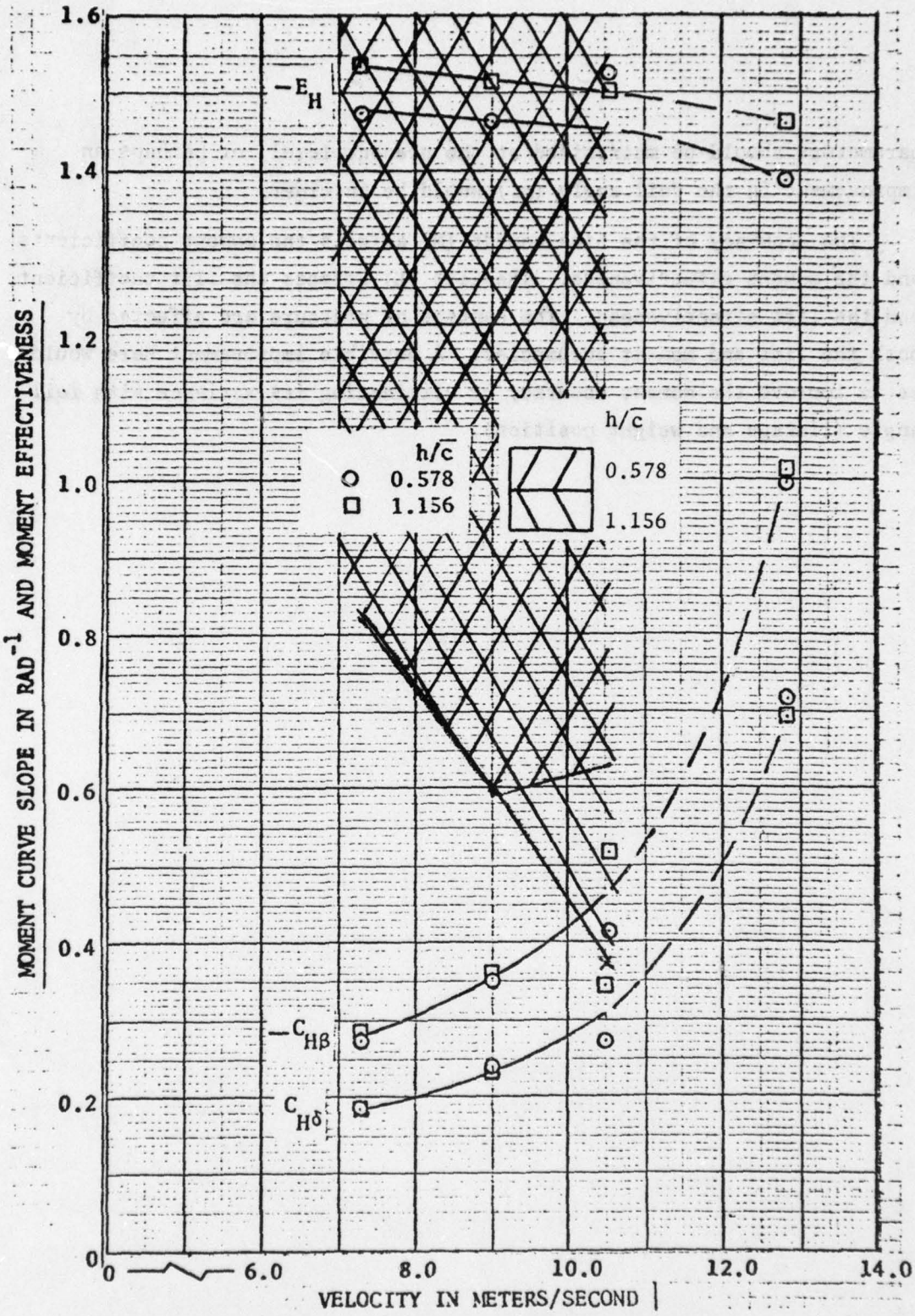

FIGURE B6b - ESTIMATED MAXIMUM ERROR IN E_H

parameters should be maintained at the present level, or perhaps an improvement in the foil angle (α) would be in order.

The accuracy of the bias moment (M) affects the moment coefficients and the moment effectiveness. The lift (L) affects the lift coefficient and the lift effectiveness. The centers of pressure are affected by both the lift and moment accuracies. A possible improvement here would be to improve the moment accuracy by eliminating its variance with foil angle (linkage and weight position).

REFERENCES

1. Remington, P.J. and E.K. Bender, "Hydrofoil Design for Minimum Control Power," Bolt, Beranek, and Newman, Inc. Report 2511 (Feb 1973).
2. Coder, D.W. and B.B. Wisler, Jr., "Hydrodynamic Equilibrium Conditions for AG(EH) Main Strut-Pod-Foil System Using Flap Incidence Control," DTNSRDC Report SPD-332-03 (Jun 1976).
3. Coder, D.W., R.M. Norton, and B.B. Wisler, Jr., "Hinge Moment Reduction for the AG(EH) Main Strut-Pod-Foil Assembly by Use of Training Edge Tabs," DTNSRDC Report SPD-332-04 (Jun 1976).

DTNSRDC ISSUES THREE TYPES OF REPORTS

1. DTNSRDC REPORTS, A FORMAL SERIES, CONTAIN INFORMATION OF PERMANENT TECHNICAL VALUE. THEY CARRY A CONSECUTIVE NUMERICAL IDENTIFICATION REGARDLESS OF THEIR CLASSIFICATION OR THE ORIGINATING DEPARTMENT.

2. DEPARTMENTAL REPORTS, A SEMIFORMAL SERIES, CONTAIN INFORMATION OF A PRELIMINARY, TEMPORARY, OR PROPRIETARY NATURE OR OF LIMITED INTEREST OR SIGNIFICANCE. THEY CARRY A DEPARTMENTAL ALPHANUMERICAL IDENTIFICATION.

3. TECHNICAL MEMORANDA, AN INFORMAL SERIES, CONTAIN TECHNICAL DOCUMENTATION OF LIMITED USE AND INTEREST. THEY ARE PRIMARILY WORKING PAPERS INTENDED FOR INTERNAL USE. THEY CARRY AN IDENTIFYING NUMBER WHICH INDICATES THEIR TYPE AND THE NUMERICAL CODE OF THE ORIGINATING DEPARTMENT. ANY DISTRIBUTION OUTSIDE DTNSRDC MUST BE APPROVED BY THE HEAD OF THE ORIGINATING DEPARTMENT ON A CASE-BY-CASE BASIS.